Day-Ahead Residential Electricity Demand Response Model Based on Deep Neural Networks for Peak Demand Reduction in the Jordanian Power Sector

Shaqour, Mahr Ayas
九州大学大学院総合理工学府環境エネルギー工学専攻

KYUSHU UNIVERSITY

Day-Ahead Residential Electricity Demand Response Model Based on Deep Neural Networks for Peak Demand Reduction in the Jordanian Power Sector

Ayas Mahr Shaqour

Supervisor
Associate Professor. Hooman Farzaneh

August 2021

Energy and Environmental System Laboratory
Department of Energy and Environmental Engineering
Interdisciplinary Graduate School of Engineering
Sciences

KYUSHU UNIVERSITY
Japan

Table of Contents

List of Figures

List of Tables

Abstract

Due to Jordan's challenges, its energy sector, from high dependency on importing around 97% of its energy resources, expensive fuels as well as a rapid increase in the integration of renewable energy, these challenges call for the integration and utilization of smart grid concepts in Jordan's power grid. A smarter grid utilizes the many types of data available from smart meters on both transmission level and end-user levels to implement high-performing machine-learning-based demand predictions as well as demand dynamic demand response systems that can enhance the operation and reliability of the power grid.

In this Thesis, a comprehensive demand response model for the residential sector in the Jordanian electricity market is introduced, considering the interaction between the power generators (PGs), grid operators (GOs), and service providers (SPs). First, an accurate day-ahead hourly short-term load forecasting is conducted, using Deep Neural Networks (DNNs) trained on 4-year data collected from the National Electric Power Company (NEPCO) in Jordan. The customer behavior is modeled by developing a precise price elasticity matrix of demand (PEMD) based on recent research on the short-term price elasticity of Jordan's residential sector and the analysis of the different types of electrical appliances and their daily operational hours according to the latest surveys. First, the DNNs are fine-tuned with a detailed feature analysis to predict the day-ahead hourly electrical demand and achieved a mean absolute percentage error (MAPE) of 1.365% and 1.411% on the validation and test datasets receptively. Then the predictions are used as input to a detailed model of the Jordanian power grid market, where a day-ahead peak-time demand response policy for the residential sector is applied to the three distribution power companies in Jordan. Based on different PEMD analyses for the Jordanian residential sector, the results suggest a potential reduction range of 4.49% to 8.19% in peak demand accompanied by a cost reduction of USD 64,263 $ to 265,411 per day for the Jordanian power sector.

Acknowledgment

First, **Alhamdulillah** for giving me the will, energy, and all of which I am blessed with.

I would like to express my greatest gratitude to my teacher and supervisor, **Associate Professor Hooman Farzaneh**, for guiding me, managing my research, and pushing me to achieve my fullest potential, of which I wouldn't have achieved any of my master's results without his support.

I would like to express my gratitude to **Professor Aya Hagishima** for her guidance through the laboratory rotation program. I would also like to give my thanks to all my teachers through my master's degree who taught me valuable knowledge related to energy and environmental engineering.

I would like to thank the **Japanese Government** represented by the Ministry of Education, Culture, Sports, Science, and Technology **(MEXT)** for providing the financial support for my research life in Japan.

I would like to express my sincerest gratitude and love to my mother **Haifa**, who always blesses me with her prayers and love, my father **Maher** may his souls rest in peace who has been my inspiration to achieve the highest standards in my life, and my amazing brother **Abdelrahman** of which I am forever proud of. I would like to express my sincerest gratitude to my aunts **Ghada** and **Hanan** for their moral support of me and my family through my Studies. I would like to thank **Sara**, for her continued support, and the light she shared with me during my research.

I am grateful for meeting my best friends **Yunus**, **Amr**, **Khaoula**, **Nisa**, and **Moustafa** for all the support and high standards they taught me.

I would like to thank **Sajid Abrar** for his support and for being an inspiration in managing his time and research and for being a support to everyone. I would like to thank **Nie Zifei**, for showing the utmost passion and hard work to his research and goals that I have ever seen, he has inspired me so much. I am thankful for the late-night conversations with my good friends **Yuchiro-san**, all the support and help **Naoto-san** has given me and all the good times spent with **Hiritomo-san** of which will not be forgotten. And for all my friends at the EES laboratory and Kyushu University for all their support, I hope to see them in the best of places.

Finally, I would like to express my thanks to my colleagues and friends at the National electric power company, **Faisal Abu Zaid**, **Almuatasim Dyab**, **Moustafa Az Zahlan**, and **Huthaifa Almogdady** for their support of my research by providing data, insights, and expertise.

Ayas Shaqour

Chapter 1: Introduction

1.1. World's Energy Challenges

The world energy demand grew by 2.3% in 2018, which is the fastest growth within the last decade [1]. The rapid increase in the global economy and population as well as the increase in heating and cooling demands, has resulted in more energy demand in certain regions, particularly in developing countries like India and China. With energy demand being on the rise, the world is faced with high dependence on fossil fuels, leading to increased greenhouse emissions, global climate change and increased health risks. As a result of this increase, CO_2 emissions went up by 1.7% to hit a new record of 33.1 Gt in 2018, with the growth of fossil fuels shown in Figure 1, [2]. Even though renewable energy is growing fast, it's not growing fast enough to meet the rise in energy demand at 1% for developed countries and 5% for developing ones [2].
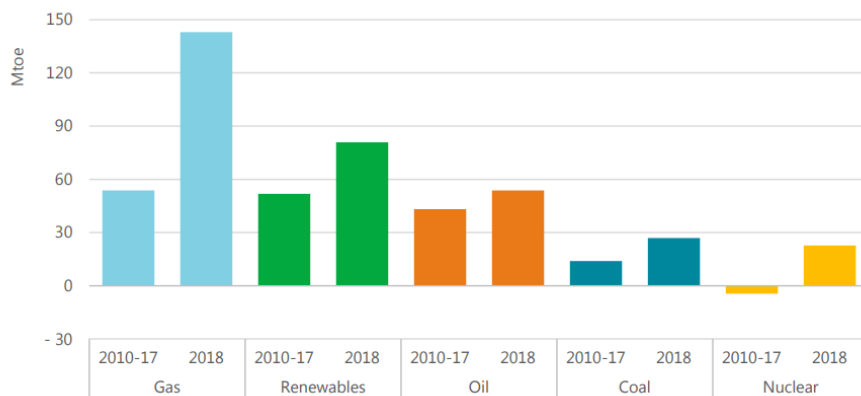
Figure 1 Average annual global primary energy demand growth by fuel, 2010-18 [1]

The world is moving into a future with higher energy demand and depleting energy sources, as well as rising environmental and health risk concerns. Hence, it's essential to have higher energy efficiency in terms of technology and usage, higher integration of renewable energy, new innovative energy storage technologies, and dependence on non-fossil fuel energy like nuclear energy.

1.2. Jordan's energy situation and Power Grids Challenges

With very limited resources, Jordan faces significant challenges in its energy sector due to heavy reliance on importing most of its energy resources. Losing access to Iraq's crude oil in 2003 and Egypt's natural gas, the country was put under critical economic conditions that had an adverse impact on both private and public sectors, placing the country under massive debt[3]. As shown in Figure 2, by 2015, the total accumulated commercial loans and the advances from the Ministry of Finance (MoF) reached 4.9 Billion JDs by the national electric power company (NEPCO), which was 18.8% of Jordan's GDP and accounted for one-quarter of the total consolidated public-sector debt, limiting the borrowing capacity of the government [4]. In 2018, the imported crude oil and natural gas accounted for 92% of the total energy requirements, constituting 10% of the country's GDP[5]. Shortage in affordable energy supplies directly affects the public sector, increasing the budget deficit and leading to revenue-boosting measures (Hike taxes and fees). In contrast, private sectors face immense production costs due to high energy costs and higher taxes, leading to lower productivity and profitability. With Jordan's annual energy demand growing at a rate of 3% [6] and the surge of Syrian refugees estimated between 660,000 and 1.26

million [7], coupled with the previous challenges mentioned, the government had a strong commitment to reform its energy sector.
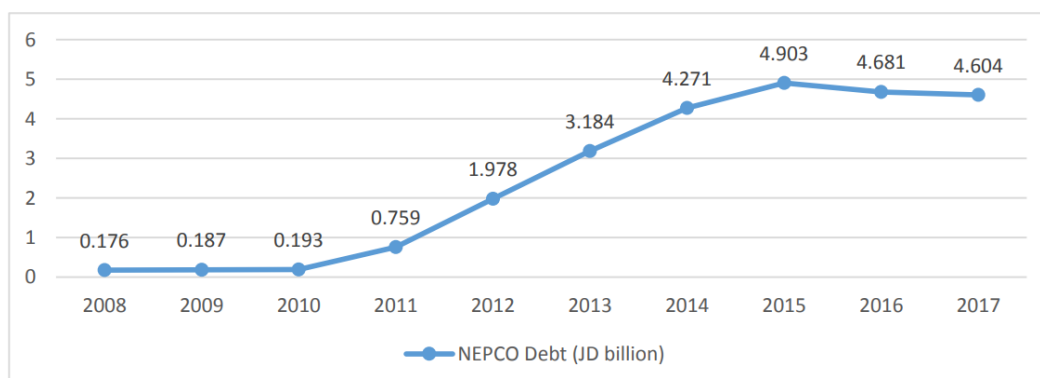
Figure 2 NEPCO Dept [4]

In 2013, the National Energy Efficiency Action Plan (NEEAP) was introduced in Jordan to set the targets for achieving 20% energy saving and increasing the share of renewable energy to cover 10% of the national energy consumption by the year 2025. To this aim, a five-year electricity tariff plan adjustment was implemented between 2013 and 2017 to increase NEPCO's revenue, and an Automatic Electricity Tariff Adjustment Mechanism (AETAM) was adopted in 2016 to reflect global oil price changes in consumer's tariffs, except those under 300 kWh per month, in order to protect poor households [4]. The Automatic tariff adjustments were applied from January 2018, as can be seen in Figure 3, when the three months moving average of the Brent crude oil price crossed the breakeven threshold of 55$ set by NEPCO and the Energy and Mineral Regulatory Commission (EMRC) in December 2017 as can be seen in Figure 4[4].
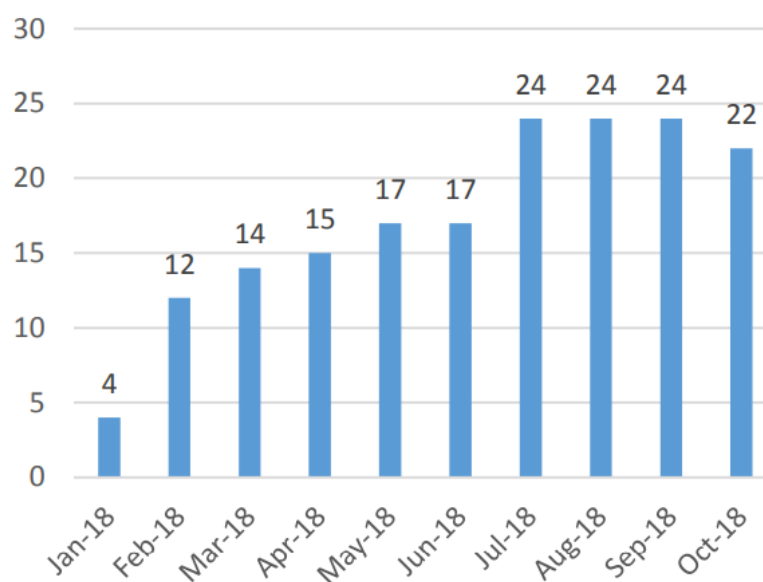
Figure 3 "Automatic Tariff Adjustments (fils per kWh)" [4]
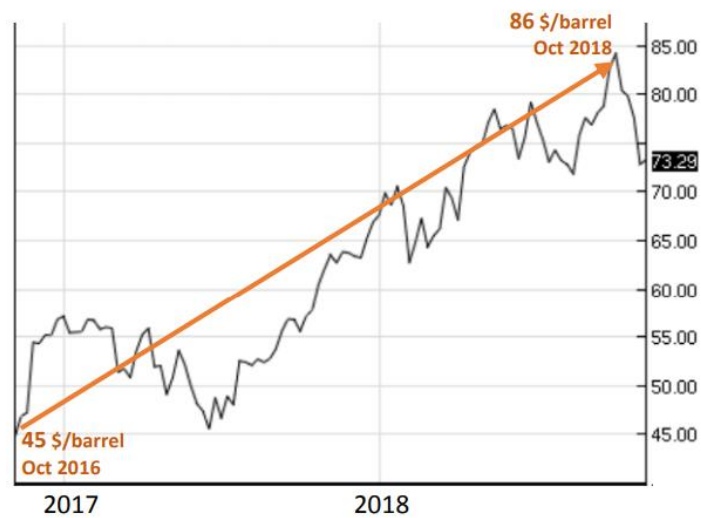
Figure 4 "Rise in Global Brent Crude Oil ($ per barrel)" [4]

Due to the tremendous efforts, financial incentives, and government promotion to attract overseas investments and expertise, there has been significant progress in the renewable energy sector, reaching a capacity of 1470 MW by late 2019, which represents 25.7% of total generation capacity, with solar accounting for approximately 75% of renewable power [8]. Renewable energy's contribution to the total electricity generation reached 15.1%, with solar energy, wind power, and hydropower accounting for 10.4%, 4.4%, and 0.1%, respectively [9]. While this sheds hope for the future of the Jordanian energy sector and increases energy resilience [10], an increase in renewable energy in both transmission and distribution levels introduces grid-level operational challenges that must be met to achieve optimized and efficient operation. Renewable energy sources such as solar and wind are non-dispatchable power units characterized by uncertainty, stochasticity, and being intermittent as they are dependent on variable weather conditions, which increase the flexibility needed to achieve supply-demand balance [11] and the need for energy storage systems [12][13]. On transmission levels, a fluctuation in renewable energy supply causes a sudden decrease or increase in power flow, while on distribution and consumer levels, a sudden change in weather conditions can lead to a reduction in renewable energy generation that causes a sudden load increase, affecting the grid voltage and frequency levels. Hence, grid operators need to rely on the frequent operation of high-ramping power supply units, which are costly to operate, where a sudden decrease in renewable energy occurs. In high renewable energy scenarios, the minimum power output of conventional power plants is an extremely sensitive factor to avoid plant shutdown, which is economically a worst-case scenario, causing challenges to conventional power generators' unit commitment and operation [14].

1.3. *Demand Response potential for Jordan*

Demand-side management (DSM) and Demand Response (DR) systems introduce a form of flexibility from the consumer side[15]. In DR systems, the power distributors and Grid Operator (GO) can influence consumers to shift, shed and reschedule their energy consumption and electrical appliances usage by providing incentives or implementing dynamic pricing methods [16]. Jordan is rapidly installing smart meters around the country, with great potential for implementing many DSM methods such as Time of Use (TOU) pricing, Peak pricing, and real-time pricing schemes. Implementation of a DR scheme targeted to the residential sector can guarantee flexibility in unit commitment planning and hourly operation to achieve optimized demand-supply matching and avoiding the need to use fast-starting and costly power units in times of high energy demand or

low renewable energy generation. With the domestic and government buildings accounting for 46.12% of the electrical energy demand in 2019, implementing the DR and DSM programs is highly recommended for the Jordanian power sector [17].

DR had already proven benefits in Jordan. A pilot project was implemented for the principal consumers of NEPCO with smart meters installed, considering incentives, compensations, and non-peak times price penalties. The pilot project resulted in 6 million $ indirect savings of operating costs and indirectly increased efficiency in the transmission system with reduced bottlenecks and recommended future expansion on commercial and residential consumers, taking into consideration the effect of renewable energy generation [18]. Figure 5 shows the power demand (MW) for a day in December-2019, together with the wind and solar (PV) energy generated through the day.
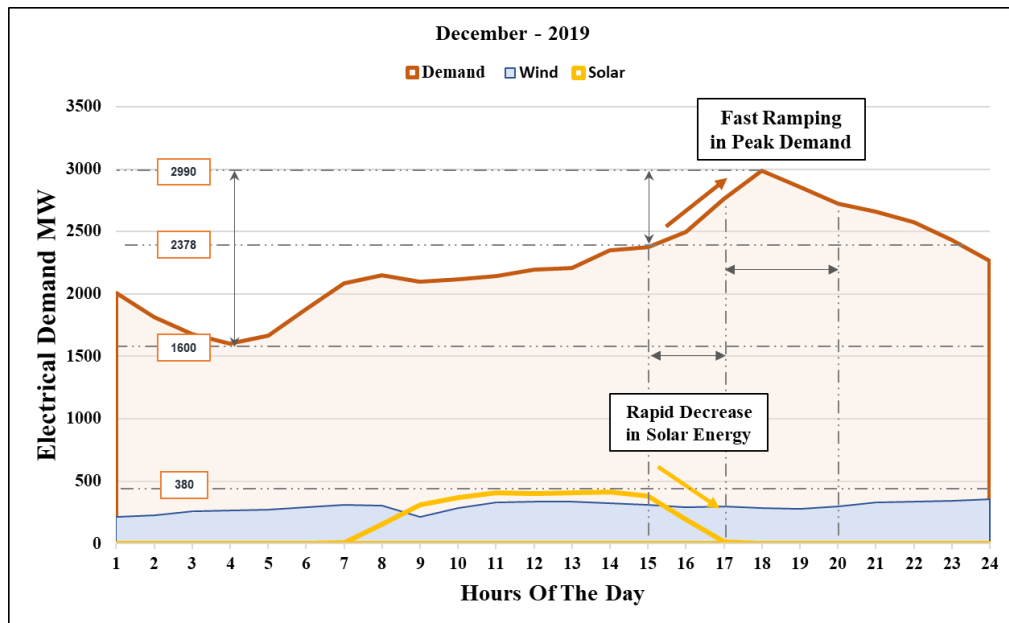
Figure 5 Jordan's Power Demand and Renewable Energy Generation for a day in winter at the end of 2019.

As can be observed in this figure, the evening peak occurs after the rapid decline in renewable energy from 3 to 5 PM, losing almost 380 MW of solar power, while gaining 612 MW in evening load peaking at 6 PM. Hence, a deficit of 992 MW needs to be provided by the GO, NEPCO, between 3 and 6 PM, which amounts to 44% of the average load (2256 MW) of that day. It would be highly favorable for the GO to shift and reduce demand from the evening peak to any other time of the day, especially that period with high solar energy. It is notable that, unit commitment planning for optimized power dispatch is based on planning which power plants to operate at what hours. Each power plant has its startup time; Combined Cycle (CC) power plants need approximately 3 hours to operate. Each power plant has different minimum generation limits, depending on whether it operates in a Single Cycle (SC) or a CC and the number of activated units. Hence, a DR scheme that targets the evening peak in winter can lead to more flexibility in power dispatch operation and shifting from peak power, which forces the GO to operate fast and expensive power plants to ensure reliable operation in peak times. The dual challenge of minimum power and the start-up time of power plants can be solved by using day-ahead unit commitment optimization that relies on day-ahead hourly predictions of the load, power plant availability, energy cost, and available power Egypt's interconnection. Figure 6 depicts the effects of influencing electrical demand consumption in peak demand periods [19][20]. The price axis represents the cost liability on the GO for meeting specific power demand in the gird, where the cost of producing energy for standard power demand is relatively low, using conventional power generators, but grows extremely high in

peak periods. The original demand represented by Demand Curve 1 is influenced by DR at peak time, leading to a decrease in demand (Demand Curve 2) and lower energy prices on the GO.
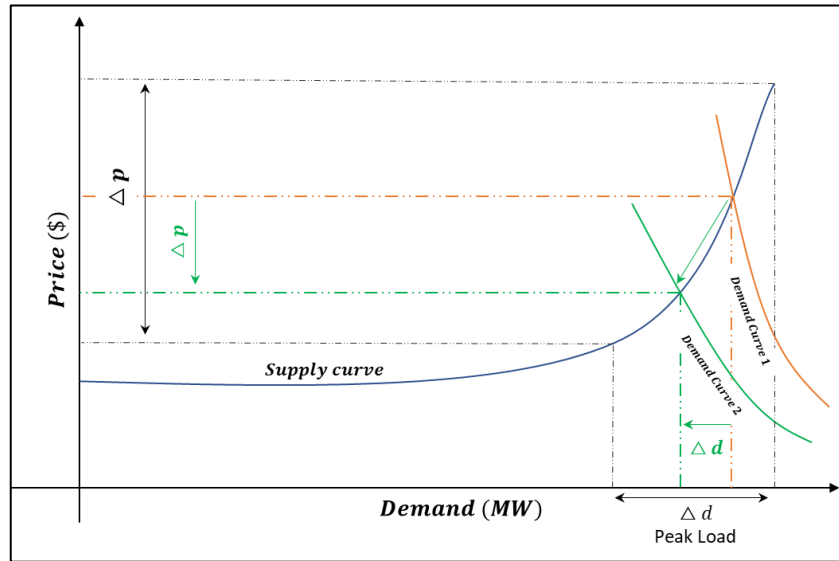
Figure 6 Standard Supply - Demand Curve of Electrical Energy Markets

1.4. Machine Learning applications in future Smart Grids

Power systems from generation to distribution are key for developing societies, providing the energy needed in terms of daily living needs, public services, and, more importantly, driving manufacturing and production. Hence, having a stable, resilient, and efficient power system is essential for the economic development and prosperity of societies. The conventional power grid was designed to carry energy from centralized big power producers to consumers, where energy flow is unidirectional. Although with the introduction of renewable energy, distributed power generation, and energy storage, power grids are faced with having to cope with bi-directional energy flow and more complex design. Today, the consumers are also playing an active role in the energy paradigm with the introduction of smart meters and demand response programs, allowing them to participate in the energy management of the grid[21]. Figure 7 shows the difference between the conventional and new power grid[22].

The concept of Smart Grid was introduced to overcome the challenges of today's power grid, by utilizing the advancements of different fields of technology, such as communication, power electronics, control, and computer science. A Smart grid is a power system that can sustain a two-way power and information flow between its different nodes, in a way that is safe, resilient and sustainable[23].

The new power grid will have the following capabilities[24]:

1. Being able to handle schedules and power transfer under uncertainty
2. Integration of renewable sources and adapting to their stochastic nature
3. Sustaining the need for higher quality and reliability of power supply
4. Sustaining optimized power flow through the transmission and distribution networks
5. Dealing with operation uncertainties and resolving unpredictable events, increasing power security
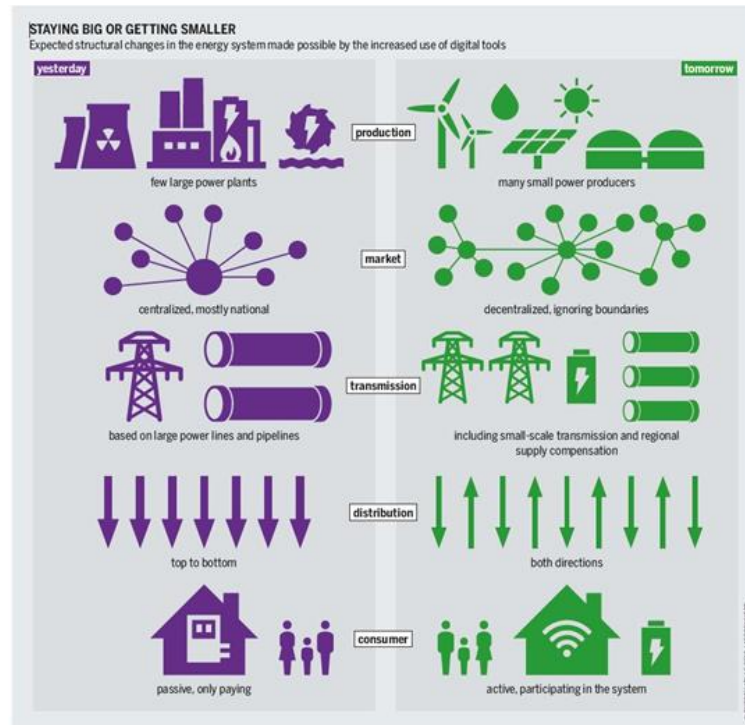
Figure 7 conventional vs. new power grid [22]

In order to meet the previous capabilities and leverage the advancements in today's technology, a lot of research is being done by research institutes and government entities, although in order to achieve each of the aforementioned, there is a series of challenges. For example, the automation and digitization of power grids will impose high security and reliability risks due to the risk of cyber-attacks and high reliability on the communication networks[25]. There are also many challenges related to renewable energy; being stochastic leaves, a space for uncertainty in energy generation in terms of magnitude and time since both PV and Wind power systems heavily rely on environmental conditions[26]. This poses challenges in power dispatch and supply-demand balancing. Furthermore, renewable energy sources also rely on power electronics such as converters and inverters, which induce many harmonics into the grid, posing power quality issues.

With the introduction and deployment of smart meters and smart metering infrastructure as well as advances in the field of ICT "Information and Communication Technologies" and IOT " The internet of things" and the introduction of smart grids and the concept of smart cities, we now have available large amounts of data related to our energy system that can be utilized and studied through advanced computational techniques powered by the advancement of computational power that has become cheaper and more affordable. This opens up a broad field of research in energy system management and energy consumption reduction through advanced data analysis leading to hidden pattern recognitions and supply-demand predictions. Figure 8 shows the bi-directional data flow in a Smart Grid[27].
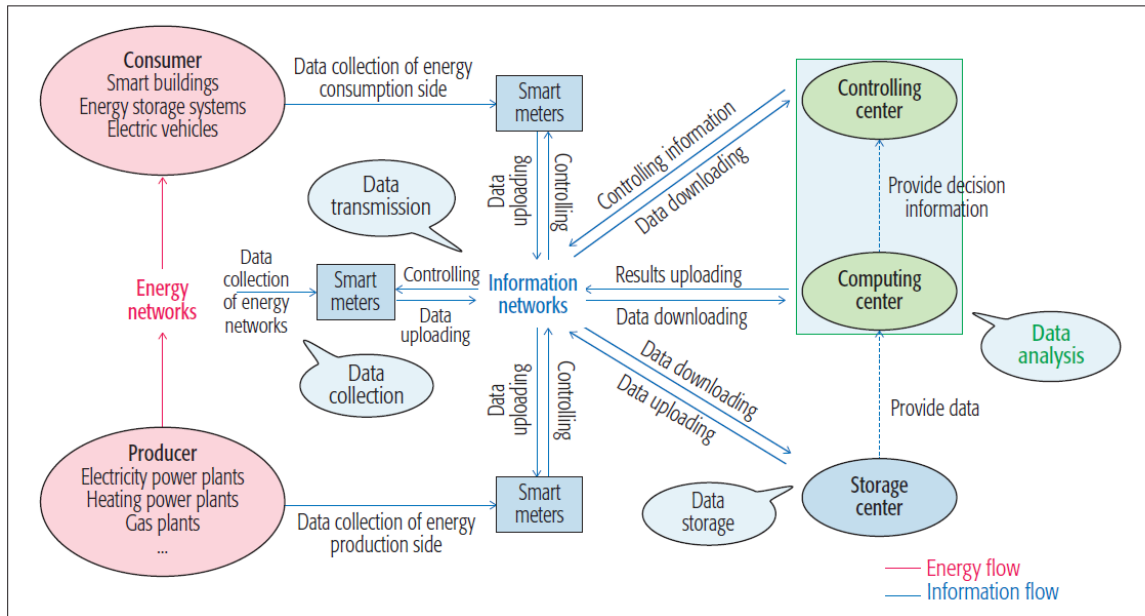
Figure 8 Data flow in Smart Grids [27]

Machine learning (ML) refers to the ability of systems to learn from given data in order to find hidden patterns or make future predictions. Machine learning is a group of various computational algorithms with instructions to make data-driven decision-making frameworks. These algorithms are developed so that they can continue from the data given and deal with big amounts of data achieving higher prediction rates than conventional algorithms. Machine learning is used in many applications from web search, filtering, recommendation systems, fault detection, image recognition and so on [28]. As shown in Figure 9, Machine learning is classified into two major classes: Supervised and Unsupervised learning. In Supervised Learning, the model is built to learn from a set of inputs or features to predict a known output or category, wherein the training process, the data is called labeled data, meaning the output data is known to us, hence, comes the name "Supervised" as we are supervising the training process feeding the data with each input and giving it the correct output to adjust its parameters in a way that decreases its prediction error in each iteration. Unsupervised learning, on the other hand, is a set of algorithms that are used on data that is not labeled or where the category is unknown to us, so these algorithms are used to detect hidden patterns or rules in the data fed, then summarizes and groups the data in a way were meaningful insights can be extracted.
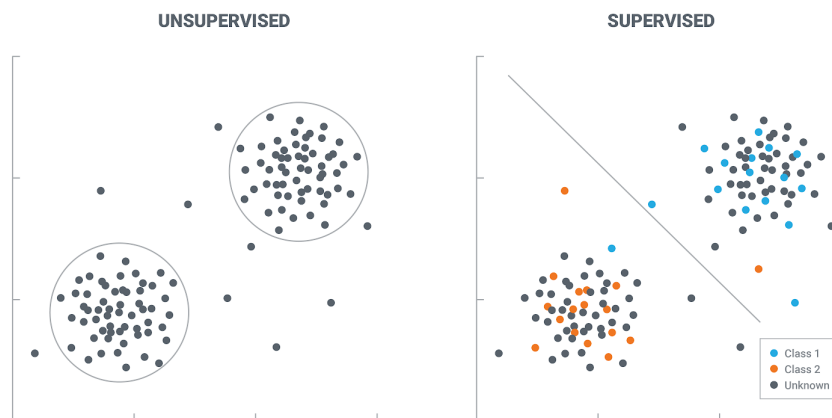
Figure 9 Supervised vs Unsupervised Learning [29]

Supervised learning can be further classified into Regression and Classification. Regression is when the output is a continuous value that can have infinite values; for example, detecting energy consumption or fuel prices, the output value can take any value. On the other hand, classification is when the predicted output is a categorical value, that is a part of a set of defined values; for example, when predicting if the system is in an error state, the output is either yes or no, or when trying to classify images to animal or non-animal and so on.

Machine learning algorithms have a range of potential applications in the field of smart grids, such as forecasting future energy demand, clustering user types into different categories, predicting future production of renewable energy sources and finding the best energy pricing. Machine learning has a big potential when it comes to smart grids utilizing the large amount of data that will be produced and that can be leveraged to achieve a more efficient and smart energy system[27]. Table 1 shows the different machine learning algorithms used for different smart grid applications [27].

Table 1 Machine learning application in smart grids [27]

Methods	Applications				
	Clustering	Demand Response	Energy Production Optimization	Energy Pricing	Monitoring and diagnostics
Linear Regression		●	●	●	
Support vector machines		●	●	●	●
Neural Networks	●	●	●	●	●
K-Means	●				
Kalman filter		●	●	●	
Gaussian Process	●	●	●	●	
Principal component Analysis (PCA)/ Independent component Analysis (ICA)/ Nonnegative matrix factorization (NMF)	●				
Learning vector quantization (LVQ)	●				

1.5. *Related Work*

DR systems can be mainly classified into time-based and incentive-based pricings as well as other subcategories such as Direct load control (DLC), Demand Bidding(DB), emergency DR programs (EDRP), Time-of-use (ToU), Real-Time Pricing(RTP), and Critical Peak Pricing (CPP)[30][31]. Aalami et al. introduced a DR model considering Interruptible/Curtailable loads as well as capacity market programs where they combined the price elasticity of the demand model with the customer benefit. Their model applied to the Iranian power grid peak load data can aid GOs in improving the power load curve, while considering customer well-being [32]. Moghaddam et al. introduced a mathematical model for incentive-based and time-based DR programs to consider the correct balance of penalty and incentive rates to achieve DR's best performance for given demand levels [33]. Baboli et al. discussed observations based on psychology and economy that consumers react differently to both incentive (reward) and price (punishment) based DR systems which are not considered in conventional DR models [20]. Qu et al. proposed an improvement to the price elasticity matrix of demand (PEMD) to unify the modeling of rigid and flexible loads by introducing a weighting factor and measured the effect of price policies and load types on calculating the elasticity matrix[34]. Wang et al. implemented an optimal strategy for both bidding and scheduling for aggregators of distributed energy resources (DER) who manage distributed solar and wind energies and battery storage systems under uncertain

consumer response to real-time pricing (RTP) considering uncertainties of renewable energy generation and consumer response[35].

The employment of DR systems depends on precise knowledge of future wholesale electricity market prices and customer demands and future renewable energy generation. Hence, researchers have combined both machine learning algorithms and DR models to overcome these challenges. Lu and Hong proposed a novel real-time incentive-based DR system that utilized both deep learning and reinforcement learning (RL) algorithms combining two Deep neural networks (DNNs) for day-ahead price and demand predictions. [36]. Wen et al. implemented a modified deep learning (MDL) algorithm to predict 24-ahead power demand, prices, and PV energy generation in incentive-based demand response models utilizing recurrent neural networks (RNN) architectures[37]. Pramono et al. presented an improvement in short-term load forecasting for DR systems using an ensemble of two DL approaches; Convolutional neural networks (CNN) and long short-term memory (LSTM)-RNN, showing higher performance over conventional models [38]. Hlalele et al. presented an optimization model that considers the combination of direct load control demand response and economic dispatch under renewable obligation policies, where the model maintains a predefined renewable energy share in the mix of different energy sources[39]. Zeng. et al. proposed a demand response modelling approach for increasing the efficiency of renewable energy deployment, which considers operational improvements and a system planning perspective. Their model captures the correlation of uncertain variables such as renewable energy generation, customer demand and changing responsiveness to DR and utilizes clustering methods to implement a scenario reduction that reduces the computational complexity of the model[40]. Balasubramanian and Balachandra formulated a modeling approach to optimally implement an incentive-based demand response to match the variations of electrical demand and supply. Their model is coupled with a focus on assessing voluntary-based consumer-centric demand response systems that are less complex and cost-effective to other methods[41].

Table 2 shows recent DR studies systems on multiple scales of the residential sector using different DR schemes.

Table 2 Recent studies on Residential DR systems

Ref.	DR Type	Study Scale	Methodology	Achievements
[42]	Hybrid Price-based DR (HPDR)	Residential micro-grid.	Day-ahead HPDR scheduling to a residential micro-grid, considering uncertainty related to generation and dispatch.	In comparison to ToU and RTP and fixed-rate (FR) pricing, HPDR, which is a combination of ToU and RTP, showed a lower decrement in the peak-to-valley index (PtV) by 12% and Coefficient of Variation Percentage (CVP) by 25% and increased social welfare by 18%.
[43]	ToU	Residential Household	DR strategies (Rule-based and Machine-Learning (ML) Based) for controlling a heat pump and thermal storage system in a smart-grid ready residential Household.	The proposed ML prediction-based smart controller under a ToU DR scheme showed superior performance reducing electricity end-use usage, utility generation cost, and carbon emission by 41.8%, 39%, and 37.9%, respectively.
[44]	Dynamic Price-based	Residential Local energy Market	Agent-based simulations for pricing strategy and demand shifting strategy	The model was simulated for a LEM with 100 households,

			under dynamic pricing DR are applied on a local electricity market (LEM) based on the German energy market.	increasing its local sufficiency by 16% through DR and local Trading, showing a 10c€/kWh reduction in annual electricity costs as well as 40% reduced peaks.
[45]	ToU	5000 Residential Households	DR strategies, using 18 months of data in Ireland where different ToU schemes were applied to 5000 Households coupled with information feeding (in-home display units (IHD), monthly billing, etc..)	The ToU DR coupled with the information feed reduced energy demands for the given household, especially in peak demand periods. However, after implementation, little DR impact was observed by changing the distance between the peak and off-peak prices.
[46]	Dynamic Price-based	2 Residential Buildings	OpenStudio and EnergyPlus to assess the effects of DR potential on HVAC systems through changing temperature set points in two residential buildings in Texas, USA	In applying two different types of real-time dynamic tariff pricing, simulation results showed that a reduction potential of 10.8% in energy costs could be achieved through the proposed DR controller without significant impact on comfort levels and savings of 24.7% peak load and 4.3% of energy for HVAC could be achieved annually.
[47]	Dynamic Price-based	Residential Household	Dynamic Price-based DR by modeling the optimal consumer response through fuzzy reasoning (FR) and Reinforcement Learning (RL)	Simulation results showed a power consumption smoothing by 15% and energy costs reduction by 18.5% can be achieved by considering consumer preferences through morning and evening demand peak periods.
[48]	ToU and Incentive-based	100 Residential Households	Simulation of two DR systems: (1) an augmented ToU DR system solved using a stochastic optimal load aggregation model. (2) an incentive-based DR is solved using a two-stage stochastic unit commitment (UC) model satisfying operational cost reduction and consumer convenience.	Simulations for one load aggregator and 100 Residential Households showed that under augmented ToU DR with 60% consumer participation level, generation costs can be reduced by 24% and load profiles' standard deviation by 42%. Although with a higher 60% consumer participation level reaching 80%, the model becomes less efficient. Although under the incentive-based DR, 77% standard deviation and 20% generation costs reductions can be achieved.

1.6. *Thesis Contribution*

Very few studies discussed the possibilities of DR and DSM in Jordan. Tawalbeh et al. addressed the potential of residential peak shaving to reduce peak demands [49]. They showed that an average of 3.5 kWh of peak load reduction per day could be achieved through adjusting the residential tariffs in peak times from 5 to 8 pm, using TOU pricing. Another research conducted by Jarad and Ashhab emphasized the potential for energy saving in the Jordanian residential sector through energy efficiency measures, where they reported a saving of 15% in energy consumption and 22% in cost could be achieved through the use of efficient lighting and solar heaters by applying for an hourly analysis program (HAP) software [50]. The insight gained from these studies highlights further the potential of DR in giving more incentives for residential and commercial users to pursue energy-efficient electrical appliances and usage. However, this potential has not yet been exploited because there is no understanding of the factors that amplify this potential. This is mainly due to the lack of a conceptual framework and methodological approach that can be applied to a robust data set to quantify the main implications of using DR applications in the Jordanian power sector. This research aims to fill the gap by presenting a detailed day-ahead price-based demand response model for the residential sector in Jordan with the following contributions:

1. A well-defined and optimized Deep Learning model for accurate day-ahead hourly short-term load forecasting (STLF) is trained on 4-years of Jordan's hourly electrical demand from 2016 to 2019. The model's architecture and input features follow state-of-the-art feature engineering based on recent research discussed in detail. Up to date, there are very few Jordanian case studies that examined daily hourly STLF rather than day-ahead hourly STLF, such as [51], where they used only one year of electrical demand data. This research proposes a new set of time series features that are novel to previous works on Jordan's electrical demand forecasting.

2. A comprehensive demand response model for the Jordanian power sector is introduced, considering the interaction between the Power Generators (PGs), GOs, and Service Providers (SPs), which uses the estimated day-ahead hourly demand STLF, considering the detailed data on generation capacities and costs of Jordan's power suppliers as well as bulk consumers' peak load and bulk supply prices. A precise PEMD estimation was implemented for Jordan's residential sector based on recent research on the short-term price elasticity of Jordan's residential and the analysis of the different types of electrical appliances and their daily operational hours according to the latest surveys and studies present. To the best of our knowledge, this is the first study in Jordan's electricity market to estimate the DR impact on the residential sector and find the potential implications in peak demand reduction and generation savings.

1.7. Thesis Outline

The rest of this thesis will be depicted as follows: Chapter 2 discusses the Jordanian power sector in detail, Chapter 3 presents the Demand response model for the Jordanian power sector, Chapter 4 introduces the hourly day-head demand prediction model, Chapter 5 shows the results of the day-ahead prediction model, Chapter 6 presents a detailed analysis of Jordan' residential sector PEMD and Chapter 6 will conclude the thesis.

Chapter 2: Jordan's Electricity Sector

2.1. Electricity sector Overview

The electrical sector in Jordan has undergone reform starting from 1996, where the generation, transmission, and distribution sectors were privatized in 1999. The overall architecture of the Jordanian electricity sector is shown in Figure 10 and is mainly composed of four layers: Generation, Transmission, Distribution, and Consumption[52]. NEPCO, operated by the government, acts as the GO of the power grid under a single buyer model as well as the transmission sector operator. The long-term strategy of the power grid is under the responsibility of the Ministry of Energy and Mineral Resources (MEMR), whereas the EMRC is responsible for establishing regulations and licensing on all levels of the power grid from generation to distribution as well as setting laws and tariffs in the electricity sector [52][53].
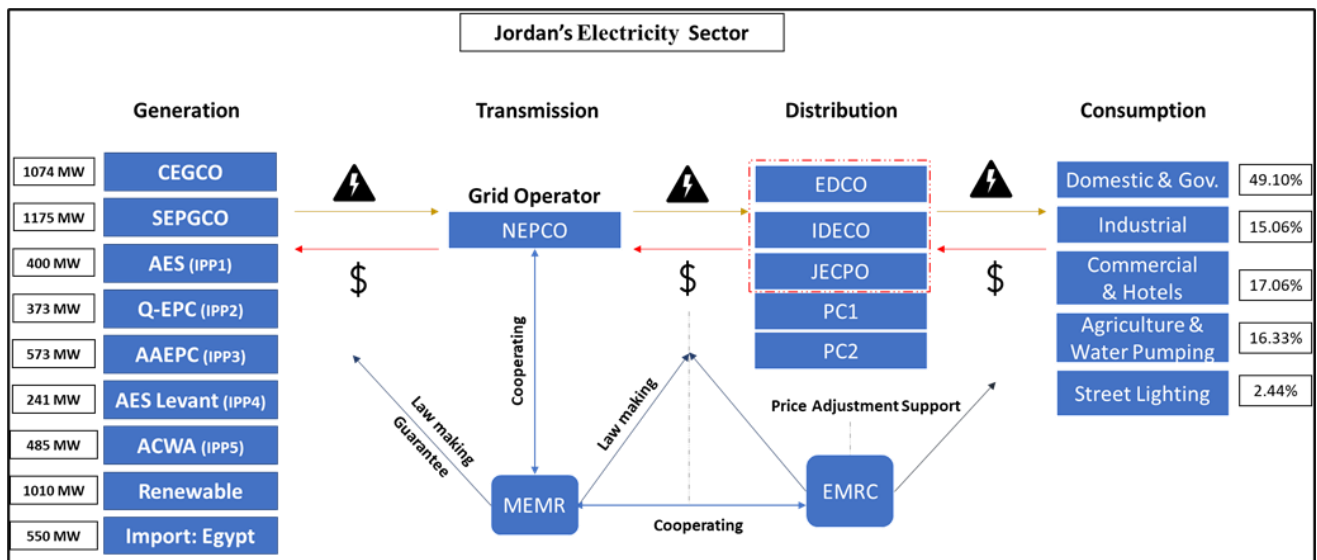
Figure 10 Jordan's Electricity Sector – 2019

2.2. Generation Sector

Jordan's power generation is mainly based on thermal power plants followed by renewable energy and Egypt's interconnections, as shown in Table 3. The Table shows the details of each respective power supplier and their generation capacities by 2019, based on the latest data from the Japan International Cooperation Agency (JICA) report [52] and the respective websites of the respective power plants' websites, where the generation capacities can be slightly higher or lower depending on hot or cold seasons. The renewable energy capacity is shown in Table 3 only includes the transmission level suppliers, not the distribution and consumer level generation. Jordan is interconnected with Egypt with a total capacity of 550 MW, utilizing a 400 kV submarine cable, where up to 250 MW can be used according to energy availability and other factors, while the rest are reserved for operational purposes [54].

Table 3 Jordanian Power Plants – 2019

Power Plants		Unit	Available Capacity	Fuel Type			Average Cost (JOD */MW)
				P	S	T	
CEGCO	ATPS	5 * ST	130 * 5 MW	NG	HFO	-	
	RISHA	2 * GT	58 MW	NG	LFO	-	203.46
	Rehab	CC	297 MW	NG	LFO	-	
SEPCO	Samra I	CC	270 MW	NG	LFO	-	
	Samra II	CC	270 MW	NG	LFO	-	61.06
	Samra III	CC	400 MW	NG	LFO	-	
	Samra IV	CC	220 MW	NG	LFO	-	
IPP	IPP1	CC	400 MW	NG	LFO	-	59.85
	IPP2	CC	373 MW	NG	LFO	-	64.89
	IPP3	DE	573 MW	NG	HFO	LFO	231.04
	IPP4	DE	241 MW	NG	HFO	LFO	121.17
	IPP5	CC	485 MW	NG	LFO	-	60.09
Egypt		-	550 MW	-	-	-	52.79
PV		-	640.5 MW	-	-	-	72.79
WIND		-	369.6 MW	-	-	-	79.94

*Jordanian dinar

The average costs shown in Table 3 are based on NEPOC's 2019 - annual report, which are calculated according to the total amount of energy purchased divided by the total amount of money paid to the respective power plants in 2019 [17]. Generation costs include many factors such as the base costs, capacity costs, daily unit start-up costs, fuel price. RISHA is a special case, where its natural gas is extracted from Jordan; hence it is always maxed out according to the available gas. IPP3 and IPP4 are the most expensive units since they are composed of small and fast starting 15 MW generators that are used in peak demand when sudden and rapid changes in energy demand occur. Renewable energy is under the contract of Take-or-Pay, where unit commitment scheduling and operation aim to utilize all the energy produced. All power plants operate on natural gas as a primary fuel, where heavy and light fuel oils (HFO & LFO) are used as secondary fuels.

The main electrical power sources in Jordan are classified into: Government-owned/ partially owned power plants, Independent Power Plants (IPPs) and the Egyptian interconnection. The government holds 100% of the shares of the Samra Electricity Power Company (SEPCO), being the largest energy producer, while having only 40% of the shares of the Central Electricity Generation Company (CEGCO), being the second-largest energy producer. The different independent power suppliers have different shareholders and private investors such as Mistui, Korea Electric Power Corporation (KEPCO) and Mitsubishi.

2.3. Transmission Sector

In 1996 the Jordanian Electricity Authority was restructured into NEPCO and had the responsibility over the power sector from generation to distribution, and then in 1999, both generation and distribution sectors were privatized[52]. Currently, NEPCO is responsible for the transmission grid, whereby at the end of 2019, the transmission level substation capacity amounted to 15265 MVA with 65 main substations with 1376 circuit kilometers of 400 KV transmission lines and 3764 circuit kilometers of 132 KV transmission lines. Nepco's peak load amounted to 3205 MW and 3380 MW in 2018 and 2019 respectively and is expected to increase by around

2.9% annually. NEPCO also ensures through its National Control Center (NCC) to provide a continuous and reliable supply of electricity linking generation and distribution, by coordinating between all key players in the power sector from different power plants to the MEMR and EMRC[17]. The main responsibilities for NEPCO are[17] [52]:

1. Acting as the system operator of the power system in Jordan and controlling demand-supply balance.
2. Being responsible for constructing, operating, and maintaining substations and transmission lines in the transmission grid.
3. Performing power system research, planning and development.
4. Acting as a single buyer of electricity from power plants and single supplier of electricity to bulk consumer.
5. Securing the fuel for the thermal power plants.
6. Being responsible for the interconnections with neighboring countries such as Egypt and previously Syria.
7. Achieving sustainable development by increasing dependency on local resources and enhancing renewable energy usage.

The following Table shows the expected increase in Electricity Demand and Electrical energy Purchasing by NEPCO from 2020 to 2040[17]:

Table 4 Electrical Demand Forecast in the Transmission sector

Year	Max. Demand*		Electrical Energy Generated**	
	MW	Growth (%)	GWh	Growth (%)
2020	3050	3.0	19850	2.9
2022	3240	3.1	21110	3.1
2025	3535	2.9	23205	3.2
2030	4058	2.8	27011	3.1
2035	4665	2.8	31446	3.1
2040	5360	2.8	36610	3.1

*Summer loads ** Sent-out (purchased)

2.4. *Distribution and end consumers*

The Distribution sector compromising the bulk energy supply is composed of three private distribution companies: Jordan Electric Power Company (JEPCO), Irbid District Electricity Company (IDECO, Jordan north area), and Electricity Distribution Company (EDCO), that distribute energy to consumers in the central, northern and southern parts of Jordan respectively [52]. Besides, two categories of large energy consumers (Principal Consumers), PC1 and PC2, are a part of the bulk energy supply. The Consumption load types and percentages are calculated according to the 2019 NEPCO report, without taking into account the PC1 and PC2, where domestic and governmental consumers reach up to 49.1% of the main energy consumption, where 6% of it accounts for the governmental buildings and 1.5% for others[17]. Table 5 shows the five bulk consumers, which are the main customers of NEPCO, with JEPCO being the largest consumer with 61.26% of peak demand, out of all the bulk

consumers. The bulk supply prices are categorized into: Day energy pricing from 8:00 – 24:00, Night energy pricing from 00:00 – 7:00, and Peak tariff, which depicts the demand capacity cost of the highest hourly electrical demand within the period of peak demand tariff as announced by MEMR in the day with the highest electrical demand as can be seen in Table 6 [55][56][57]. The peak periods are between 5 PM and 9:30 PM, representing the evening peak where the demand is highest throughout the year. The total peak demand of the three distribution companies accounts for almost 96% of the total peak demand in the bulk consumer, which shows there is great potential for the DR system targeting their respective consumers. As previously discussed, domestic and governmental buildings account for almost 49% of their energy consumption.

Table 5 Bulk supply prices and Peak Demand 2019

Bulk Consumers	Bulk Supply Price			Peak Demand (MW)	Peak Demand %
	Day (Fils/kWh)	Night (Fils/kWh)	Peak (JD/kW/ Month)		
JEPCO	71.90	61.88	2.98	2129.9	61.26%
EDCO	74.02	64.07	2.98	580.8	16.70%
IDECO	58.20	48.29	2.98	622.7	17.91%
PC1	237	170	2.98	71.6	2.06%
PC2	124	109	2.98	72.1	2.07%

Table 6 Peak Tariff Periods for 2020

Periods		Period of Peak Demand Tariff
Start	End	
2021-01-01 - 00:00	2021-01-31- 24:00	(17:00 – 20:00)
2021-02-01 - 00:00	Wintertime End 24:00	(17:30 – 20:30)
Summertime starts - 00:00	2021-06-30 - 24:00	(18:30 – 21:30)
2021-07-01 - 00:00	2021-08-15 - 24:00	(18:00 – 21:00)
2021-08-16 - 00:00	2021-09-30 - 24:00	(17:30 – 20:30)
2021-10-01 - 00:00	Summertime End - 24:00	(18:00 – 21:00)
Wintertime starts - 00:00	2021-12-31 - 24:00	(17:00 – 20:00)

Chapter 3: Day-ahead Demand Response modeling

3.1. Day-ahead Demand Response Model

A dynamic price or incentive-based hourly DR is extremely invasive to consumers since they are less likely to have enough time to reschedule their demands well ahead of time and be more stressful for residential consumers. Hence, a day ahead DR model is more appropriate for residential consumers, having enough time to adjust the loads impacting their electricity bills the most, and incentivizing them to increase their efficiency in energy usages, such as optimizing their heating and cooling loads. The proposed DR model in this study is depicted in Figure 11, which is supposed to be implemented by the GO targeting the Residential consumers.
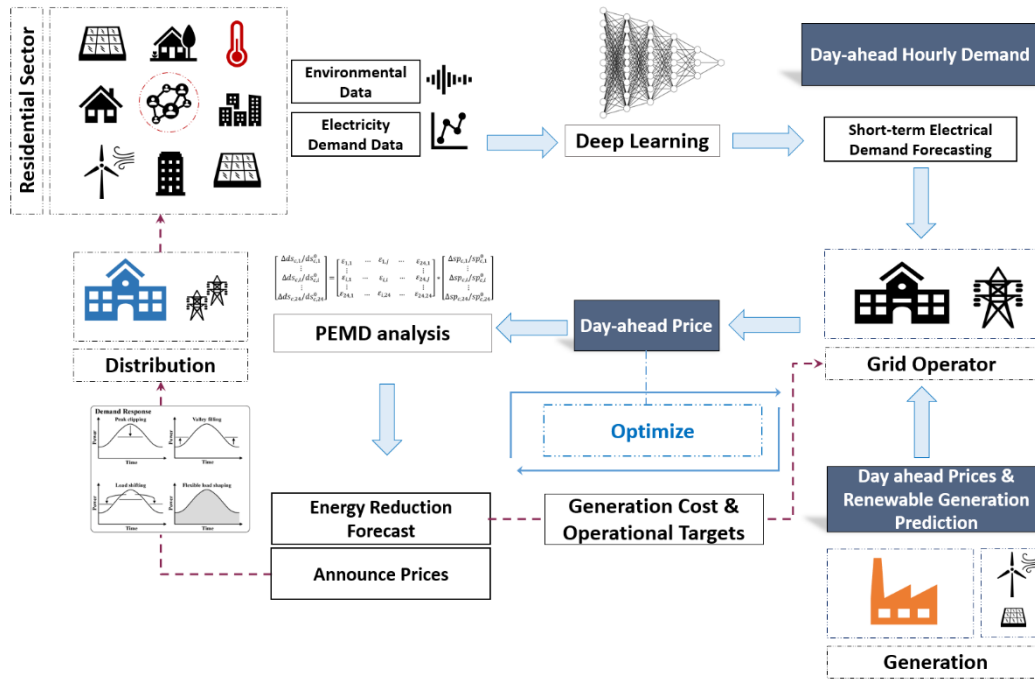
Figure 11 Proposed Day-ahead Demand Response Model for Jordan in this study

Precise day-ahead information on electrical demand, generation availability, generation costs, and the expected amount of renewable energy generated is highly crucial to implementing the DR system [19]. The GO (NEPCO) aims to reduce the cost of energy production, especially at peak periods, to reduce the expensive energy purchased from IPP3 and IPP4, while increasing the demand in off-peak periods to maximize its net profit. The DR system can influence consumer behavior from peak to off-peak and allow the grid higher flexibility acting as a safety margin in cases of high expected demand. NEPCO's main responsibility is to implement a precise day-ahead hourly demand prediction to estimate the demand every hour for the next day. Since the GO, as per grid regulations, provides the fuel for the power plants, the day-ahead cost of energy purchase is correlated to fuel prices known by the GO; therefore, the generation costs are given. Furthermore, the GO utilizes the PEMD to predict the effects of different prices on the residential consumers and decide the best price to achieve the required goals relating to peak demand reduction and off-peak filling by increasing the prices at peak loads and reducing them at off-peak periods. It is noted that the prices are announced to the distribution companies at the start of each

day, where they announce them to their consumers through specially designed schemes.

In this study, it is assumed that the generation schedule is given through unit commitment analysis done by the GO by communicating with the power suppliers, where the renewable energy plants also provide the renewable generation predictions. The profit-seeking maximization model of the GO, considering the Jordanian power grid consumers, excluding the energy exports, can be expressed by:

$$Max \quad \sum_{d=1}^{D}\sum_{h=1}^{H}\left(\sum_{c=1}^{C} I_{c,h}(sp_{c,h}, ds_{c,h}) - \sum_{ps=1}^{PS} C_{ps,h}(bp_{ps,h}, dp_{ps,h})\right) + \sum_{c=1}^{C} PCI_C (dp_c, dpp_c) \tag{1}$$

Subject to:

$$ds_{c,h} = ds_{c,h}^{0}\left[1 + \varepsilon_h \frac{sp_{c,h}-sp_{c,h}^0}{sp_{c,h}^0} + \sum_{\substack{h'=1, \\ h'\neq h}}^{24} \varepsilon_h' \frac{sp_{c,h'}-sp_{c,h'}^0}{sp_{c,h'}^0}\right] \tag{2}$$

$$spp_{c,h,Min} \geq sp_{c,h} \geq spp_{c,h,Max} \tag{3}$$

Where $I_{c,h}$ is the income at hour $h \in \{1,2..24\}$ from the bulk consumer of type $c \in \{1,2,..5\}$, which is a function of bulk supply price ($sp_{c,h}$)and the demand sold ($ds_{c,h}$) at hour h for consumer c. $C_{ps,h}$ is the cost purchasing power from power supplier $ps \in \{1,2,..PS\}$ at hour $h \in \{1,2..24\}$, which is a function of the buying price ($bp_{ps,h}$) estimated by the average prices shown in Table 3, and the demand purchased ($dp_{ps,h}$). At each hour h, all the costs of purchasing demand from each ps depict the total hourly cost depending on which power plants were utilized, according to the unit commitment by the GO. PCI_C is the peak capacity income per consumer c which is a function of the highest demand peak (dp_c) for the respective consumer c and their demand peak price (dpp_c). ps denotes the total power supply units utilized at the respective hour. $spp_{c,h,Min}$ and $spp_{c,h,Max}$ are the upper and lower ranges of the bulk supply price, as determined by the GO.

ε_h and ε_h' represent the self and cross-price elasticities of demand, respectively, where they capture the effect of electricity price change for customers on their electricity consumption. This relationship lies at the heart of DR systems to determine the price set by utilities to achieve economic benefits in the power market and technical benefits related to the operation of the power system [21]. To capture the price elasticity of demand on 24 hours under the assumption that the rescheduling of the production doesn't go beyond a 24-hour interval, the PEDM is formulated as [21][22]:

$$\begin{bmatrix} \Delta ds_{c,1}/ds_{c,1}^0 \\ \vdots \\ \Delta ds_{c,i}/ds_{c,i}^0 \\ \vdots \\ \Delta ds_{c,24}/ds_{c,24}^0 \end{bmatrix} = \begin{bmatrix} \varepsilon_{1,1} & \cdots & \varepsilon_{1,j} & \cdots & \varepsilon_{1,24} \\ \vdots & & & & \vdots \\ \varepsilon_{i,1} & \cdots & \varepsilon_{i,i} & \cdots & \varepsilon_{i,j24} \\ & & & & \vdots \\ \varepsilon_{24,1} & \cdots & \varepsilon_{24,j} & \cdots & \varepsilon_{24,24} \end{bmatrix} * \begin{bmatrix} \Delta sp_{c,1}/sp_{c,1}^0 \\ \vdots \\ \Delta sp_{c,i}/sp_{c,i}^0 \\ \vdots \\ \Delta sp_{c,24}/sp_{c,24}^0 \end{bmatrix} \tag{4}$$

The PEMD relates the effect of the change of price in any hour of the day depicted by i to the change in demand of the hour itself as well as other hours depicted by j. $\varepsilon_{i,i}$ represents the self-elasticity, which relates the change of price in the period i to the change in demand in that period, whereas $\varepsilon_{i,j}$ represents the cross-elasticity, relating the change of demand in hour i to the change in price in another period j, which are shown as ε_h and ε_h' in Eq (2), respectively.

The proposed model was developed under the following assumptions:

1. Daily environmental and residential demand data are available with an hourly sample rate.
2. The day-ahead generation electric power prices are available as a single value for each power plant.
3. The day-ahead selected power plants for dispatch by unit commitment are available for each day.
4. Both self-elasticity and cross elasticities for each hour are known and available for the grid operator each day, where they were assumed constant in this research.
5. The demand response algorithm is run and implemented at 00:00 of the new day, when the final demand hour of the previous day is received, then the new prices are announced up to 24 hours.
6. The response to the change in prices for the residential sector is assumed at the distributer level, where when the distributer receives the new prices, they have their methods of implementing the DR to each different section and types of their consumers by means of having the same effect as if the prices where directly increased for the consumers.

3.2. Price Elasticity of Demand Matrix

The price elasticity of demand in economic theory, as previously mentioned, depicts the relationship between the change in demand relative to the change of price and is formulated as[58]:

$$\varepsilon = \frac{\Delta q/q_o}{\Delta p/p_o} \tag{5}$$

Where ε is the elasticity for a specific time period, q_o is the initial quantity of demand in that period, p_o is the initial price, Δq is the change in demand quantity in relevance to the change in price Δp. Highly Elastic demand is depicted by a large ε where demand is highly sensitive to price. As previously discussed and in order to capture the price elasticity of demand on a 24-hours period, the following equation is used [34][35]:

$$\begin{bmatrix} \Delta q_1/q_{1_o} \\ \vdots \\ \Delta q_i/q_{i_o} \\ \vdots \\ \Delta q_{24}/q_{24_o} \end{bmatrix} = \begin{bmatrix} \varepsilon_{1,1} & \cdots & \varepsilon_{1,j} & \cdots & \varepsilon_{1,24} \\ \vdots & & \vdots & & \vdots \\ \varepsilon_{i,1} & \cdots & \varepsilon_{i,i} & \cdots & \varepsilon_{i,24} \\ \vdots & & \vdots & & \vdots \\ \varepsilon_{24,1} & \cdots & \varepsilon_{24,j} & \cdots & \varepsilon_{24,24} \end{bmatrix} * \begin{bmatrix} \Delta p_1/p_{1_o} \\ \vdots \\ \Delta p_i/p_{i_o} \\ \vdots \\ \Delta p_{24}/p_{24_o} \end{bmatrix} \tag{6}$$

The PEMD relates the effect of the change of price in any hour of the day depicted by i to the hour itself as well as other hours depicted by j. $\varepsilon_{i,i}$ represents the self-elasticity, which relates the change of price in the period i to the change in demand in that period and is described as:

$$\varepsilon_{i,i} = \frac{\Delta q_i/q_{i_o}}{\Delta p_i/p_{i_o}} \tag{7}$$

Whereas $\varepsilon_{i,j}$ represents the cross-elasticity, relating the change of demand in hour i to the change in price in another period j is represented by:

$$\varepsilon_{i,j} = \frac{\Delta q_i/q_{i_o}}{\Delta p_j/p_{j_o}} \tag{8}$$

In the case of a price increase, the self-elasticity is always negative for a given our i and all the respective j elements for that column are negative. Finally, for any given hour i, the total change in demand for that hour is the amount that is shed depicted by the self-elasticity and the amount that gets redistributed to other hours represented by the cross-elasticity and is given by:

$$\frac{\Delta q_i}{q_{i_o}} = \varepsilon_{ii} * \frac{\Delta p_i}{p_{i_o}} + \sum_{\substack{j=1, \\ j \neq i}}^{24} \varepsilon_{ij} * \frac{\Delta p_j}{p_{j_o}} \tag{9}$$

Where Equation 9 is used to predict the electrical demand at a given hour i, given the change in prices and the elasticity matrix elements for the ith column. Finally, by substituting q for d (standing for electrical demand), the electrical demand output from the DR for hour i is predicted by [20]:

$$d_i = d_{o_i} + \varepsilon_{ii} * d_{o_i} * \frac{\Delta p_i}{p_{o_i}} + \sum_{\substack{j=1, \\ j \neq i}}^{24} \varepsilon_{ij} * d_{o_i} * \frac{\Delta p_j}{p_{o_j}} \tag{10}$$

This equation is the basis of equation 2 that was presented in the model discussed in the last section.

3.3. Consumer behavior modeling

The PEMD reflects the consumer response to a DR program represented by the values of self and cross elasticities and their distribution in the PEMD, where different DR policies and consumer response patterns to the price change can impact the estimation of the PEMD. Figure 12 represents the two types of PEMD modeling a day-head DR policy (a) and an hour-ahead DR policy $(b)\&(c)$. In day-ahead DR polices, prices are announced one day earlier or at the start of the day, where consumers can re-schedule their demand for each interval i of the day, hence all elements in the PEMD can be non-zero. Whereas in hour-ahead DR, consumers can only reschedule the price of the next hour, where they only have information on the current price and hour ahead price, hence it is unlikely that they can reschedule their demands ahead of time, making all cross-elasticities above the diagonal zero[34]. Some researchers considered all off-diagonals to be zero in this case [35].

Figure 12 PEMD under Different Policies: (a) Day-ahead DR, (b)&(c) Hour-ahead DR

The PEMD estimation is also correlated to how consumers in different markets reschedule their demands to different hours of the day, represented by the cross elasticities' distribution in the PEMD. Figure 13 shows the

different types of consumer rescheduling, which can be assumed into five different categorical behaviors[58]:
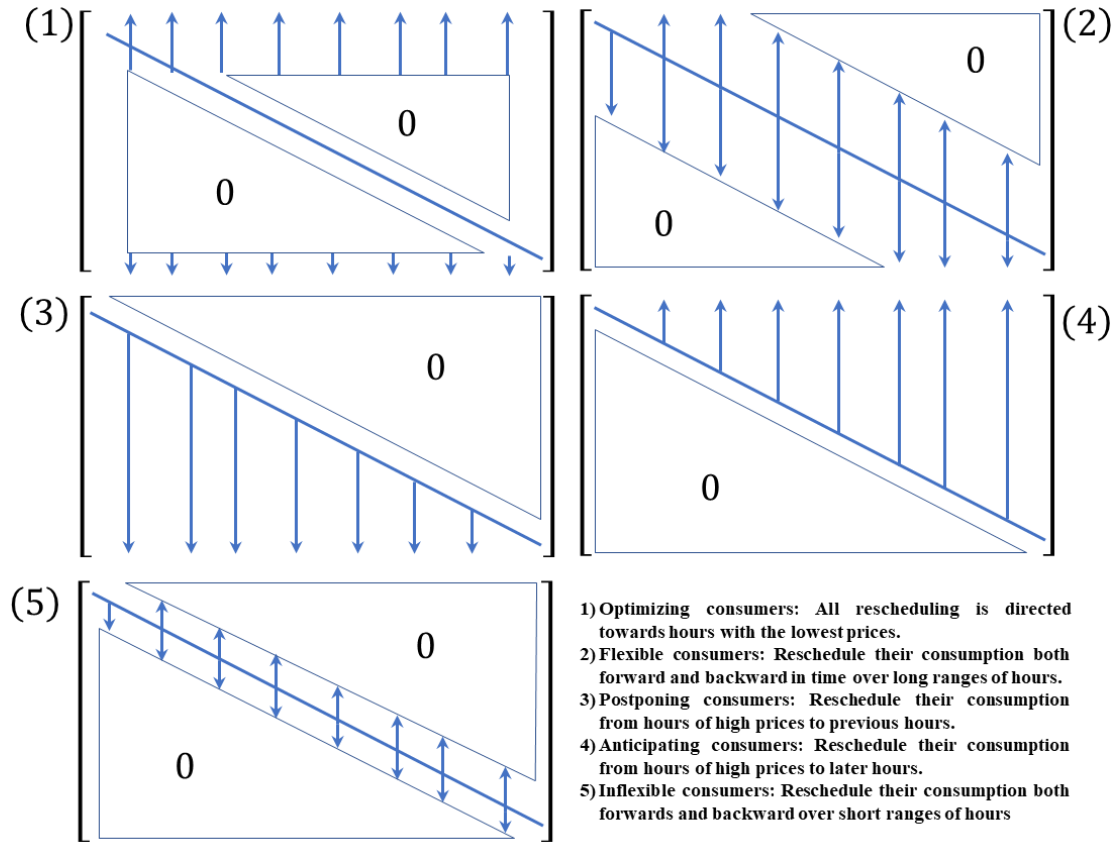
Figure 13 **Different Consumer rescheduling behaviors in DR markets**

The categories of behaviors for day-ahead demand response are (1), (2), and (5), where the last two are the most probable, as it's unlikely that consumers are extremely optimized to fully reschedule their demand to hours of least price. The difference between flexible and inflexible consumers is the time horizon to where demand at a certain hour is rescheduled to other hours of the day, depicted by the arrow lengths in Figure 13. The selection of this horizon is based on a detailed analysis of the types of loads that exist, where water heating, for example, can be shifted to a larger time horizon prior to periods of high demand than other appliances such as lighting [59].

Chapter 4: Deep Neural networks for day-ahead short-term load forecasting

4.1. Machine learning and neural networks

Neural Networks is a machine learning algorithm used for supervised learning, in which the algorithm trains the computer to learn from given data and make future regression predictions or classifications. The name comes from the analogy of neural networks to the human brain since it is constituted of thousands of simple nodes called neurons, each of these neurons are connected in a dense matter, in layers called hidden layers. The data is fed into the neural network in a forward manner called "Forward Propagation" then, the neurons in each layer between the input and output layers receive the transformed data from all connected neurons to its input and sends the data combinations to all neurons connected to its output. Figure 14 represents a general overview of a neural network[36]. Due to the intricate connections and non-linear activations of neural networks, a neural network can model any non-linear function[60].
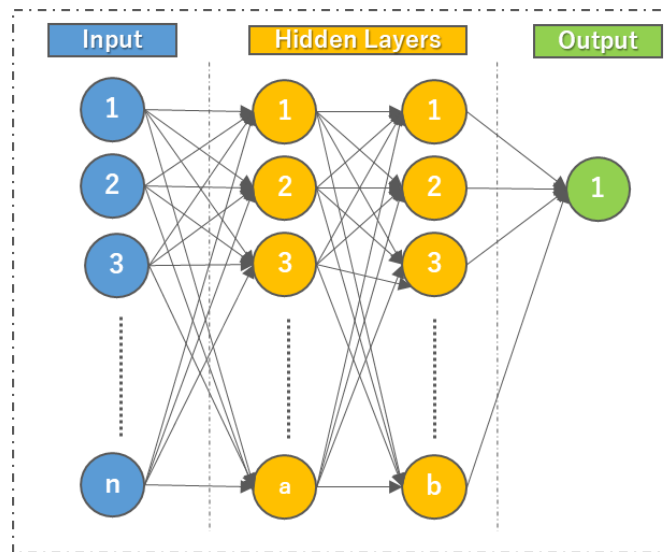
Figure 14 Neural Network Representation

Every vertical layer between the input and output layers is called a hidden layer and consists of several neurons. Every neuron in the hidden layers consists of several inputs, weights, a bias, output, and an activation layer. The biases and weights represent a linear regression, and their output is fed into a non-linear activation function.

4.2. Neuron Network modeling

Neurons are the building blocks of a neural network, as shown in Figure 15 [61]. A single neuron consists of wights and biases as well as an activation/transformation function that maps the input of the neuron to its output. A single neuron is very similar to a logistic regression, where a linear model is fed into a non-linear transformation such as the sigmoid function, which intern limits the outputs and transforms it into a probability metric bound between 0 and 1.
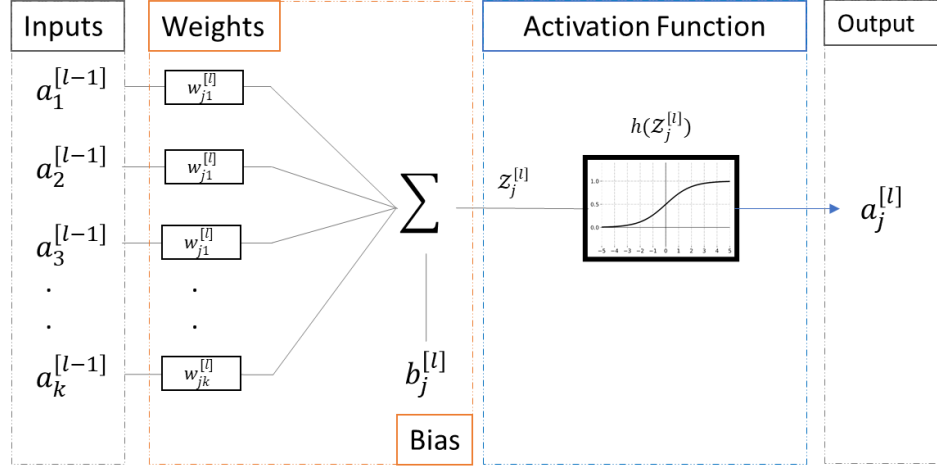
Figure 15 A Single Neuron

The following equations govern the mathematical representation of a neuron with a sigmoid activation in vector notation:

$$Z_j^{[l]} = w_j^{[l]^T} * x^{(i)} + b_j^{[l]} \tag{11}$$

$$Sigmoid: g(Z) = \frac{1}{1 + e^{-Z}} \tag{12}$$

Equation 11 represents the output of the neuron j in the hidden layer l, where w is the weight vector of that neuron, b is the bias and $x^{(i)}$ is the ith training example from the input layer. Equation 12 represents the activation function, which is called the Sigmoid function, as shown in Figure 15. The General formula for the output of each neuron in a certain layer is depicted as follows with a non-vector notation:

$$a_j^{[l]} = g^{[l]} \left(\sum_k w_{jk}^{[l]} a_k^{[l-1]} + b_j^{[l]} \right) = g^{[l]} \left(z_j^{[l]} \right) \tag{13}$$

Where $a_j^{[l]}$ is the activation (Output) of the jth neuron in layer l , $g^{[l]}$ is the activation of the neuron in that layer, $a_k^{[l-1]}$ is the kth input to that neuron from the previous layer. $b_j^{[l]}$ is the bias of the jth neuron in layer l. $w_{jk}^{[l]}$ is the kth weight in the jth neuron in layer l.

4.3. Activation Functions

Activation functions introduce a form of non-linearity to the model and apply a transformation to the inputs of the neurons and decide the activation level of each neuron, wherein the case of the sigmoid function, the output is bound between 0 and 1 as if deciding if the neuron is turned on or off. The choice of activation function greatly affects the performance of training the network, where each function has different characteristics related to the non-linear regions it has, region boundary, and the computational costs of the function and its derivation. Each function has different mathematical properties related to approximation and optimization theory[62]. The following Table 7 shows some of the popular activation functions currently in use and their comparison based on [63]:

Table 7 Activation Functions and their comparison
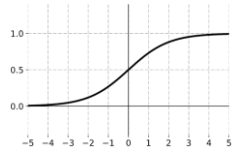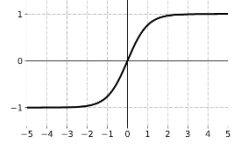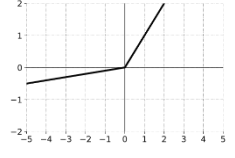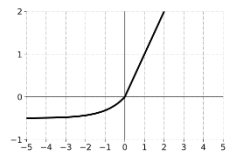
Name	Equation	Derivative	Shape	Advantages	Dis-Advantages
Sigmoid	$g(z) = \left(\dfrac{1}{(1+e^{-z})}\right)$	$g'(z) = g(z)(1-g(z))$		▪Easy to understand. ▪Mostly Utilized in shallow networks. ▪Used as output layer for classification. [64]	▪Slow Convergence ▪Non-Zero-centered output. ▪Gradient Saturation ▪Sharp Damp Gradient during backpropagation ▪Vanishing Gradients [63]
Tanh (Hyperbolic Tangent)	$g(z) = \dfrac{e^z - e^{-z}}{e^z + e^{-z}}$	$g'(z) = 1 - g(z)^2$		▪Zero centered output ▪Enhanced backpropagation ▪Better performance of Sigmoid [63][65]	▪Vanishing Gradients ▪Achieves a Gradient of 1 only at 0 input. [63]
Relu (Rectified Linear Unit)	$g(z) = \max(0,z)$ $= \begin{cases} z, & \text{if } z \geq 0 \\ 0, & \text{if } z < 0 \end{cases}$	$g'(z) = \begin{cases} 1, & \text{if } z \geq 0 \\ 0, & \text{if } z < 0 \end{cases}$		▪Most widely used [66] ▪Fast Convergence [28] ▪Better performance and generalization over sigmoid and tanh [67] ▪Has linear characteristics. No Exponentials or Divisions[68].	▪Can Overfit easily in comparison to Sigmoid [69] ▪Dead neurons in the negative input region, because the gradient in that region is zero and the parameters do not get updated [68].
Leaky Relu	$g(z) = \begin{cases} az & \text{for } z \leq 0 \\ z & \text{for } z > 0 \end{cases}$	$g'(z) = \begin{cases} 1, & \text{if } z \geq 0 \\ a, & \text{if } z < 0 \end{cases}$ $a \sim 0.01$		▪Solves the dying neurons problems by introducing a non-zero gradient in the negative region and having Better Sparsity [70]	▪It is comparable to the Relu, except having non-zero gradients over the entire duration.
Elu (Exponential Linear Unit)	$g(z)$ $= \begin{cases} z, & \text{if } z > 0 \\ \alpha(e^z - 1), & \text{if } z \leq 0 \end{cases}$	$g'(z) = \begin{cases} 1, & \text{if } z \geq 0 \\ g(z) + a, & \text{if } z < 0 \end{cases}$		▪Avoids dying neuron. ▪The saturation plateau in the negative region allows for more enhanced learning of robust representations. ▪Faster learning and better generalization. ▪Better Sparsity. [71]	Values are not centered around zero, although it is closer than the Relu towards that. [72]

Table 7 introduces popular activation functions, showing their equations, derivatives, shapes, and both advantages and disadvantages. The learning process in a network is composed of millions of mathematical

operations, which is a computationally demanding task. Hence, the choice of activation functions and their computational and mathematical complexities is an important factor for achieving optimum results. According to research, the Rectified Linear Unit is one of the most popular activation functions currently in use due to its higher speed of converging. According to research, it has been said to train six times faster than the tanh function[73]. Each of the activation functions gives different characteristics to the model; both the tanh and the sigmoid functions are much slower to converge when using gradient descent due to their nonlinear saturation regions with a very low slope. The activation of the output layer depends on the type of prediction, in regression we can emit the final activation or use Relu for only positive output values, but for binary classification problems, the Sigmoid function since is used and in the case of multi-class classification, the soft-max activation is used. Finally, the Elu function is used in the research as it is an improved version of the high-performing Relu function.

4.4. Optimization algorithms

After setting up a neural network, the main objective is to update all the weights and biases in the hidden and output layer in a way that increases the prediction accuracy of the model. Initially, all the weights should be set randomly and not initialized to zero. Then the weights are updated with the following steps:

1. Input the training data into the network and propagate it to the output layer.
2. Calculate the error between the predicted value and the ground-truth/real value.
3. Back propagate the loss through the network to obtain the gradients.
4. Use the gradients to update the weights of the network.

First, the cost function allows the calculation of the error between the predicted and real value. The mean squared error cost function is used for regression problems and is as followed:

$$Cost: J_{mse}(\hat{y}, y) = \frac{1}{m} \sum_{i=0}^{m} (\hat{y}^{(i)} - y^{(i)})^2 \tag{14}$$

$J_{mse}(\hat{y}, y)$ is the summation of the mean square errors across all training data samples, $where$ $\hat{y}^{(i)}$ is the prediction value and $y^{(i)}$ is the real output, m is the number of training examples. There are different types of cost functions depending on the type of output being regression or classification. Regression problems utilize the MSE function due to its derivation characteristics for the backpropagation. Classification problems utilize the cross-entropy cost function.

$$J(\theta)_{min} = min\{Cost: J_{mse}(\hat{y}, y)\} \tag{15}$$

The goal is to minimize the cost function $J(\theta)$. θ represents the weights and biases of the model, where the Cost function depends on them. Equation 14 represents the Mean Squared Error (MSE) cost function that is used for regression models. The total error calculated is used to measure the performance of the training process at each iteration and its derivation is fed back with backward propagation where the parameters (θ)s of the model representing the weights and biases are updated using gradient descent:

$$\theta_{t+1} = \theta_t - \eta \cdot \nabla_{\theta_t} J(\theta_t), \tag{16}$$

In the above Equation, each weight θ_t at training step, t is updated by calculating the partial derivative $\nabla_{\theta_t} J(\theta_t)$ of the error function $J(\theta_t)$ relative to each parameter θ_t in the network using the chain rule. η denotes the learning rate and determines the speed of gradient descent, where choosing a very big value might cause the model not to converge towards the global minimum or too low a value slows down the learning process. By iterating with forwarding and backward propagation, the parameters of the model are updated in a way that drives the error down until it reaches the required error rate. Then the model can be used for the specified task it is designed for.

As mentioned previously, back-propagation is a gradient descent algorithm that updates the parameters of the model to decrease the error "Cost Function". There are many variations to the application of gradient descent, with the most prominent version called Adam. To have fast and more efficient convergence towards the global minimum in any given network, certain improvements are added to Equation (16), including moving average to the updates, decreasing oscillations in the search space, reducing descent time, and computational time resources. The following Table 8 shows three of the most popular algorithms in use today[74]:

Table 8 Popular optimization algorithms for Neural Networks

Name	Modified gradients	Update Rule	Parameters
Momentum [75]	$v_t = \gamma v_{t-1} + \eta \cdot g_t$	$\theta_{t+1} = \theta_t - v_t$	$\gamma = 0.9$ $\eta = Learning\ Rate$
RMSprop [76]	$E[g^2]_t = \gamma E[g^2]_{t-1} + (1-\gamma)g_t^2$	$\theta_{t+1} = \theta_t - \dfrac{\eta}{\sqrt{E[g^2]_t + \epsilon}} g_t$	$\eta = learning\ rate$ $\gamma = 0.9$ $\varepsilon = 10^{-8}$
Adaptive Moment Estimation **Adam** [77]	$m_t = \beta_1 m_{t-1} + (1-\beta_1)g_t$ $v_t = \beta_2 v_{t-1} + (1-\beta_2)g_t^2$ $\widehat{m}_t = \frac{m_t}{1-\beta_1^t}, \hat{v}_t = \frac{v_t}{1-\beta_2^t}$	$\theta_{t+1} = \theta_t - \dfrac{\eta}{\sqrt{\hat{v}_t} + \epsilon} \widehat{m}_t$	$\eta = learning\ rate$ $\beta_1 = 0.9$ $\beta_2 = 0.999$ $\varepsilon = 10^{-8}$

where g_t is the gradient of the objective function relative to the parameter θ_i to be updated at time step t where $g_{t,i}$ is represented as[74]:

$$g_{t,i} = \nabla_{\theta_t} J(\theta_{t,i}) \tag{17}$$

$E[g^2]_t$ abbreviated as m_t in Adam, represents the running average at time step t, which is a function of the previous running average $\gamma E[g^2]_{t-1}$ and the current gradient g_t. β_1 represents the γ parameter of Momentum, while β_2 represents the γ parameter of RMSprop. As can be seen, Adam is a combination of both RMSprop and Momentum, leading to its high performance in practice compared to similar adaptive learning methods[74].

4.5. Performance Metrics

In order to measure the performance of the prediction model, different performance indicators are used. The following three equations representing the Mean Absolute Error(MAE), Mean Squared Error(MSE), the R^2 error and (Mean Percentage Absolute Error) MAPE will be used to evaluate the performance of the neural network model[78][79]:

Table 9 Error Metrics for measuring prediction performance

Metric	Type	Equation	Characteristics
MAE	Scale Dependent	$\frac{1}{m}\sum_{i=1}^{m}\|y_i - \hat{y}_i\|$	• The absolute term avoids mutual cancelation between positive and negative errors. • Skewness cannot be determined
RMSE	Scale Dependent	$\sqrt{\frac{1}{m}\sum_{i=1}^{m}(y_i - \hat{y}_i)^2}$	• Avoids mutual cancelation between positive and negative errors. • Large errors and outliers are penalized more, and small errors less.
MAPE	Percentage Based	$\frac{1}{m}\sum_{t=1}^{n}\|\frac{y_i - \hat{y}_i}{y_i}\|$	• Dimensionless and can be compared across different data sets. • Must be used with caution when y_i is close to 0.
R2	Percentage Based	$1 - \frac{\sum_{i=1}^{m}(y_i - \hat{y}_i)^2}{\sum_{i=1}^{m}(y_i - \bar{y})^2}$	• Bound between 0 and 1 (Higher is better) • Judges how well the model fits the Data.

Where y_i is the real value for input i, $\hat{y}_i$ is the predicted value, m is the number of training input vectors (Observations). $\bar{y}$ is the mean of the real values y_i. The Mean Absolute error can clearly indicate the average error in relation to the real values. The MAPE metric is the main performance indicators used to comparing model performance across different studies with data having different scales time series regression analysis. The final model performance is compared across all the data splits mentioned using the mean absolute percentage error (MAPE), and the root means square error (RMSE) [80].

4.6. *Improving generalization and avoiding overfitting/High Variance: Dropout, Regularization, and early stopping*

Deep neural networks can have a large number of parameters to learn and adapt to the training data, although one of the major problems concerned is overfitting the network to the training data where the model becomes characterized with high variance, with high performance on the training data and the noise that comes with it, while achieving less performance on the validation and test sets[81]. The following techniques are used to overcome the challenge of achieving good generalization of the network on data it has never been trained on.

4.6.1. Dropout

Dropout is a technique presented by [82] where it turns off neurons in selected layers with a certain probability in order to reduce the overfitting of the model. At each training epoch, each layer turns off neurons randomly with a certain probability between 0 and 1. This helps in reducing overfitting and noise or outlier overfitting while training the model on the training data. Although, this is not used during validation or testing data. Dropout is applied to each layer separately and does not need to be applied to every layer. The percentages seen in Figure 16 represent the assigned dropout probability each neuron has in a specific layer. The algorithm is presented in the following figure:
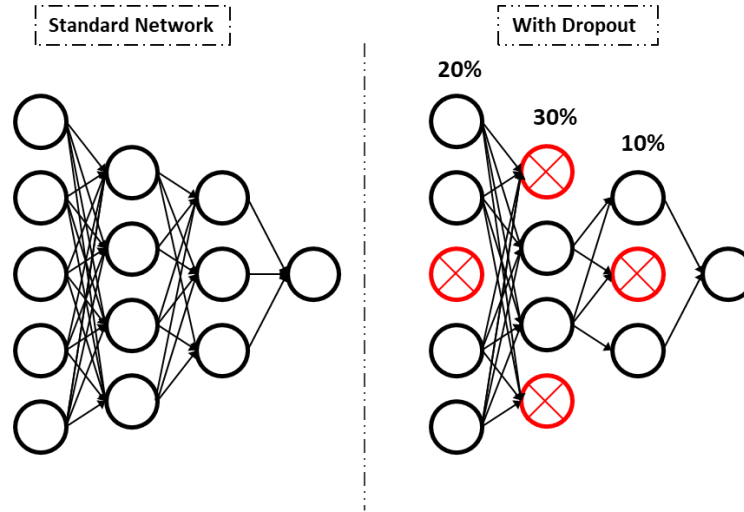
Figure 16 Dropout

4.6.2. Ridge Regression ($l2$ Regularization) and Lasso Regression ($l1$ Regularization)

Ridge Regression ($l2$ Regularization) and Lasso Regression ($l1$ Regularization) are referred to as shrinkage methods in statistical theory [81] and are represented as follows:

$$J(\theta) = \frac{1}{m}\sum_{i=1}^{m}(h_\theta(x^{(i)}) - y^{(i)})^2 + \frac{\lambda}{m}\sum|\theta| \tag{18}$$

$$J(\theta) = \frac{1}{m}\sum_{i=1}^{m}(h_\theta(x^{(i)}) - y^{(i)})^2 + \frac{\lambda}{m}\sum\theta^2 \tag{19}$$

$\sum|\theta|$ is the sum of all the absolute weights in the neural network and equation 18 represents the ridge

regression, while equation 19 represents the Lasso regression with the difference of taking the square of every weight then summing them. λ is complexity or hyper parameter that controls the amount of penalty for large coefficients in the model. These regressions add a value to the original $J(\theta)$ in equation (5) that is used to reduce the variance problem of the model overfitting to the training data, the noise and outliers that can come with it.

4.6.3. Early stopping:

The Back propagation algorithm is an optimization algorithm that searches for the best weights and biases within every neuron to achieve the least error possible, although, with every iteration of the back propagation, two main scenarios can occur: (1) on a macro level, the training can start to overfit the training data and diverge on the validation/development data. (2) on a micro level, the error oscillates a lot, even in regions with the lowest error. Hence, early stopping is a technique used to stop the training of the neural network at the best training iteration, avoiding the region of divergence between validation and training errors as well as finding the least error iteration/epoch that achieves the best generalization possible depicted by the validation data set[83]. Figure 17 illustrates early stopping on a macro-level perspective, while the latter will be discussed later.
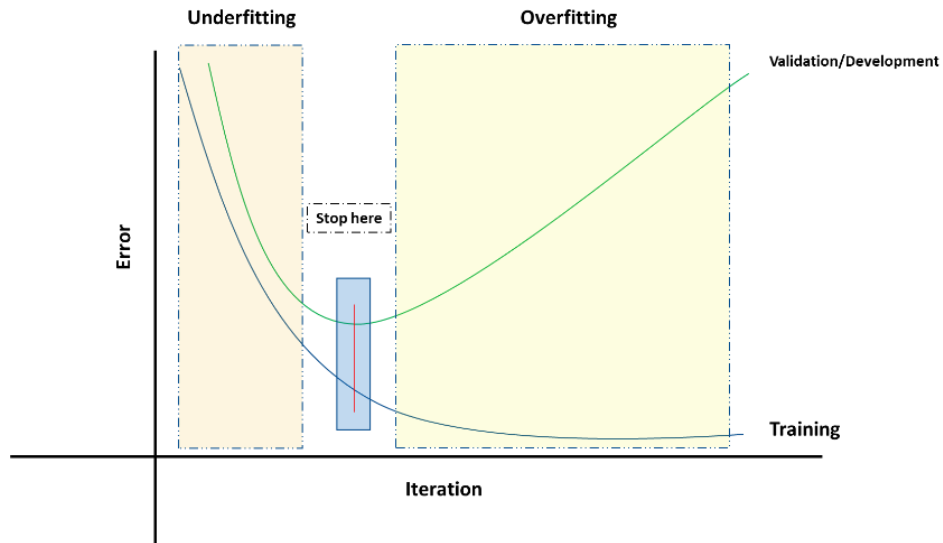
Figure 17 Early Stopping

4.7. Feature Selection Methodologies

Feature selection is one of the essential steps to building a high-performing machine learning predictor, as well as selected and designed features improves the performance of the prediction algorithm, reduces its training and run time, and makes it more cost-effective [84]. Although, there are many advanced techniques and methods used for selecting the best features for a machine learning algorithm, this subsection introduces the methods used in this research. Machine learning algorithms are bound by the data available that correlates to the target variable to be predicted; hence, the best subset should be selected out of the potential available variables.

4.7.1.   Physical relation and expert domain knowledge

A deep understanding of the physical relation between variables and deep knowledge in the field being studied, can affirm the need to use a certain variable in the prediction model. For example, in energy demand, meteorological data has been found to be of most importance as independent variables where they carry essential information for the predictions related to energy demand. This is due to their direct physical and phycological impact on energy consumption behavior[85].

4.7.2.   Correlation metrics and the Pearson Correlation Coefficient

Many statistical methods are used to determine the correlation and covariance between two variables. These methods do not explicitly measure or claim the causal relationship between variables but shed insights on the direction of change of one variable in relation to the other. Correlation measures the monotonic relation between two variables; this relationship describes whether the increase in one variable is accompanied by an increase or decrease in the other, where there is a relationship governing the change in magnitude of both variables. A positive correlation means that when one variable has high values, the other tends to also have high values. A negative correlation is one where a higher value in one variable is associated with lower values in the other. The Pearson Correlation coefficient is a common and widely used index that measures the linear correlation between two continuous random variables[86]. Assuming Y is the predicted continues variable and X_i is the predictor variable i, the Pearson correlation coefficient is defined as[84]:

$$\mathcal{R}(i) = \frac{\text{cov}(X_i, Y)}{\sqrt{\text{var}(X_i)\text{var}(Y)}} \tag{20}$$

Where cov represents the covariance between the two variables and var represents the variance of each variable. The estimate of $\mathcal{R}(i)$ is given by the following equation[84]:

$$R(i) = \frac{\sum_{k=1}^{m} (x_{k,i} - \overline{x_i})(y_k - \bar{y})}{\sqrt{\sum_{k=1}^{m} (x_{k,i} - \overline{x_i})^2 \sum_{k=1}^{m} (y_k - \bar{y})^2}} \tag{21}$$

Where $R(i)$ *is the* Pearson Correlation coefficient between the predicted variable y and the predictor variable x_i. m represents the number of samples, $\overline{x_i}$ and $\bar{y}$ represent the mean of the values of the variable x_i and target variable y respectively. The difference between the Person correlation coefficient and covariance is that it is a dimensionless measure of covariance bound by the range of [-1,1], where 1 represents the highest positive linear correlation and -1 the highest negative linear correlation. On the other hand, covariance depends on the measurement scale of the selected variables and its value cannot be easily interpreted in a relative sense to rank different features[84].

4.7.3.   Sensitivity analysis

Machine Learning methods are black-box methods, where their performance highly depends on the available data and variables that correlate to the target variable. Correlation metrics, physical and logical inferences on the relationship between different variables might not fully justify the inclusion of a particular feature, where correlation does not imply causation [79], and the inclusion of parameters that are in themselves corelated can cause causation multicollinearity, which can lead to redundancy. Perfectly

corelated variables can be redundant where they offer no additional information to the model, although a very high correlation can cause variable complementarity. Adding to the previous points, a variable that is insignificant on its own can lead to increasing the prediction performance when added to other variables. The same is said when two variables are insignificant on their own can be useful together[84]. Hence, taking a different subset of the target features in question and training multiple models then evaluating the effect of adding each feature is a method that can be used to discover useful and redundant features. This method is considered a brute force method, where if there are x number of variables there are 2^x different combinations. For the case of this research, we test different feature combinations as shown in the following Figure 18.
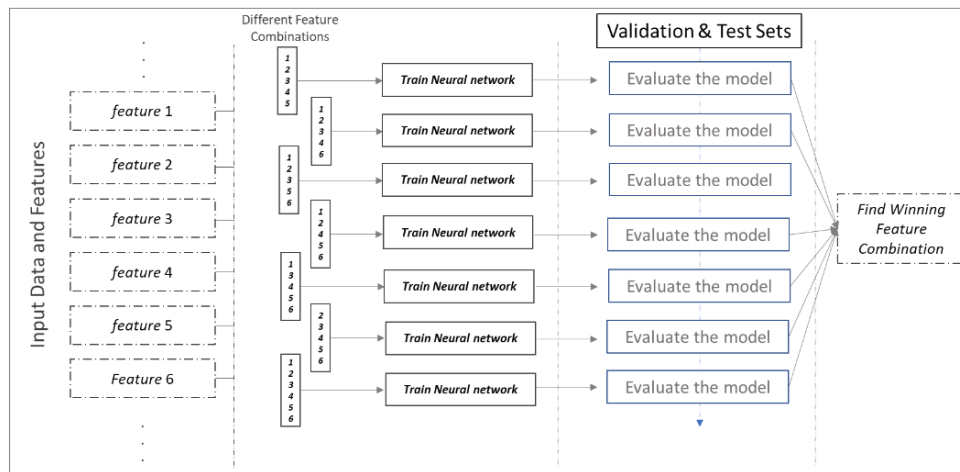
Figure 18 Sensitivity Analysis for feature Selection

Chapter 5: Day-ahead Short-term Load forecasting Results

5.1. Jordan's electrical demand data analysis

In this study, the 4-years hourly electrical demand of NEPCO between 2016 and 2019 is used to train the deep learning model to predict the day-ahead hourly STLF for the Jordanian power grid, which is shown in Figure 19. It can be observed that, the highest peaks out of all the years happened in 2019, reaching 3380 MW in winter. It is due to the increase in urbanization, growth in population, as well as the rise in penetration of different types of electrical appliances to households, while for the same year, the lowest demand was recorded at 1195 MW in spring.
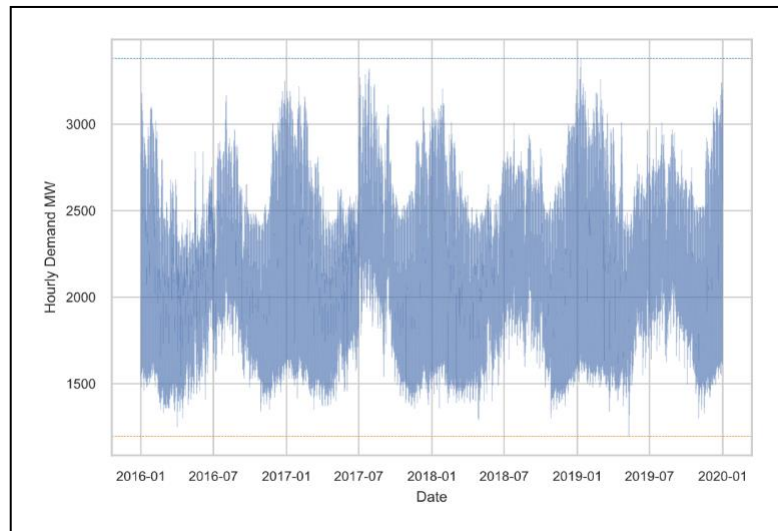
Figure 19 Yearly variation in Jordan's Electrical Demand
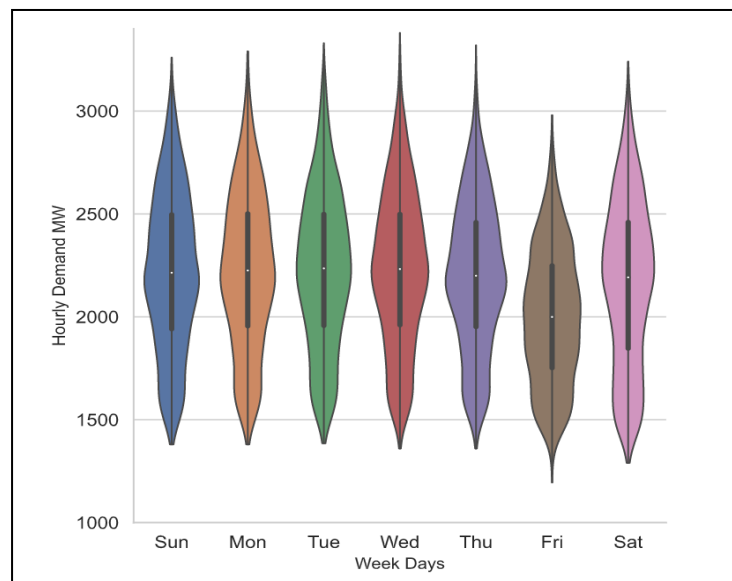
Figure 20 Weekly variation electrical demand, 2016-2019

The electrical demand is a highly complex time series that is a function of human daily and seasonal behaviors and weather conditions, making it heterogeneous and uncertain. In Figure 20, the weekly variation of the electrical demand is represented by the probability density distribution for different days of the week. An apparent increase in peak demand occurs from Saturday through Wednesday, then declining towards Friday, where Friday and Saturday represent the weekend holidays. As previously shown in Figure 5, the daily demand is also affected by the hour of the day, where the peak demand occurred for that specific day at 6 PM, while the lowest occurred at 4 AM. Hence, time-series features such as an hour of the day, day of the week, as well the day of the year carry essential information for the STLF[87]. In Figure 21, and for each quarter of the year (Q1-Q4), where Q1 represents the first 3 months starting from January, the variation of hourly demand with the temperature change is shown. Electrical demand peaks at winter (end of Q4 – Q1) and summer (end of Q2 – Q3) temperatures, as consumers are more likely to use space heating and cooling. On days characterized with thermal comfort between 20 and 30 ℃, the average demand is lower. The curves on top and to the right of the figure show the probability density distribution for demand and temperatures per quarter. The third quarter depicting two thirds of the summer season had the highest demands on average.
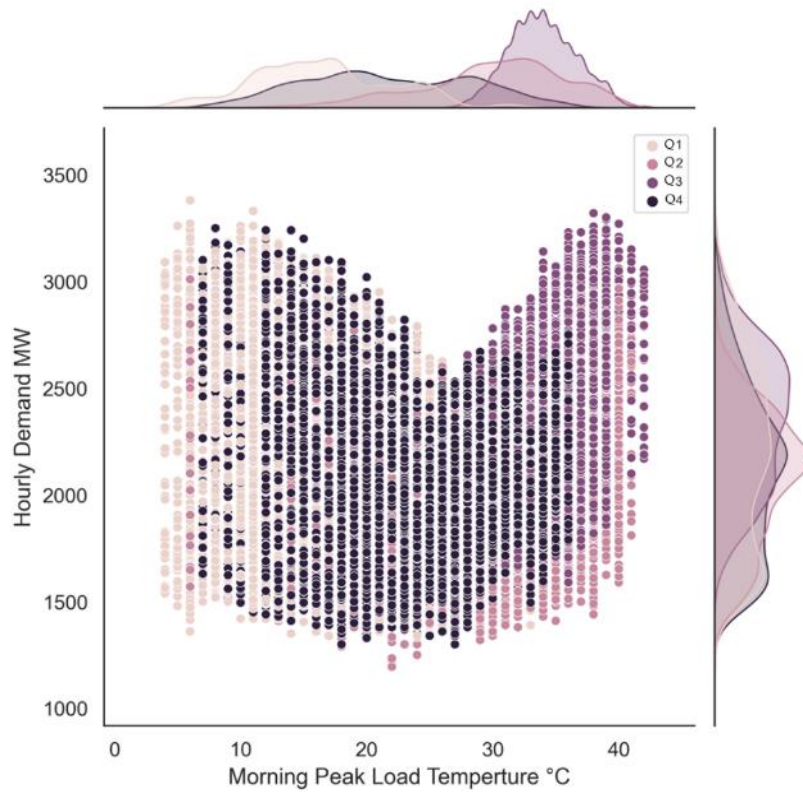
Figure 21 Demand vs. Morning Peak Load Temperatures, 2016-2019

Finally, the autocorrelation analysis represents the correlation of the demand at a certain hour to its lagged values shown in Figure 22, indicating which previous hours of the demand hold the highest correlation to be used as predictive features in STLF[23][60].
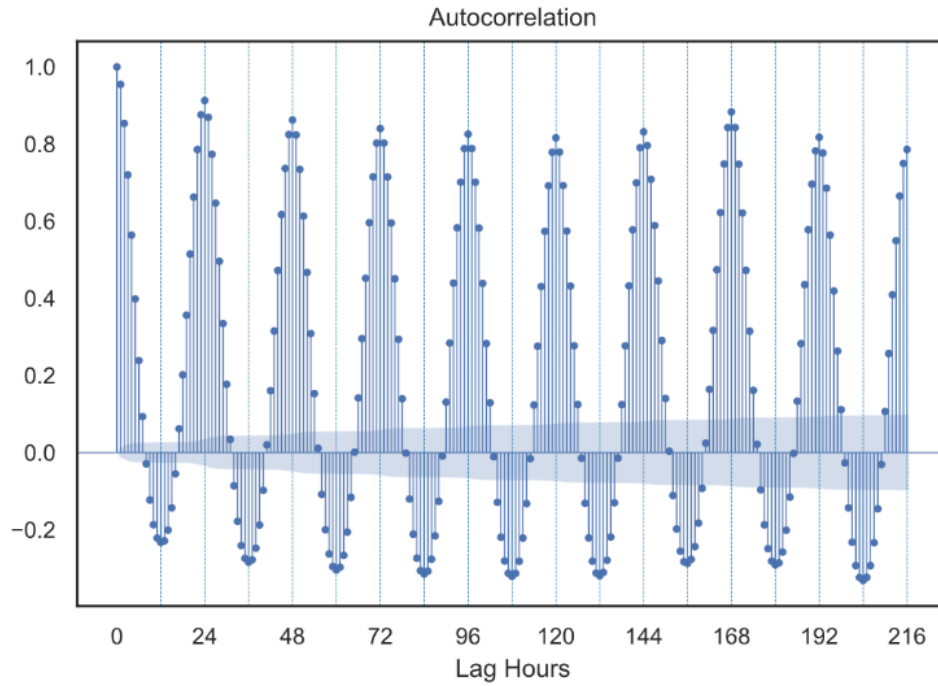
Figure 22 Autocorrelation of the electrical time-series signal with previous hours

Lagged demands at (-1, -24, -168, -48) hours showed the highest correlation, respectively, representing the demand at the same hour in the previous two days in the current week and the same day in the prior week. Table 10 illustrates the exogenous features related to demand at the hour to be predicted. The endogenous features related to the demand at previous hours of the week are given in Table 11.

Table 10 Exogenous input features related to demand at the hour to be predicted

No.	Exogenous Input Features	Range
1	Morning Peak-Load Time Temperature °C	4 - 42
2	Evening Peak-Load Time Temperature °C	2 - 37
3	Minimum Load-Time Temperature °C	-1 - 34
4	Hour of the day	1 - 24
5	Day of the Year	1 - 366
6	Week of the Year	1- 53
7	Normal Day	[0,1]
8	National Holiday	[0,1]
9	Ramadan	[0,1]
10	Sunday	[0,1]
.	.	[0,1]
16	Saturday	[0,1]

Table 11 Endogenous input features related to the demand at previous hours of the week

No.	Endogenous Input Features	Range
1	lagged Demand (-24 hours)	1195 - 3380
2	lagged Demand (-25 hours)	1195 - 3380
3	lagged Demand (-26 hours)	1195 - 3380
4	lagged Demand (-48 hours)	1195 - 3380
5	lagged Demand (-49hours)	1195 - 3380
6	lagged Demand (-50 hours)	1195 - 3380
7	lagged Demand (-168 hours)	1195 - 3380
8	lagged Demand (-169 hours)	1195 - 3380
9	lagged Demand (-170 hours)	1195 - 3380
10	lagged Demand (-192 hours)	1195 - 3380
11	lagged Demand (-193hours)	1195 - 3380
12	lagged Demand (-194hours)	1195 - 3380

In the above tables, the first three features are assumed to be collected from day-ahead weather predictions at the times of the expected morning, evening, and minimum peak times of the day where the demand is to be predicted. Features 4 to 16 represent the time series features, specifying the hour of the day, day of the week, day of the year, week of the year, and whether the day is a national holiday, the month of Ramadan, or a typical day[36], [87]. The lagged demand features were selected according to the autocorrelation analysis, where [36] considered the previous two days only, which can make a problem when weekends are involved as discussed by [87], hence, the same day and its previous day from the last week were used as inputs to the model.

5.2. *Deep learning model's training and optimization results*

The training and tunning process for the proposed deep neural network model used in this study depicted in Figure 24, is used to predict the day-ahead 24-hour demands. The model predicts the day-ahead demand at a specific hour h starting from the end of the previous day; the model is run 24 times to predict the next day's hourly demand hour by hour. The 4-year hourly demand dataset was split into 90% training data to train the model, 5% validation data to tune the hyperparameters and select the best architecture, and 5% testing data coupled with the last month of 2019 used as a final test of the model's generalization performance. Achieving high prediction accuracy is essential for the DR model and is achieved through careful feature selection coupled with selecting an optimal neural network architecture.
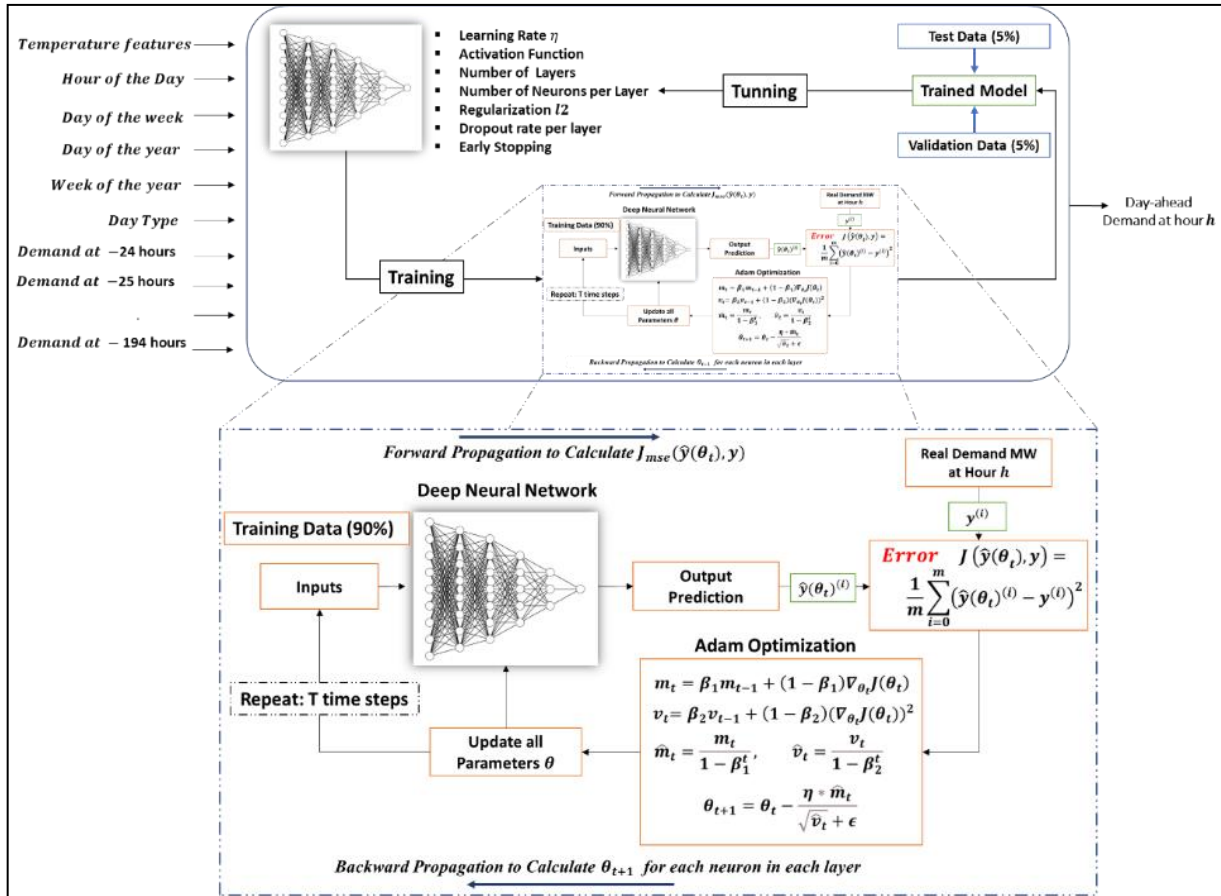
Figure 23 Tuning and Training of the Day-ahead Deep Learning model for demand prediction at hour h

Before the features are input into the model, the non-categorical features were normalized using Z-Scoring:

$$z_{norm}^{(i)} = \frac{z^{(i)} - \mu}{\sqrt{\sigma^2 + \varepsilon}} \tag{16}$$

Where $z_{norm}^{(i)}$ is the normalized data sample for one feature, $z^{(i)}$ is the sample point to be normalized, μ is the mean of that feature samples, σ^2 is the variance of the feature samples, and ε is used to avoid division by zero. Normalizing Data accelerates the Gradient descent learning rate, where the different scales of features can make certain weights and parameters update faster than others, making the gradient descent slower to converge to lower errors. An important notice is that for each feature set, the mean and variance are computed from the training data and are also used to normalize all the dataset splits.

A sensitivity analysis was used to select the final model's hidden layers' (referred to as HL) configuration shown in Table 12:

Table 12 Final Deep Neural Network Architecture

Layers	HL-1	HL-2	HL-3	HL-4	Output-L
#Neurons	1024	512	256	128	1
Activation	elu	elu	elu	elu	-
Dropout Probability	0.1	0.1	0	0	-
$l2$ paramater	0.18	0.18	0.18	0.18	-

The architecture starts with a high number of neurons, then descends to lower numbers, which aligns with recent works such as [85], and the elu activation function showed slightly higher performance than the relu activation function. Dropouts were only applied to the first two layers, which showed better performance in combination with $l2$ regularization. Table 13 shows the final performance results for the training, validation, and testing data.

Table 13 Final Deep learning model results on Training, Validation and Testing Data

Data	MAPE%	RMSE	R2
Training	1.205%	31.17	0.9932
Validation	1.365%	38.39	0.9897
Testing	1.411%	43.18	0.9871

The MAPE error for the test data achieved a 1.411% error, just above the validation and training error; hence, the model achieves good generalization and high accuracy. Finally, the predictions of the last month of 2019, which is the final test of the model as it was not used to train the model, similar to the validation and testing data, are shown in Figure 24. The final model prediction results achieved a MAPE error just above the testing data at 2.03% since it is the hardest to predict at the end of the training period. This shows the importance of the continuous training of the model every day when new data is acquired to sustain high accuracy and generalization. Most of the high errors depicted by the lower part of Figure 24 occur from 8 AM to 12 PM. As will be discussed later, improved prediction models should focus on this period of the day for improvement.
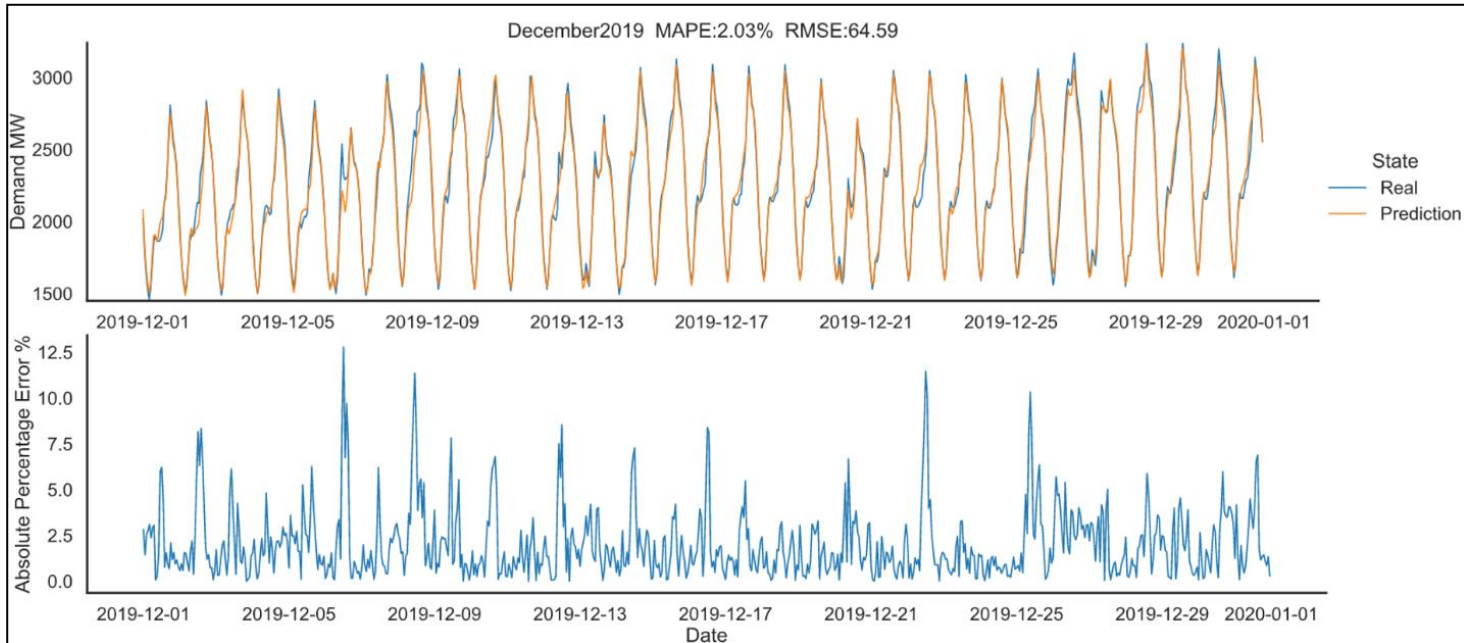
Figure 24 December-2019 prediction results

To better investigate the occurrence of high errors in the proposed prediction in Figure 24, Figure 25 depicts the hourly Absolute Percentage Error for each day in December 2019, where each day has been labeled according

to its weather description as observed in NEPCO's data. First, the relatively high errors can occur between 8:00 and 17:00, with the largest errors being mainly in the range of 10:00 to 13:00 around noon time. High prediction errors can occur for many reasons that cause an abnormal change in consumer behavior or affect the production of PV energy on distribution levels. It can be observed in the figure that rainy days such as the 6th,8th, and 9th of December had very high errors during noon, this can be related to more people staying in the door as well as a reduction in distribution and consumer level PV production that the grid operator sees as a sudden increase in electrical demand as was observed in Figure 13. Cloudy days, depending on the area of cloud coverage in Jordan and the time of cloud coverage, can also disrupt PV generation, as can be seen in both the 2nd and 10th of December from 11:00 to 17:00. On the 25th, the Christmas holidays could be a critical factor for the change in morning load between 8:00 and 10:00, causing higher errors in the period. Finally, regarding Sunday, the 22nd of December, a sudden change in demand was traced for the 4 Sundays from the 1st to the 22nd, for example, at 11:00 going from 1876 MW, 2519 MW, 2354 MW to 2118 MW on the 22nd. The first major increase in demand was due to both the rainy day observed and a large decrease in temperature, dropping from a 21°C morning on the temperature on the 1st to a 12°C on the 8th, then the temperature slowly rose to 13 °C then 18 °C at the 22nd. Since the model relies on the demand from the same day at the previous week as one of its features, these sudden changes in weather conditions can have a significant impact on any specific day that has a large change in demand, especially at certain periods, and especially that Sunday depicts the starting day of the working day in Jordan.
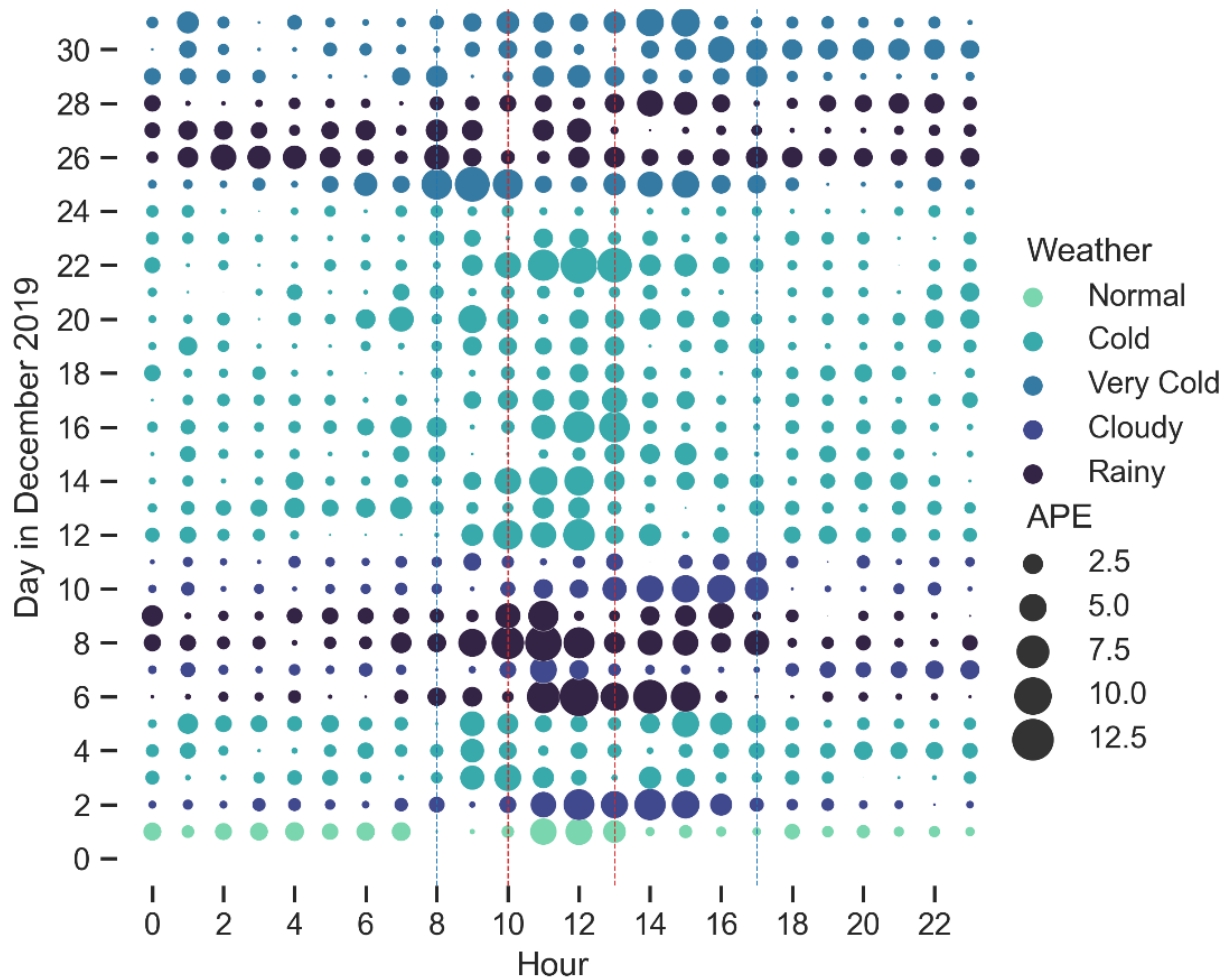
Figure 25 Absolute percentage error of the forecasted results in December 2019 and related weather conditions.

Chapter 6: PEMD analysis results and the dispatching scenario

6.1. Jordan's residential sector PEMD analysis

Pre-implementation of DR requires a well-established estimation of the PEMD to analyze the impact of price ranges on demand. The short-term price elasticity is the best estimation for self-elasticity (ε_h) as it shows the negative relationship between price and demand change in short periods. Based on an analysis of residential tariffs for the periods between 1984 to 2014, the short-term price elasticity of electrical demand for the residential sector in Jordan is estimated at -0.0575[59].

Although, since price responsiveness of demand varies at different hours of the day, two scenarios are assumed: (1) ε_h is assumed constant for every hour, (2) ε_h is assumed to be double in peak periods. Hourly cross-elasticity represents the amount of energy shifted from one hour to other hours of the day, both backwards and forwards in time. To estimate the amount of potential shiftable energy in peak load hours and its time horizon, a detailed analysis of the different loads impacting DR and their penetration in the residential sector is conducted, which is represented in Table 14.

Table 14 Power consumption and Penetration rates of different electrical appliances in Jordan's Residential Sector

Appliance	Penetration Rate (%)[1]	Watts[4]	H/Day
Vacuum cleaner	68%	1200	0.5
Dishwasher	7%	1800	1
Washing Machine	97%[2]	1800	1.5
Water heater (Electrical/ Gas)	79% * 0.5[2,3]	4000	3
AC	32%	1800	12
Freezer	16%	200	12
Refrigerator	98%	200	12
Microwave	54%	1500	0.5
Laptop/PC	31%	120	3
TV	98%	200	3
Lighting	100%	420	6

1. Jordan's department of statistics survey in 2017 [88]
2. [89]
3. The water heating penetration is assumed at 50% for the electrical-based and 50% for the gas-fired
4. JICA's report on the electricity sector master plan [52]

The data in Table 14 was used to estimate the normalized weight of each appliance's energy consumption relative to other appliances, which is shown in Figure 26. The figure depicts an estimation of the weight of each appliance's share of the residential electrical demand for the loads discussed in this study, where it is more

probable that it holds in the evening load period when consumers return from work and need to use both water and space heating.
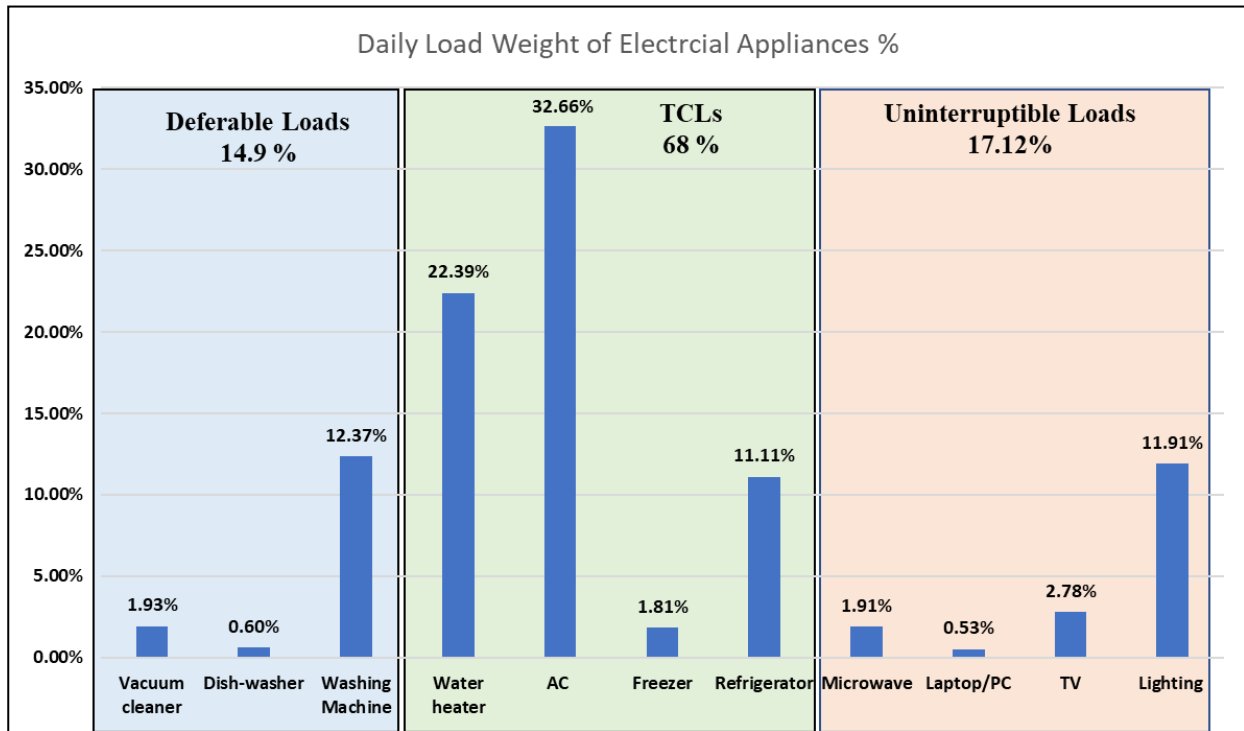
Figure 26 Daily Load Weights of Electrical Appliances in Jordan's Residential Sector

Residential loads can be classified into different types according to their flexibility and DR characteristics: Thermostatically controlled loads (TCLs), Deferrable Loads, Uninterruptible Loads [90]. TCLs are highly correlated to temperature and environmental factors, where due to their thermal storage properties, their demand can be more flexible with a lower impact on consumer comfort. Deferrable Loads refer to appliances that are flexible to use and can also be shifted with low impact on consumer comfort. Finally, uninterruptible Loads refer to the appliances that require continuous energy demand while being used and are highly correlated to consumer comforts where they usually have little DR potential. Both TCLs and Deferrable Loads are estimated to represent 82.9% of the residential sector which amounts to a significant potential for DR in Jordan's residential sector. Water heating and deferrable appliances can be easily shifted in peak demand periods resulting in peak shaving. According to the previous discussion, cross-elasticity is estimated under two scenarios related to the amount of energy re-allocated in peak time:

1. **A lossless-case scenario**: Reduced energy at a certain hour is re-allocated into other hours of the day without a loss in total energy consumption. Hence, the summation of all cross elasticities in every column in the PEMD is equal in magnitude to the self-elasticity at that hour.

2. **A 75% re-allocation scenario**: 75% of the reduced demand is re-allocated to other hours, and 25% is not used by the consumers, such as lighting, TV, or AC usage that users simply do not use again. Therefore, the summation of all cross elasticities in every column in the PEMD is equal in magnitude to 75% of the self-elasticity at every hour.

6.2. Peak period DR policy impact on PEMD estimation

The proposed DR policy in this study is implemented by changing the peak-period prices only to reduce the peak-load according to operational and security goals of the GO, which has a direct impact on the estimation of the DR behavior of the residential sector. The period of DR is assumed to start one hour before (4 -5) PM and after (8-9) PM the announced peak periods that were discussed in Table 6 for the winter season are constant for the whole period. The PEMD under this price policy in the winter peak-time is depicted in Figure 27, where it incentivizes consumers to shift their energy consumption outside of the peak demand period only due to the constant peak period price. Since the prices only change in the peak period, the areas on the left and right of the peak period are ignored and were considered zero based on the policy proposed.
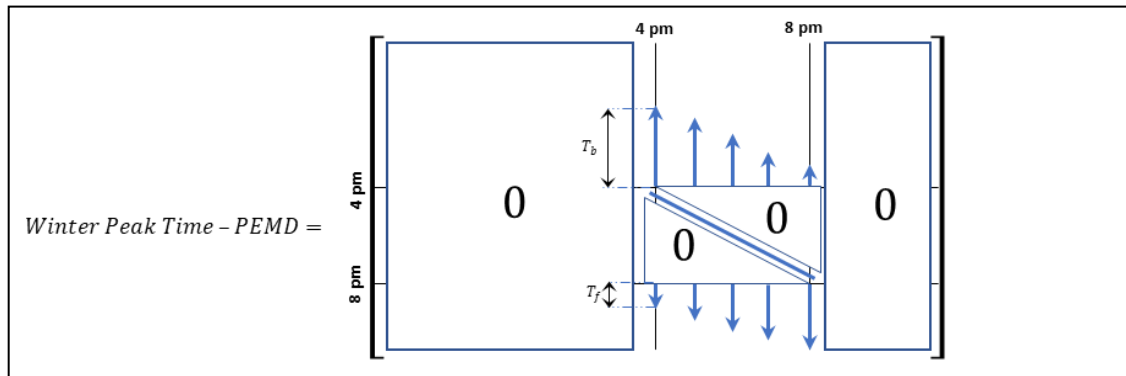
Figure 27 Winter Peak Time - PEMD under the proposed DR policy

Consumers are inclined to shift their demand to the closest hours outside of the peak period [91], as depicted in Figure 27. The time-horizon (T_b: backward time horizon and T_f: forward time horizon) of the demand re-allocation depends on the type of appliances shifted. In the case that most of the appliances shifted are deferrable loads or water heating, it is assumed that the time-horizon of shifting is 4 hours closest to the hour under peak pricing, where the cross-elasticates have the same value as reported in Table 15. It is also assumed that, in the last hour of the peak period, a part of their demand is shifted to the next day after 24:00, which is not considered in the current PEMD models. If more AC usage is shifted, the weight of the cross-elasticity of the peak hour period is doubled for the closest 2 hours, as represented in Table 16.

Table 15 Base self-elasticity, lossless PEMD with no AC shifting Scenario

Time*	16:00	17:00	18:00	19:00	20:00
12:00	+0.0144	0	0	0	0
13:00	+0.0144	+0.0144	0	0	0
14:00	+0.0144	+0.0144	+0.0144	0	0
15:00	+0.0144	+0.0144	+0.0144	+0.0144	0
16:00	-0.0575	0	0	0	0
17:00	0	-0.0575	0	0	0
18:00	0	0	-0.0575	0	0
19:00	0	0	0	-0.0575	0
20:00	0	0	0	0	-0.0575
21:00	0	+0.0144	+0.0144	+0.0144	+0.0144
22:00	0	0	+0.0144	+0.0144	+0.0144
23:00	0	0	0	+0.0144	+0.0144

*at 23:00 for example, it indicates the period of (23:00 – 24:00)

Table 16 Base self-elasticity, lossless PEMD with AC shifting Scenario

Time	16:00	17:00	18:00	19:00	20:00
12:00	+0.0096	0	0	0	0
13:00	+0.0096	+0.0096	0	0	0
14:00	+0.0192	+0.0192	+0.0096	0	0
15:00	+0.0192	+0.0192	+0.0192	+0.0096	0
16:00	-0.0575	0	0	0	0
17:00	0	-0.0575	0	0	0
18:00	0	0	-0.0575	0	0
19:00	0	0	0	-0.0575	0
20:00	0	0	0	0	-0.0575
21:00	0	+0.0096	+0.0192	+0.0192	+0.0192
22:00	0	0	+0.0096	+0.0192	+0.0192
23:00	0	0	0	+0.0096	+0.0096

Table 17 shows the structure of the finalized PEMD in this study. Cases 1 to 4 represent the base self-elasticity which equals the short-term self-elasticity for the residential sector of Jordan, while Case 5 to 8 assume that the peak period will have double the elasticity. Cases [1,2,5,6] represent a lossless PEMD, where the summation of the cross-elasticities is equal to the cross elasticity in magnitude, while their counterparts take the 75% case scenario mentioned previously. Finally, cases [3,4,7,8] consider more AC usage participated in DR, where the second level of cross elasticity (L2) with double the weights of (L1) is used, as was shown in Table 15 and Table 16.

Table 17 Finalized PEMD

Case Scenarios	Self-Elasticity	Cross Elasticity—L1	Cross Elasticity—L2
C1		$-(-0.0575/4)$	-
C2	-0.0575	$-(-0.0575/6)$	$-2\times(-0.0575/6)$
C3		$-(0.75\times(-0.0575))/4$	-
C4		$-(0.75\times(-0.0575))/6$	$-2\times(0.75\times(-0.0575))/6$
C5		$-(-0.115/4)$	-
C6	-0.115	$-(-0.115/6)$	$-2\times(-0.115/6)$
C7		$-(0.75\times(-0.115))/4$	-
C8		$-(0.75\times(-0.115))/6$	$-2\times(0.75\times(-0.115))/6$

6.3. *Dispatching scenario and prediction performance*

To simulate a real dispatch case scenario, the unit commitment and dispatched power plants for a day in December- 2019 were acquired coupled with the expected demands for that day as predicted by NEPCO. The detailed information of the dispatched power plants is given in Table 18. All units for that day operated with combined cycles with their real capacities shown. The available power from Egypt is assumed at 150 MW for the whole day with priority above IPP4 and Risha's power at maximum capacity with its cost not considered, being

based on natural gas extracted from Jordan. The real hourly PV and wind energy from renewable power plants are assumed to be the predicted values and are subtracted from the demand, then the table is used to find the cheapest combination.

Table 18 Power Plant Dispatched for the Cases-study in December 2019

Unit	Name	Cost (JD/MW)	Min. Demand (MW)	Max. Demand (MW)
1	**Risha**	0	33	33
2	**AES CC**	59.85	210	410
3	**ACWA CC**	60.09	210	360
4	**SAMRA 4 CC**	61.06	127.5	220
5	**SAMRA 3 CC**	61.06	192.5	420
6	**SAMRA 1 CC**	61.06	210	310
7	**QPC CC**	64.89	210	424
8	**Wind**	72.79	0	-
9	**PV**	79.94	0	-
10	**Egypt**	52.79	0	150
11	**IPP4**	121.17	0	240
12	**IPP3**	231.04	0	570

Figure 28 shows the real and predicted values of electricity Sunday, 8th of December 2019, as well as the PV and wind generation, where Sunday represents the start of the working week in Jordan. The proposed model's prediction achieved a MAPE of 3.59% and is compared to NEPCO's prediction, which performed worse. One reason is that NEPCO's prediction is usually provided before 4 PM on the previous day, while our model achieves the prediction of the whole day at the end of the previous day. Nevertheless, the proposed model achieved higher results throughout the period. It is to be noted that, hour 0:00 indicates the average demand from 0:00 to 1:00.
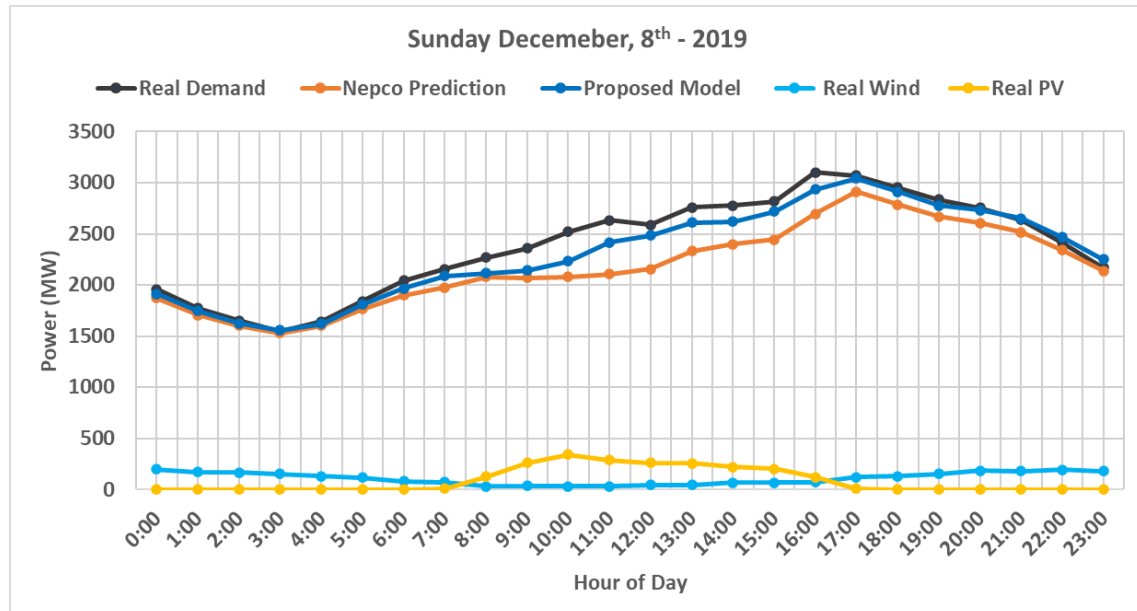
Figure 28 Selected case study day in December 2019

Chapter 7: Final model's results

7.1. *Day-ahead Demand Response model for the selected case study Scenarios*

The proposed Day-ahead DR system for the residential sector's demand is shown in Figure 29, which was applied to a selected day in December 2019. The contribution of JEPCO, IDECO, and EDCO in providing the total residential electricity demand is considered about 32.4%, 5.08%, and 9.98%, respectively. This is calculated by multiplying the peak power of each distribution company by the percentage of residential and commercial energy consumption for each company. The estimated demand is also used to calculate the amount of power purchased from each power plant, after deducting the usage of the renewable power. Finally, after the peak bulk prices are selected for each distribution company, the model is applied to each PEMD case scenario to estimate the potential generation cost savings, peak demand reduction, and load factor improvements.
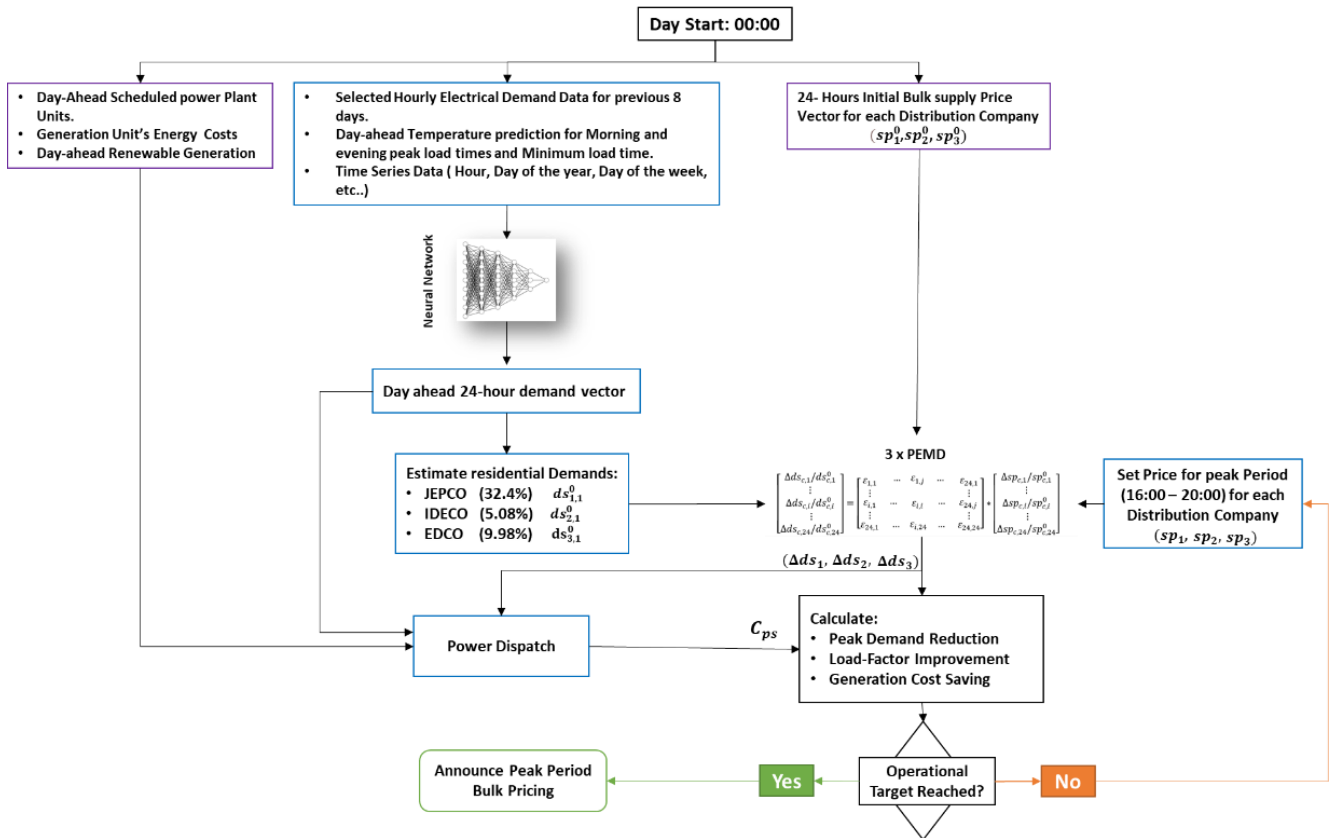

Figure 29 Applied Day-ahead DR Model for a selected day

7.2. Sunday 8-12-2019 – Case study Analysis

The Day-ahead DR model was applied to all the PEMD case scenarios discussed in Table 17, assuming the maximum peak prices $spp_{c,h,Max}$ for the period of each distribution company to be set at 200%, 250%, and 300% of their initial values. The three different price scenarios were applied to the profit maximization model presented in Equation 1 by maximizing the daily profit from the three distribution companies without considering the monthly capacity charge. Figure 30 shows the impact of applying the proposed DR model on Sunday, 8th of December 2019, considering all case scenarios and the dispatch model depicted in section 6.3. The profit maximization model always selects the maximum peak price for the given price scenarios.
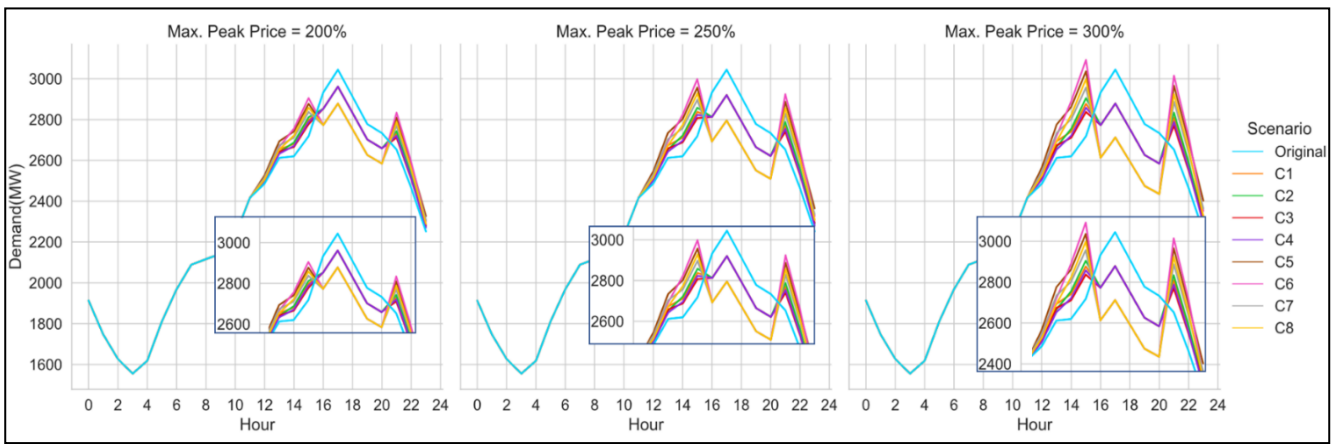
Figure 30 Hourly Demand impact of DR-model under different case scenarios

It can be observed that, the PEMD cases scenarios [C1 – C4] show a lower peak drop in the peak period due to having lower price elasticity in comparison to [C5 – C8], indicating the higher the peak period price, the higher the peak drops in the peak period. The periods after and before the peak period, especially from 2-4 PM and 9-11 PM, are extremely important. This is because the demand removed from the peak period is rescheduled towards them. Therefore, the new peaks might form, especially in case scenarios with high self-elasticities [C5 – C8], indicating the more demand is reduced in the peak period, the higher the new peaks' demand is. C6 represents the worst-case scenario, especially at higher peak prices, representing a lossless-PEMD with double the weight for the closest two hours outside the peak period. C2 represents the highest new peak formed among the cases [C1 – C4], although since it has half the self-elasticity of C6, the new peak was not as severe.

There is a clear trade-off between the demand reduced from the peak period and newly formed peaks. Figure 31 shows the peak reduction percentage for the whole day for each case scenario. C6 shows an increase in the peak by -1.46% at 300% peak price. It is noted that, in the case scenarios with low self-elasticity [C1- C4], a price increase leads to a steady decrease in the day's peak demand. In contrast, in the cases scenarios with high self-elasticity [C5-C8], higher prices can lead to a lower day's peak reduction due to the newly formed peaks. More than 5%-day peak reduction can be achieved in most cases except for C2 and C6, which are the worst cases among all case scenarios. C6 was the only scenario to show an increase in peak demand at 300% peak price, which is due to two main reasons: first, C6 depicts the high self-elasticity scenario where consumers are highly responsive to the price change, leading to more demand being shifted to hours outside of the peak period. Secondly, C6 depicts the scenario with both the lossless case where all demand removed from any hour will be allocated to other hours

and the case where the weight of demand shifted to the closest two hours is doubled. Hence, the higher the price increase, the more demand is re-allocated with a higher concentration on the hours outside the peak period being 15:00 and 21:00, as seen in Figure 19. Other cases such as C5 had a slightly less bad case at 300% peak prick as there was an even redistribution of demand reallocated to the surround-ing 4 hours of the peak period, making the newly formed peak less than C6, while in C8, there was 25% less demand shifted, making the new peaks also less than C6. Alt-hough the peak price is low enough in high elasticity scenarios, even with more de-mand shifted to closer hours, a high peak reduction can still be achieved.
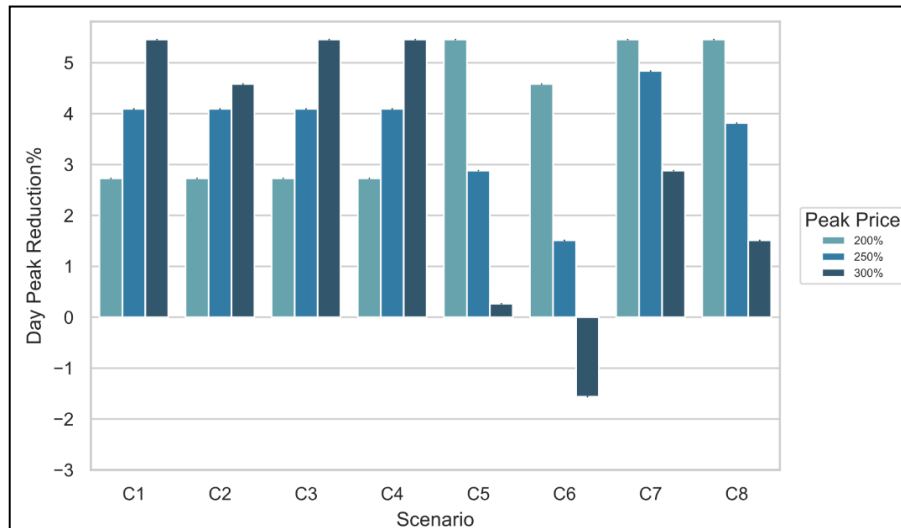
Figure 31 Day Peak Demand Reduction%

The load factor is calculated by dividing the mean demand for the whole day by the maximum demand. Figure 32 represents the comparison between the load factor for each scenario with the original demand. The results show that, the load factor can be improved around 5%, by setting high prices in low self-elasticity cases and lower prices in high self-elasticity cases.
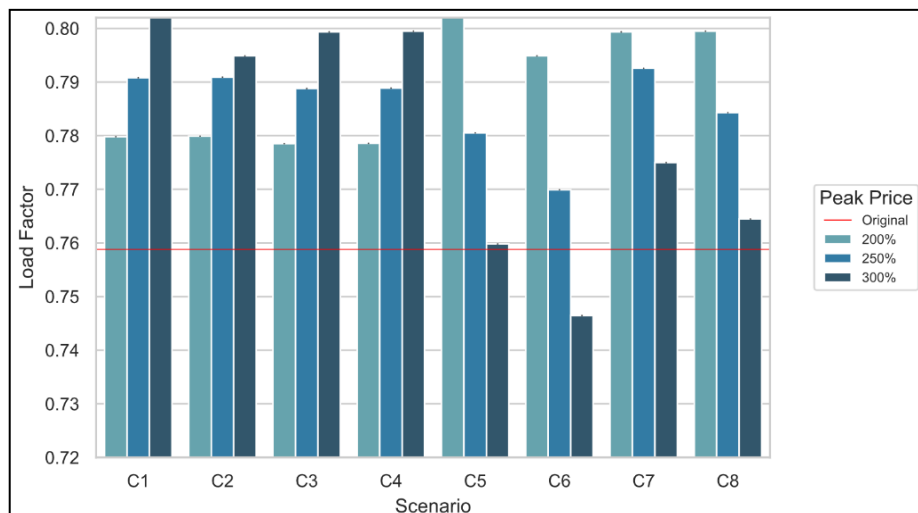
Figure 32 Load Factor analysis

The main objective of the DR program is to reduce energy consumption from costly peak power suppliers. Figure 33 shows the amount of saving in electricity usage from IPP3, which is the most expensive power plant, where both cases C8 and C7 achieved the highest savings, especially at 250% peak pricing. It is also notable that, the

worst-case scenario (C6) at 300% peak pricing also achieved savings, which is mainly because the new high peak formed at 9 PM has a smaller width (time horizon) than the original peak and drops more sharply, whereas, for the peak formed at 3 PM, PV power was available. This shows the importance of shifting demands towards periods where renewable energy is available, where in this case, even if the peak demand increased, the overall demand from IPP3 can still be reduced. Cases [C3, C4, C7, C8] achieved better savings in both self-elasticity scenarios, since 25% of the demand reduced at each hour in the peak period is removed from the grid.
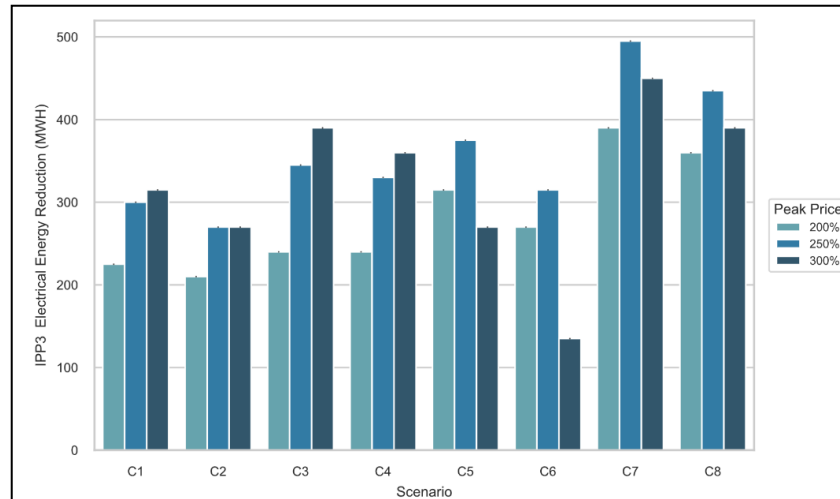
Figure 33 Savings in electricity purchased from supplier IPP3

Figure 34 shows the energy cost savings in all scenarios. Energy cost-saving doesn't follow the same pattern as energy saving because the decrease in electricity purchased from IPP3 causes an increase in IPP4 power usage in hours, where the demand rises from 2 PM to 4 PM and 9 PM to 11 PM. The best- and worst-case scenarios in cost-saving are C7 at 300% peak and C2 at 250%, with the detailed results of the peak reduction, load factor, and cost-saving for each case scenario are reported in Table 19, and 20 and the best results based on peak prices for each case are highlighted in green.
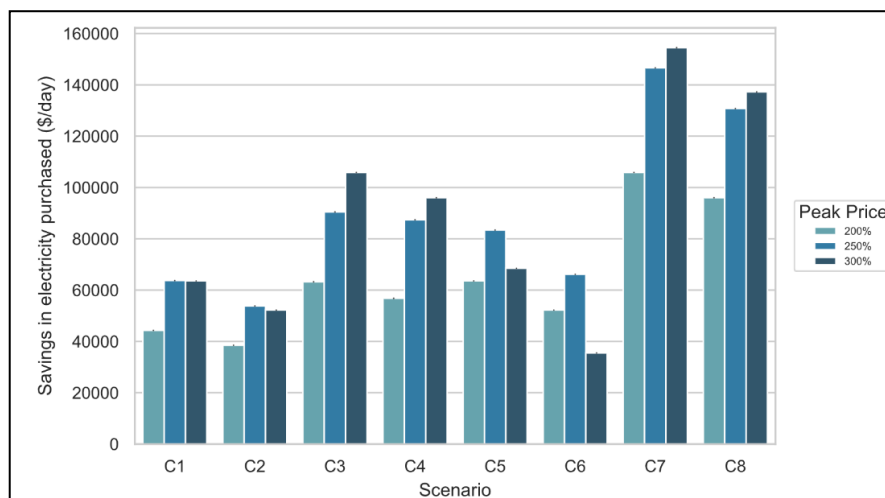
Figure 34 Cost Saving

Table 19 Cases [C1 - C4] Results

Case	C1			C2			C3			C4		
Peak Price	200%	250%	300%	200%	250%	300%	200%	250%	300%	200%	250%	300%
Peak Reduction (%)	2.729	4.093	5.458	2.729	4.093	4.582	2.729	4.093	5.458	2.729	4.093	5.458
Load Factor	0.780	0.791	0.802	0.780	0.791	0.795	0.779	0.789	0.799	0.779	0.789	0.799
Cost Saving ($/day)	44323	63726	63586	38517	53856	52213	63264	90487	105859	56801	87448	95989

Table 20 Cases [C5-C8] Results

| Case	C5			C6			C7			C8		
Peak Price	200%	250%	300%	200%	250%	300%	200%	250%	300%	200%	250%	300%
Peak Reduction (%)	5.458	2.880	0.266	4.582	1.511	-1.456	5.458	4.841	2.880	5.458	3.814	1.511
Load Factor	0.802	0.781	0.760	0.795	0.770	0.747	0.799	0.793	0.775	0.799	0.784	0.764
Cost Saving ($/day)	63586	83397	68514	52213	66149	33376	105859	146619	154505	95989	130769	137257

The results revealed that, in the case scenarios with base self-elasticity, the best improvement on all indicators could be achieved by increasing the prices, especially in C3 and C4, where due to the low-price elasticity in the peak time, newer high peaks after and before the peak period were not formed, as less energy was removed from the peak period. In these cases, peak demand reduction ranged from 4.582% to 5.458%, load factor rose to (0.780 – 0.802), and cost savings ranged from 53,856 \$ to 105,859 \$ per day. The higher the peak period price elasticity, the higher demand shifts from the peak period caused newer peaks to form at high energy prices.

The highest energy cost reductions do not align with the other indicators, ranging from 66,149\$ to 154,505 \$. This indicates that the prices should be set based on the priority of the GO, whether direct profit in terms of cost-saving has higher priority or indirect profits by peak reduction and load factor improvement that increase operational performance. The power plant shares for the C7 having the best cost-saving at 300% peak price can be seen in Figure 35, where the share of power purchased from IPP3 was reduced from 1.49% to 0.68%.
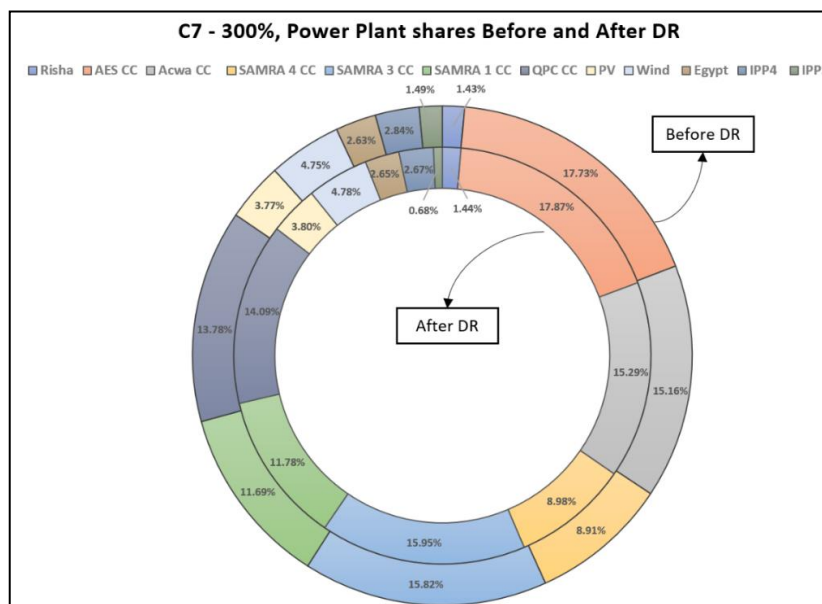
Figure 35 Power plant shares for the Case of C7-300% before and after DR

7.3. Days with the highest demand case study

In order to obtain a more comprehensible result on the effectiveness of the proposed DR model, 3 more days with the highest demand from December in 2019 were selected. Friday the 27th and Saturday the 28th have been selected to represent the weekends with the highest demand through December, while Sunday the 29th had the highest demand from the weekdays, as shown in Figure 36 alongside the previously discussed case in the previous section. The detailed results for each day are discussed in the following subsections.
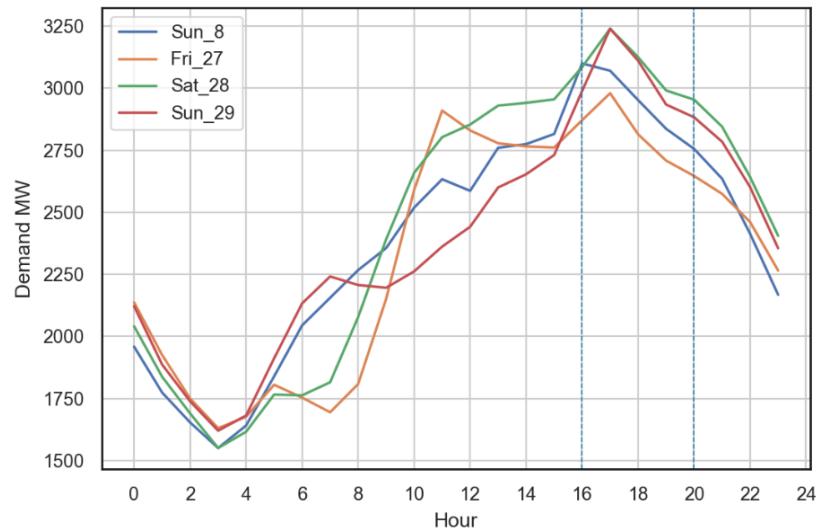
Figure 36 3 Extra Selected days within December 2019

7.3.1. Friday (27-12-2019)

Friday's demand is the most unique from the four selected case study days, where there exist two peaks, 2910 MW at 11 AM and 2980 MW at 5 PM, depicting a unique behavior at the start of the weekend holiday in Jordan as depicted in Figure 37, with a prediction performance of 1.84% MAPE Error. The results for this day are illustrated in Figures 38 to 40.
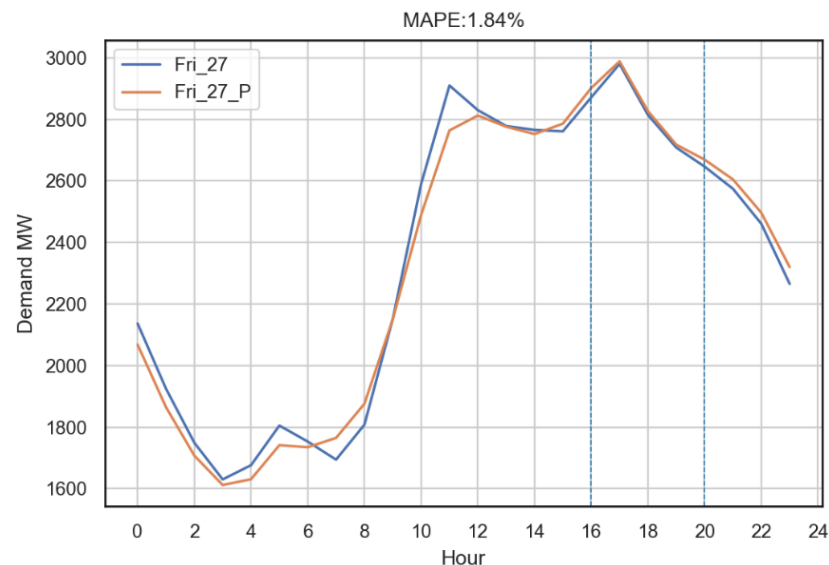
Figure 37 Friday (27-12-2019) prediction performance
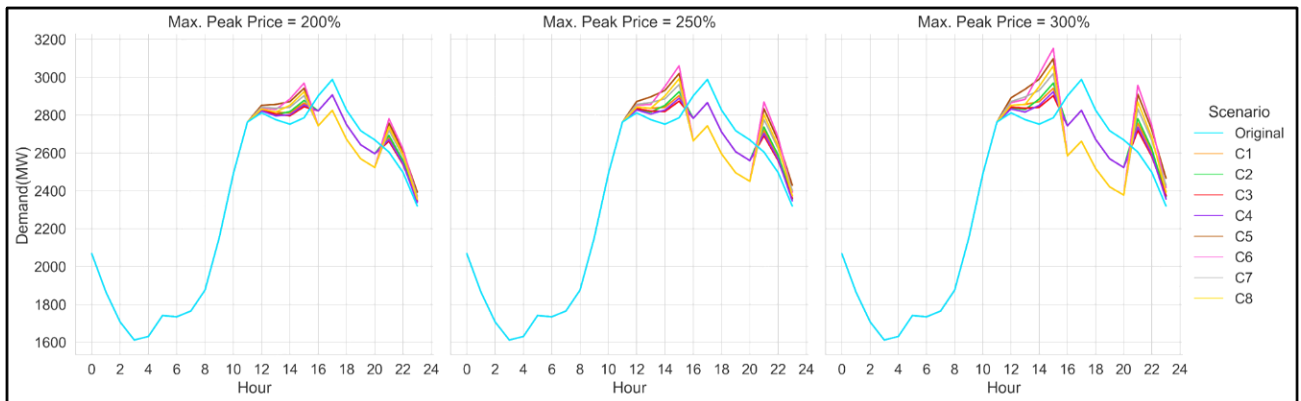
Figure 38 DR-model output under different case scenarios (Friday-27th)
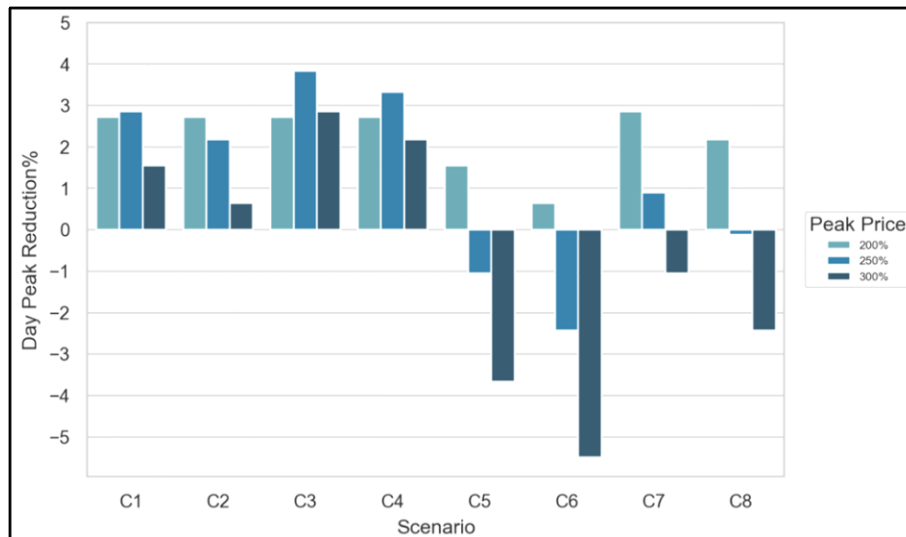
Figure 39 Peak Reduction (Friday - 27th)
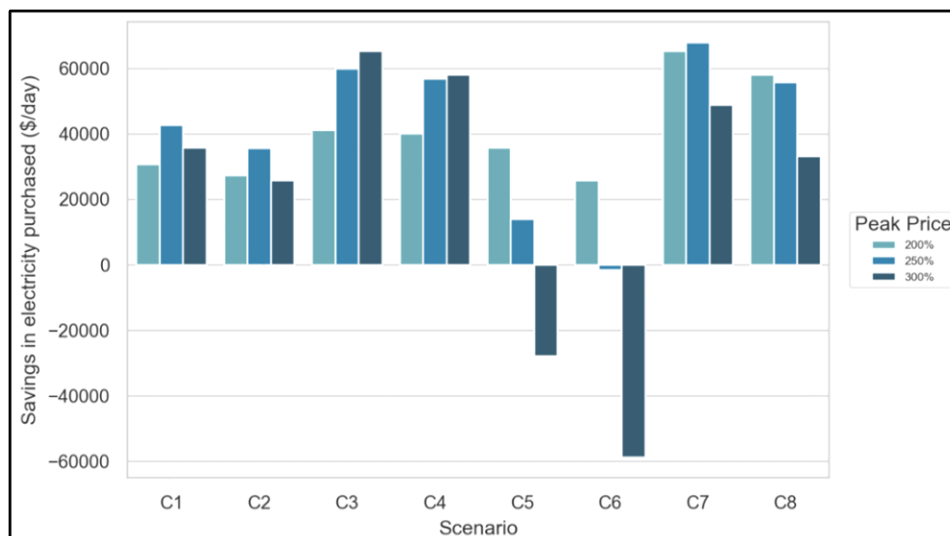
Figure 40 Saving in Purchased Energy (Friday - 27th)

7.3.2. Saturday (28-12-2019)

Saturday is also another weekend, although it only has one 3240 MW peak at 5 PM and is closer in shape to the weekdays with the difference of noticeably higher demands from the period of 9 AM to 5 PM as can be seen in Figure 41. The prediction model achieved a MAPE error of 2.04% and the results for this case study are depicted by 42 to 44.
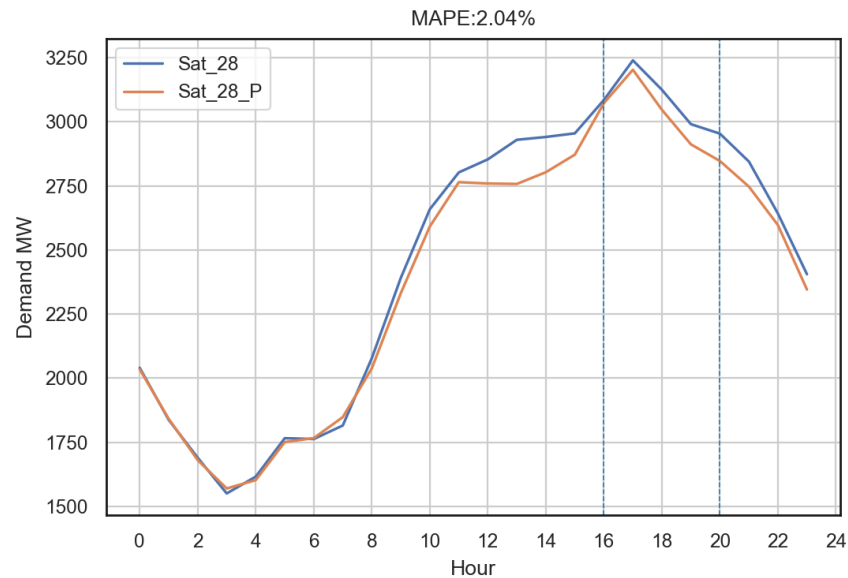
Figure 41 Saturday (28-12-2019) prediction performance
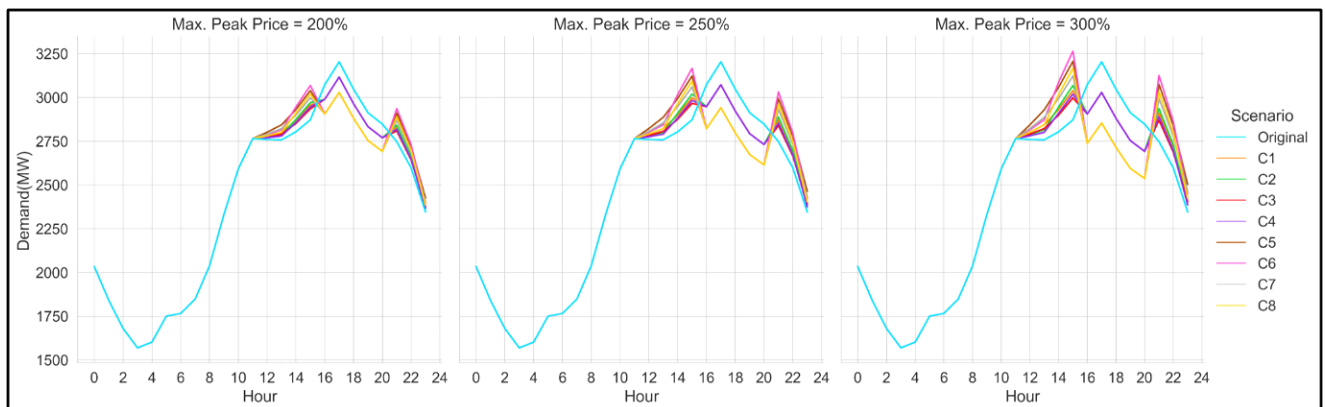
Figure 42 DR-model output under different case scenarios (Saturday -28th)
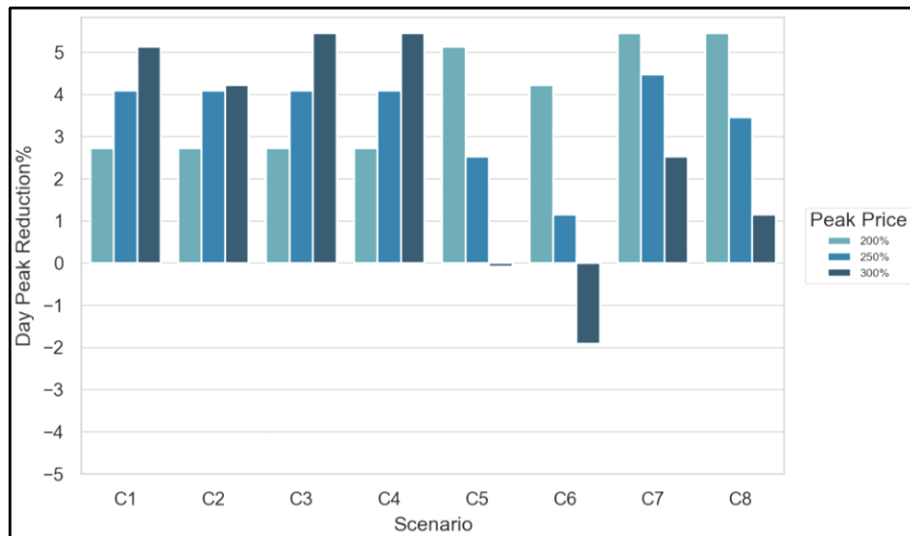
Figure 43 Peak Reduction (Saturday - 28th)
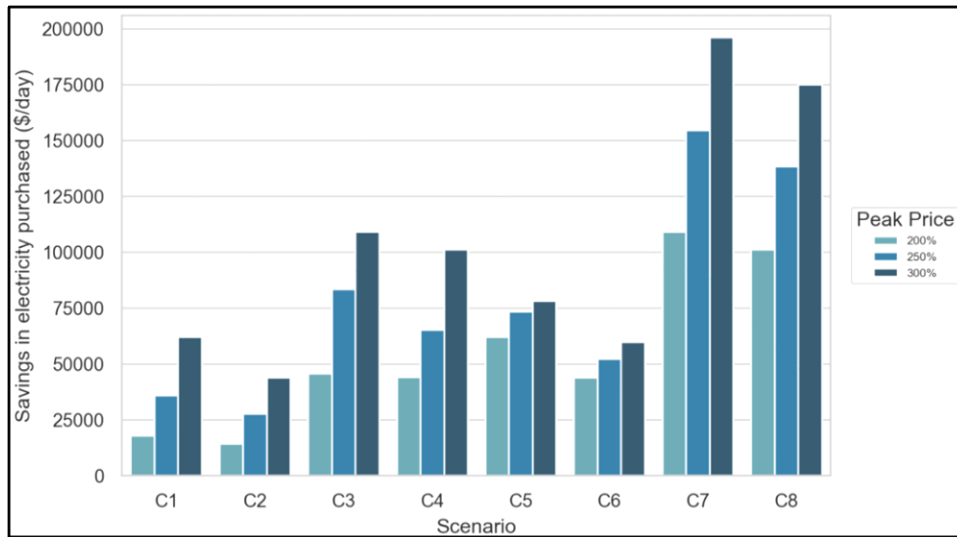
Figure 44 Saving in Purchased Energy (Saturday - 28th)

7.3.3. Sunday (29-12-2019)

Finally, the last Sunday of 2019 showing the highest demand of the month was used in this analysis. The prediction model achieved a MAPE of 1.68% performance and its demand reaches 3240 MW at peak time, as shown in Figure 45. The results for this day are shown in Figures 46 to 48.
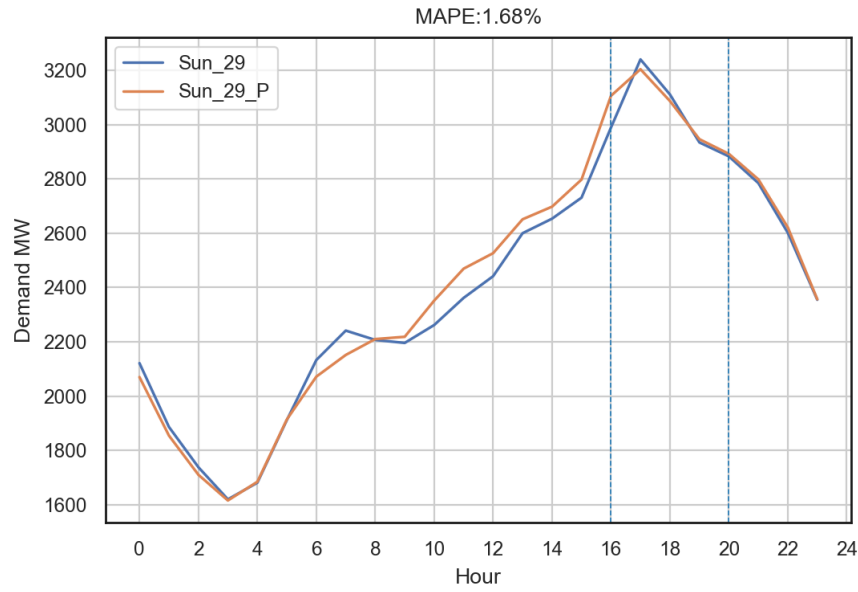
Figure 45 Sunday (29-12-2019) prediction performance
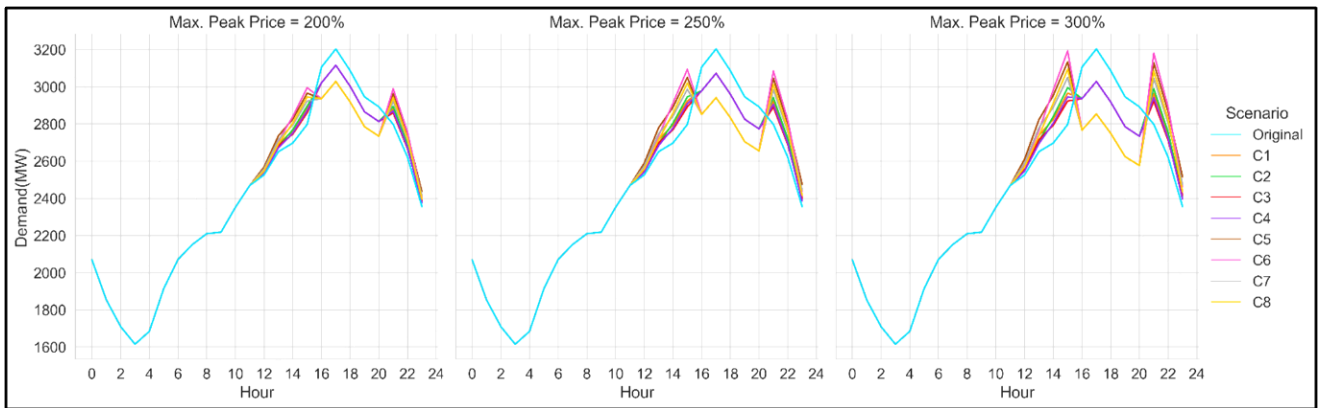
Figure 46 DR-model output under different case scenarios (Sunday -29th)
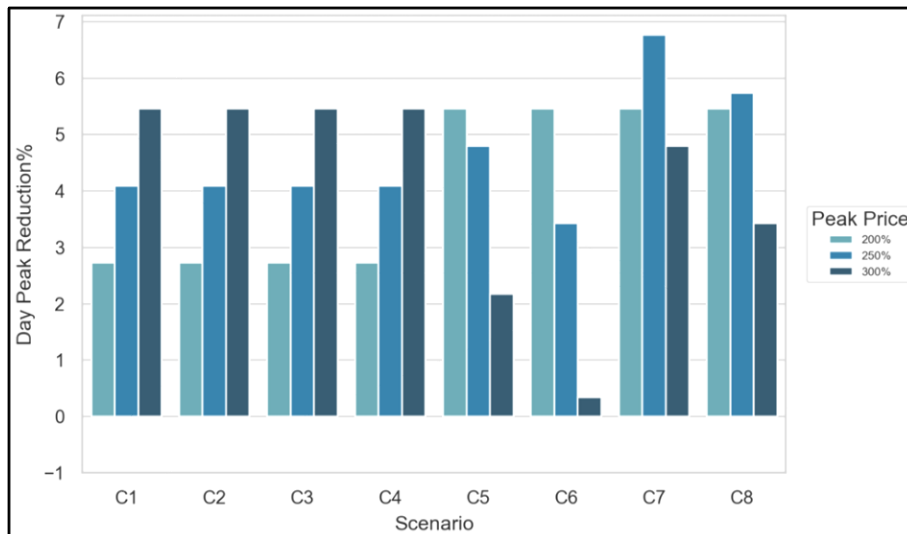
Figure 47 Peak Reduction (Sunday - 29th)
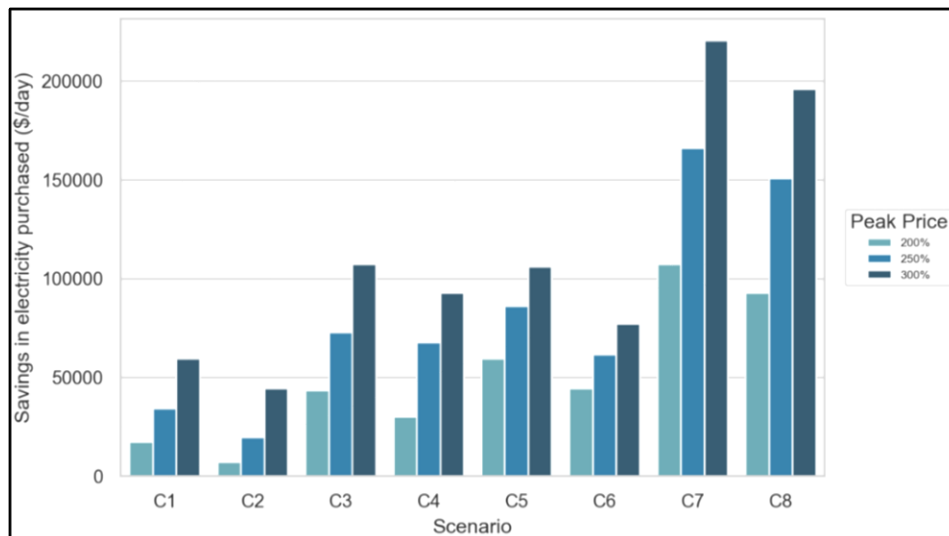
Figure 48 Saving in Purchased Energy (Sunday - 29th)

7.4. Case Studies Discussion

The results of each of the four presented days can be seen in Table 21, showing the best and lowest results in terms of Peak Reduction, Load factor, and Cost Saving.

Table 21 Final Results of the DR model on various days

| Day	Best Results			Lowest Results		
	Peak Reduction (%)	Load Factor	Cost Saving ($/day)	Peak Reduction (%)	Load Factor	Cost Saving ($/day)
Sunday - 8	5.458	0.802	154505	4.582	0.795	53856
Friday - 27	3.839	0.816	67951	0.642	0.792	25767
Saturday - 28	5.458	0.799	196245	4.217	0.791	43774
Sunday - 29	6.770	0.792	220581	5.458	0.782	44334

It can be depicted from both the previous table and the previous section that Friday – 27th was the worst-case scenario out of all the selected days, were due to its double peak and demand pattern between the peaks especially, it was easier for a new high peak to form, which showed the lowest peak reduction potential at only 0.642% and its best results also were relatively lower than all other days at 3.839%. Its cost-saving also had the lowest range from 25,767 $ to 67,951 $, showing that a better peak period DR plan must be implemented to consider the double peaks present.

On the other side, Sunday – 29th showed the highest peak demand reduction at 6.770% and a reduction in the cost of purchased energy, reaching 220,581 $ at best and 44,334 $ in the worst scenario. This day had the best results as mentioned since it had the highest peak demand; hence, the higher the peak demand is and the closer it is to the peak period, increasing the potential benefits that can be obtained. Saturday the 28th and Sunday the 8th both had similar range savings at 196,245 $ and 154,505$ respectively, were due to the higher peak demand of Saturday, it had better savings.

7.5. Results for the month of December 2019

The model was finally applied to the whole month of December - 2019 to show the general potential of applying the proposed DR model in the winter season for Jordan's residential sector. Figures 49 – 51 show the peak reduction, load factor improvements, and cost savings achieved for every day in December, with the horizontal lines showing the weekends being Friday and Saturday. The "best" indicates that case scenario that had the very highest result such as (C7-300%) in Figure 48, while "Min" depicts the minimum achievable result out of all the case scenarios such as (C2-300%) from the same figure, while "Worst" indicates the lowest achievable results (C2-200%). In terms of peak reduction observed in Figure 49, the best results had a maximum potential of 8.19% with an average of 6.04%, while the minimum results had a maximum of 5.46% and an average of 4.49%. It could also be noticed that there were only 4 days in the month where the model and peak period price policy showed low performance in terms of the minimum achievable results, which is due to the demand curve's unique behavior in those days. The load factor improvement results shown in Figure 50 had an average of 0.05 and 0.034 for the best and minimum results, respectively, and followed the same trend as Figure 49. As for the cost-saving results depicted by Figure 51, the average for the best and minimum results were 154,890 $ and 64,263 $, respectively. The highest best cost-saving was observed at 265,411$ Saturday the 21st, where it can be observed that most Saturdays on the 7th, 14th, 21st, and 28th showed high-cost saving potential consistently, especially in relevance to Fridays that showed the lowest cost-saving potential.
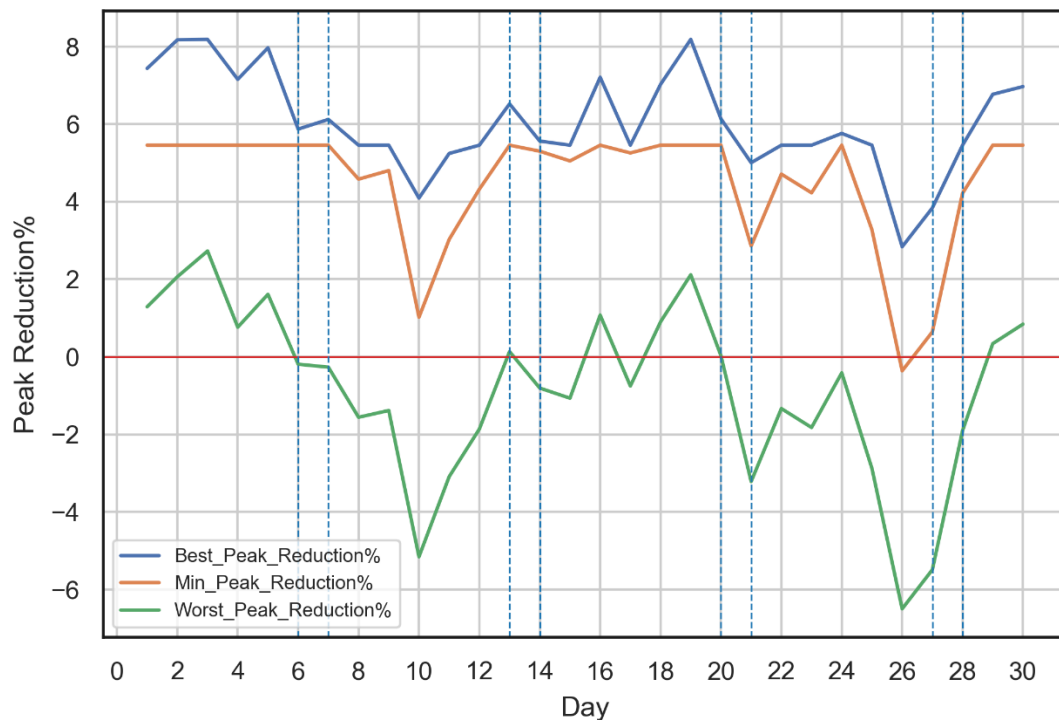
Figure 49 DR Peak Reduction for December 2019
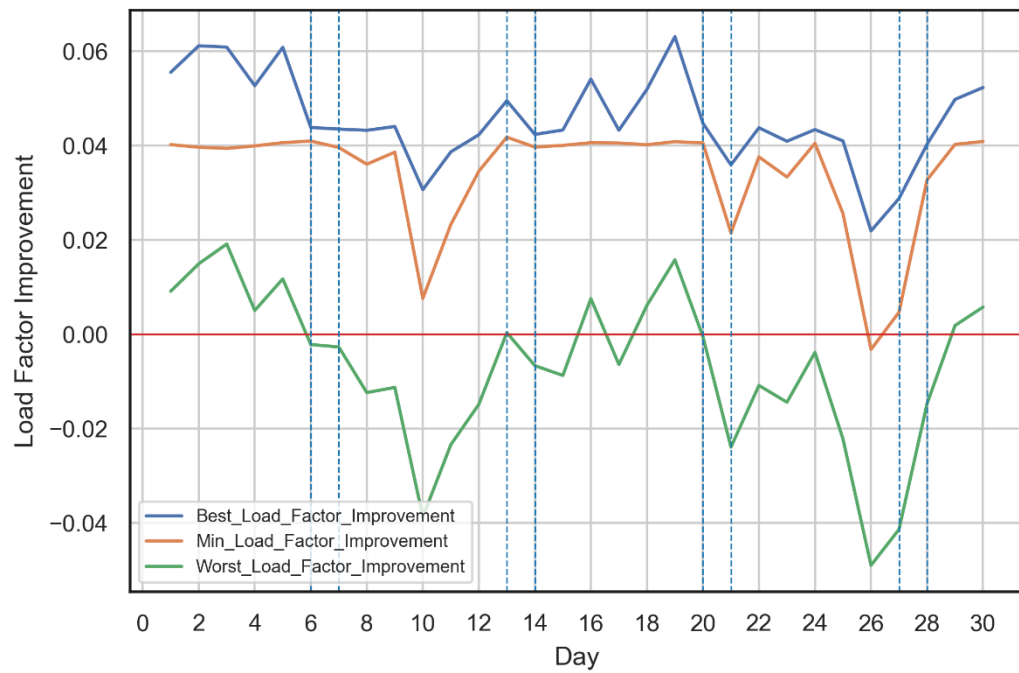
Figure 50 DR Load factor improvement for December 2019
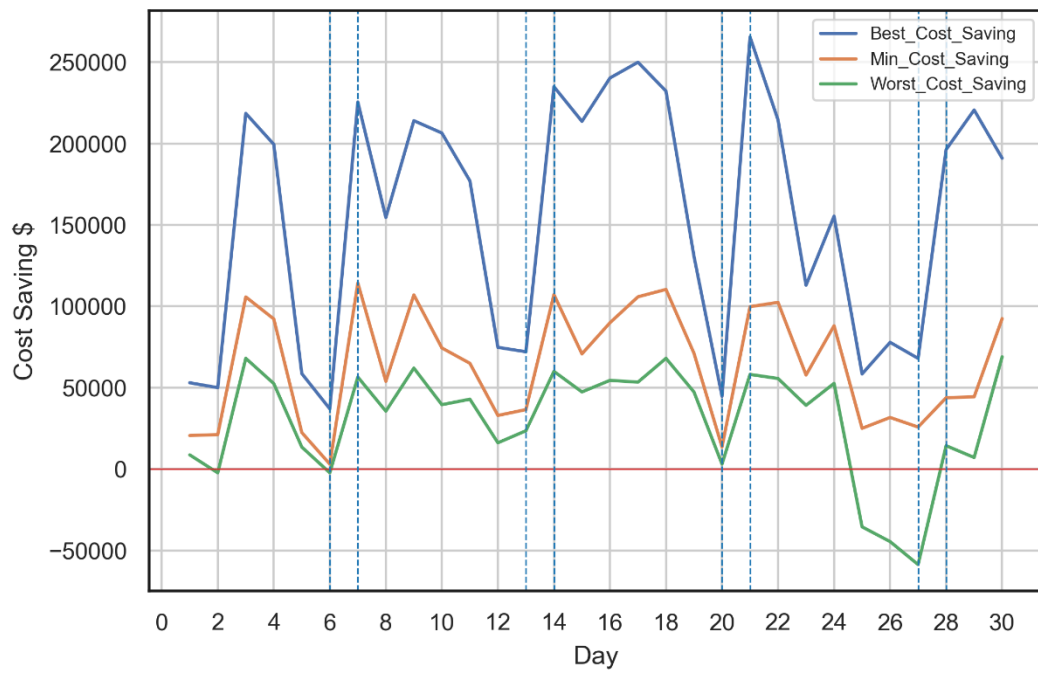
Figure 51 DR Cost saving for December 2019

Chapter 8: Conclusion

This research aimed at presenting a comprehensive demand response model for the Jordanian power sector, based on the maximization of the profit for the service provider, considering its interaction with the power generators and customers. To this aim, a peak period, Day-ahead DR based on the deep neural networks model, was introduced, and applied to the residential sector, which holds a large portion of the daily demand. The hourly Day-ahead demand prediction, which is one of the main inputs to the DR model, was achieved by training a deep neural network on 4-years of demand data showed perfect estimation with a MAPE error of 1.411% on the first test data set and 2.03% on the second one at the end of the four years training period. Besides, a precise PEMD estimation of Jordan's residential sector was based on recent research on the short-term price elasticity of Jordan's residential and the analysis of the different electrical appliances and daily operations. The results of the DR model applied for multiple case scenarios of the PEMD showed that peak reductions, load factor improvements, as well as high potential for significant cost saving could be achieved with the proposed DR model.

Current Model Limitations:

The proposed model at its current state faces the following limitations that should be taken into consideration for further development. First, due to the unavailability of a detailed electricity dispatching model for the Jordanian power sector, this part was simplified. Therefore, only the average prices and costs of the dispatched power plants were used in this study. By obtaining and including a more general and comprehensive dispatch model, more accurate modeling of the profit and saving calculation can be achieved, and a more precise optimization can be implemented. Second, in the presented model, the hourly residential demand of each distribution company was assumed to be a constant percentage of its share of the peak demand. Third, the hourly renewable energy power is considered given data to the model provided by each renewable power plant. Thus, a comprehensive prediction model should be combined with the current DR model to assess the impact of the climate conditions on balancing electricity supply and demand and predicting the demand response. In the presented model and due to the lack of full data related to weather conditions, these features were not fully integrated aside from the temperature.

Future Work:

For future work, the DR model can be further investigated and extended to consider the following:

1. Periods outside of the peak demand: While the current model focused on the periods of peak demand, utilizing the periods of off-peak and valleys to absorb demand from the peak periods through carefully selected pricing policies will be investigated. This will aid in increasing the load factor and decreasing the newly formed peaks surrounding the peak period, hence, leading to better cost savings and compensating consumers for the increase in prices in the peak periods.

2. Prediction model improvement with weather variables: As was noticed in the analysis of the error rates in the day-ahead demand prediction model, the weather variables and peak periods had the highest errors, by not only influencing consumer behaviour to deviate from their expected values but also can affect the PV generation on the consumer side that is not seen by the grid operator, leading to an unexpected spike in demand. Thus, by taking into consideration the weather variables and finding a solution to this challenge, prediction errors can be further lowered.

3. PV and Wind Day-ahead forecasting: While in the current model, the actual day-ahead hourly renewable energy values were used in the dispatch model, a prediction model can be constructed and optimized to handle this part by collecting more weather data related to PV and Wind generation.

4. Dispatch model improvement: The current dispatch model can be further improved to include the actual powerplant economic dispatch equations of the Jordanian power grid, to achieve a more accurate cost analysis of energy purchased from powerplants.

5. Investigating different DR models and policies: As previously discussed, there exist many types of DR models such as incentive paced, spot pricing, etc., where the benefits and impact of such models on achieving the DR objectives can be compared and tested.

Future Policy Recommendations:

The discussions and results of this work showed the impact of utilizing smart grid concepts such as DR systems and the utilization of machine learning algorithms to harness the available data more efficiently and produce high-performing prediction models. On this basis, the following future policy recommendations are proposed for the Jordanian government, MEMR, EMRC, NEPCO, and all other key parties in the power sector, to hasten the development of a smarter Jordanian power grid, especially in pushing the progress towards DR integration towards all consumption sectors and enabling R&D in the utilization of power grid data and advanced AI & ML algorithms to achieve energy savings, higher renewable penetration, and a reliable and optimized future power grid:

1. This work highlighted the effectiveness of DR systems in Jordan and many others worldwide; we strongly

advocate an action-oriented approach early on to implementation, by mitigating residential DR barriers from consumer to supplier sides that halts engagement, wide market completion, and the implementation of innovative methods. The governments and related institutes should start by closing the distance and leading the first mile from static and standard tariffs towards a dynamic and type-based tariff system to capture the real potential and responsiveness, especially on the verge of country-wide installation of Smart meters.

2. While industrial-based DR was implanted in Jordan successfully in a pilot project, this research has proven the benefit of moving the DR paradigm towards the residential sector. With the large portions of demand clustered in it, it proved to be an asset to dealing with the challenge of demand ramping in peak periods. Hence, directing assists in both the policy and research paradigm to facilitate and establish a smooth transition towards implementing a residential DR is essential early on.

3. With residential end consumers being the core of the proposed DR response model, they should not be treated as a challenge but as an opportunity that should be well integrated into the energy efficiency ecosystem, not only with price-based incentives but as caring to reduce the energy consumption of their country and have a shared goal of decarbonization and having a greener energy system. Consumers should be made aware of DR impacts and DR enabling technology such as storage systems, automation technologies, and renewable energy that can all act in a supportive manner within as a cluster of integrated solutions.

4. This work argued that not only great DR potential on weekdays can be delivered, but also on Saturdays, although Fridays had the furthest demand behaviour from the rest of the week and lowest potential. Higher emphasis should be made towards weekdays and Saturdays to further optimize the DR potential, while a more dynamic and customized DR for unique demand behaviours related to days such as Friday should be investigated separately to maximize the DR potential. The underlying demand behaviours of both normal and unique days should be well examined to enable smart and innovative designs for residential DR deployment.

5. Also, as shown in detail, in the case of high consumer responsiveness to the price change, a high increase in prices should be strongly avoided. It can lead to increasing the off-peak loads significantly, leading to newly formed peaks in some cases. DR policies should also aim at moving consumers towards shifting their loads more evenly and outwardly outside of the peak period, rather than just shifting them close to the peak period through awareness campaigns, especially concerning highly impactful electrical appliances to DR potential.

With that said, both the government and all key players in the power sector must take action to hasten the development of DR response systems for the different sectors of the Jordanian electricity sector and take into consideration policies to further increase the deployment of residential smart meters. Furthermore, research towards viable DR programs both price and incentive-based that attract the residential and different sectors in Jordan's power sector should be implemented, as well as pushing awareness campaigns to the importance of DR systems and mature energy usage to achieving a smarter grid that can handle the increasing challenges faced by high demands and high penetration of renewable energies as well as achieve environmental goals. Also, the government should provide more incentive to enable researchers and related personals by implementing policies that can facilitate easier access to available data, expertise and connect said parties further to accelerate development and research in these promising areas.

References

[1]   IEA, "Global energy demand rose by 2.3% in 2018, its fastest pace in the last decade," 2019. https://www.iea.org/news/global-energy-demand-rose-by-23-in-2018-its-fastest-pace-in-the-last-decade.

[2]   IEA, "Global Energy and CO2 Status Report," *Oecd-Iea*, no. March, p. 15, 2018, [Online]. Available: https://www.iea.org/publications/freepublications/publication/GECO2017.pdf.

[3]   W. Bank, "International Bank For Reconstruction And Development Program Document For A Proposed Loan With The Concessional Financing Facility Support In The Amount Of Us$250 Million To The Hashemite Kingdom Of Jordan For A Second Programmatic Energy And Water Secto," 2016. [Online]. Available: https://documents1.worldbank.org/curated/en/803731480820472849/pdf/1480820471543-000A10458-Jordan-Energy-Water-DPL-PD-11112016.pdf.

[4]   W. Bank, "Implementation Completion And Results Report (Ibrd-85300) On Ibrd Loans With The Concessional Financing Facility Support In The Aggregate Amount Of Us$500 Million To The Hashemite Kingdom Of Jordan For The First And Second Programmatic Energy And Water Se," 2018. [Online]. Available: http://documents1.worldbank.org/curated/en/222301546546705732/pdf/icr00004657-12282018-636818041906584165.pdf.

[5]   M. of E. and M. R. Jordan, "Energy 2019 -Facts & Figures," 2019. https://www.memr.gov.jo/ebv4.0/root_storage/en/eb_list_page/bruchure_2019.pdf.

[6]   G. Abu-Rumman, A. I. Khdair, and S. I. Khdair, "Current status and future investment potential in renewable energy in Jordan: An overview," *Heliyon*, vol. 6, no. 2, p. e03346, 2020, doi: 10.1016/j.heliyon.2020.e03346.

[7]   G. Tsourapas, "The Syrian Refugee Crisis and Foreign Policy Decision-Making in Jordan, Lebanon, and Turkey," *J. Glob. Secur. Stud.*, vol. 4, no. 4, pp. 464–481, 2019, doi: 10.1093/jogss/ogz016.

[8]   G. Abu-Rumman, A. I. Khdair, and S. I. Khdair, "Current status and future investment potential in renewable energy in Jordan: An overview," *Heliyon*, vol. 6, no. 2, p. e03346, 2020, doi: 10.1016/j.heliyon.2020.e03346.

[9]   NEPCO- National Electric Power Company, "Annual Report 2019 NEPCO," 2019. [Online]. Available: https://www.nepco.com.jo/store/DOCS/web/2019_en.pdf.

[10]   T. Hinokuma and H. Farzaneh, "Hybrid Renewable Energy System to Power a University," 2021.

[11]   J. Ma, V. Silva, R. Belhomme, D. S. Kirschen, and L. F. Ochoa, "Evaluating and Planning Flexibility in Sustainable Power Systems," *IEEE Trans. Sustain. Energy*, vol. 4, no. 1, pp. 200–209, 2013, doi: 10.1109/TSTE.2012.2212471.

[12] A. Shaqour, H. Farzaneh, Y. Yoshida, and T. Hinokuma, "Power control and simulation of a building integrated stand-alone hybrid PV-wind-battery system in Kasuga City, Japan," *Energy Reports*, vol. 6, pp. 1528–1544, 2020, doi: 10.1016/j.egyr.2020.06.003.

[13] Y. Yoshida and H. Farzaneh, "Optimal design of a stand-alone residential hybrid microgrid system for enhancing renewable energy deployment in Japan," *Energies*, vol. 13, no. 7, 2020, doi: 10.3390/en13071737.

[14] S. Impram, S. Varbak Nese, and B. Oral, "Challenges of renewable energy penetration on power system flexibility: A survey," *Energy Strateg. Rev.*, vol. 31, no. April, p. 100539, 2020, doi: 10.1016/j.esr.2020.100539.

[15] D. S. Kirschen, A. Rosso, J. Ma, and L. F. Ochoa, "Flexibility from the demand side," in *2012 IEEE Power and Energy Society General Meeting*, 2012, pp. 1–6, doi: 10.1109/PESGM.2012.6344828.

[16] P. D. Lund, J. Lindgren, J. Mikkola, and J. Salpakari, "Review of energy system flexibility measures to enable high levels of variable renewable electricity," *Renew. Sustain. Energy Rev.*, vol. 45, pp. 785–807, 2015, doi: 10.1016/j.rser.2015.01.057.

[17] NEPCO- National Electric Power Company, "Annual Report 2019 NEPCO," 2019.

[18] M. Alnabulsi and A. Ibrahim, "Jordan Embraces Demand Response: Rapid load growth in Jordan motivates the use of a cost-effective demand-response management system.," 2017. https://www.tdworld.com/grid-innovations/asset-management-service/article/20969752/jordan-embraces-demand-response.

[19] D. S. Kirschen, "Demand-side view of electricity markets," *IEEE Trans. Power Syst.*, vol. 18, no. 2, pp. 520–527, 2003, doi: 10.1109/TPWRS.2003.810692.

[20] P. T. Baboli, M. Eghbal, M. P. Moghaddam, and H. Aalami, "Customer behavior based demand response model," *IEEE Power Energy Soc. Gen. Meet.*, pp. 1–7, 2012, doi: 10.1109/PESGM.2012.6345101.

[21] F. B. Beidou, W. G. Morsi, C. P. Diduch, and L. Chang, "Smart grid: Challenges, research directions and possible solutions," *2nd Int. Symp. Power Electron. Distrib. Gener. Syst. PEDG 2010*, pp. 670–673, 2010, doi: 10.1109/PEDG.2010.5545803.

[22] D. Bartz and E. Stockmar, "Energy Atlas 2018 Facts and figures about renewables in Europe," *Heinrich Böll Found.*, 2018, [Online]. Available: www.foeeurope.org/energyatlas%0Awww.boell.de/energyatlas.

[23] G. Dileep, "A survey on smart grid technologies and applications," *Renew. Energy*, vol. 146, pp. 2589–2625, 2020, doi: 10.1016/j.renene.2019.08.092.

[24] J. Momah, *Smart Grid Fundamentals of Design and Analysis*. 2012.

[25] D. B. Rawat and C. Bajracharya, "Cyber security for smart grid systems: Status, challenges and perspectives," *Conf. Proc. - IEEE SOUTHEASTCON*, vol. 2015-June, no. June, pp. 1–6, 2015, doi: 10.1109/SECON.2015.7132891.

[26] I. M. Eleftheriadis and E. G. Anagnostopoulou, "Identifying barriers in the diffusion of renewable energy sources," *Energy Policy*, vol. 80, pp. 153–164, 2015, doi: https://doi.org/10.1016/j.enpol.2015.01.039.

[27] Z. Ma *et al.*, "The role of data analysis in the development of intelligent energy networks," *IEEE Netw.*, vol. 31, no. 5, pp. 88–95, 2017, doi: 10.1109/MNET.2017.1600319.

[28] Y. Lecun, Y. Bengio, and G. Hinton, "Deep learning," *Nature*, vol. 521, no. 7553, pp. 436–444, 2015, doi: 10.1038/nature14539.

[29] Lawtomated.com, "supVsUnsup." [Online]. Available: https://lawtomated.com/supervised-vs-unsupervised-learning-which-is-better/.

[30] H. A. Aalami, M. P. Moghaddam, and G. R. Yousefi, "Modeling and prioritizing demand response programs in power markets," *Electr. Power Syst. Res.*, vol. 80, no. 4, pp. 426–435, 2010, doi: 10.1016/j.epsr.2009.10.007.

[31] H. Farzaneh, L. Malehmirchegini, A. Bejan, T. Afolabi, A. Mulumba, and P. P. Daka, "Artificial intelligence evolution in smart buildings for energy efficiency," *Appl. Sci.*, vol. 11, no. 2, pp. 1–26, 2021, doi: 10.3390/app11020763.

[32] H. A. Aalami, M. P. Moghaddam, and G. R. Yousefi, "Demand response modeling considering Interruptible/Curtailable loads and capacity market programs," *Appl. Energy*, vol. 87, no. 1, pp. 243–250, 2010, doi: 10.1016/j.apenergy.2009.05.041.

[33] M. P. Moghaddam, A. Abdollahi, and M. Rashidinejad, "Flexible demand response programs modeling in competitive electricity markets," *Appl. Energy*, vol. 88, no. 9, pp. 3257–3269, 2011, doi: 10.1016/j.apenergy.2011.02.039.

[34] X. Qu, H. Hui, S. Yang, Y. Li, and Y. Ding, "Price elasticity matrix of demand in power system considering demand response programs," *IOP Conf. Ser. Earth Environ. Sci.*, vol. 121, no. 5, 2018, doi: 10.1088/1755-1315/121/5/052081.

[35] F. Wang *et al.*, "Day-ahead optimal bidding and scheduling strategies for DER aggregator considering responsive uncertainty under real-time pricing," *Energy*, vol. 213, 2020, doi: 10.1016/j.energy.2020.118765.

[36] R. Lu and S. H. Hong, "Incentive-based demand response for smart grid with reinforcement learning and deep neural network," *Appl. Energy*, vol. 236, no. December 2018, pp. 937–949, 2019, doi: 10.1016/j.apenergy.2018.12.061.

[37] L. Wen, K. Zhou, J. Li, and S. Wang, "Modified deep learning and reinforcement learning for an incentive-based demand response model," *Energy*, vol. 205, p. 118019, 2020, doi: 10.1016/j.energy.2020.118019.

[38] D. L. S. L. Forecasting, "Deep Learning-Based Short-Term Load Forecasting," 2019.

[39] T. G. Hlalele, J. Zhang, R. M. Naidoo, and R. C. Bansal, "Multi-objective economic dispatch with residential demand response programme under renewable obligation," *Energy*, vol. 218, p. 119473, 2021, doi: 10.1016/j.energy.2020.119473.

[40] B. Zeng, Y. Liu, F. Xu, Y. Liu, X. Sun, and X. Ye, "Optimal demand response resource exploitation for efficient accommodation of renewable energy sources in multi-energy systems considering correlated uncertainties," *J. Clean. Prod.*, vol. 288, p. 125666, 2021, doi: 10.1016/j.jclepro.2020.125666.

[41] S. Balasubramanian and P. Balachandra, "Effectiveness of demand response in achieving supply-demand matching in a renewables dominated electricity system: A modelling approach," *Renew. Sustain. Energy Rev.*, vol. 147, no. October 2020, p. 111245, 2021, doi: 10.1016/j.rser.2021.111245.

[42] H. J. Monfared, A. Ghasemi, A. Loni, and M. Marzband, "A hybrid price-based demand response program for the residential micro-grid," *Energy*, vol. 185, pp. 274–285, 2019, doi: 10.1016/j.energy.2019.07.045.

[43] F. Pallonetto, M. De Rosa, F. Milano, and D. P. Finn, "Demand response algorithms for smart-grid ready residential buildings using machine learning models," *Appl. Energy*, vol. 239, no. February, pp. 1265–1282, 2019, doi: 10.1016/j.apenergy.2019.02.020.

[44] E. Mengelkamp, S. Bose, E. Kremers, J. Eberbach, B. Hoffmann, and C. Weinhardt, "Increasing the efficiency of local energy markets through residential demand response," *Energy Informatics*, vol. 1, no. 1, pp. 1–18, 2018, doi: 10.1186/s42162-018-0017-3.

[45] V. Di Cosmo, S. Lyons, and A. Nolan, "Estimating the impact of time-of-use pricing on irish electricity demand," *Energy J.*, vol. 35, no. 2, pp. 117–136, 2014, doi: 10.5547/01956574.35.2.6.

[46] J. H. Yoon, R. Bladick, and A. Novoselac, "Demand response for residential buildings based on dynamic price of electricity," *Energy Build.*, vol. 80, pp. 531–541, 2014, doi: 10.1016/j.enbuild.2014.05.002.

[47] F. Alfaverh, M. Denai, and Y. Sun, "Demand Response Strategy Based on Reinforcement Learning and Fuzzy Reasoning for Home Energy Management," *IEEE Access*, vol. 8, pp. 39310–39321, 2020, doi: 10.1109/ACCESS.2020.2974286.

[48] Z. Wang, U. Munawar, and R. Paranjape, "Stochastic Optimization for Residential Demand Response with Unit Commitment and Time of Use," *IEEE Trans. Ind. Appl.*, vol. 57, no. 2, pp. 1767–1778, 2021, doi: 10.1109/TIA.2020.3048643.

[49] N. Tawalbeh, H. M. Abusamaha, and A. Al-Salaymeh, "Demand side management and its possibilities in jordan," *J. Ecol. Eng.*, vol. 21, no. 1, pp. 29–33, 2020, doi: 10.12911/22998993/113417.

[50] H. Jarada and M. S. Ashhab, "Energy savings in the Jordanian residential sector," *Jordan J. Mech. Ind. Eng.*, vol. 11, no. 1, pp. 51–59, 2017.

[51] O. Techniques, L. Alhmoud, and Q. Nawafleh, "Short-term load forecasting for Jordan's Power System Using Neural Network based Different," in *2019 IEEE International Conference on Environment and Electrical Engineering and 2019 IEEE Industrial and Commercial Power Systems Europe (EEEIC / I&CPS Europe)*, 2019, pp. 1–6, doi: 10.1109/EEEIC.2019.8783979.

[52] Japan International Cooperation Agency (JICA), "Project for the Study on the Electricity Sector Master Plan in the Hashemite Kingdom of Jordan Final Report," no. February, 2017, [Online]. Available: https://openjicareport.jica.go.jp/pdf/12283693_01.pdf.

[53] NEPCO- National Electric Power Company, "NEPCO Transmission Grid Code," [Online]. Available: https://www.emrc.gov.jo/echobusv3.0/systemassets/$rk0lzm8.pdf.

[54] NEPCO- National Electric Power Company, "Electricity Interconnection Projects."

https://www.nepco.com.jo/en/electrical_interconnection_en.aspx#:~:text=Jordan is electrically interconnected with,capabilities of (550) MW .

[55] EMRC - Jordan, "Electricity Tariff." https://www.emrc.gov.jo/EchoBusV3.0/SystemAssets/Electricity_Sector/pdfs/08ad1e0d-f03f-4e52-96f6-2936634dcc9c_guidea_2020.pdf.

[56] EMRC, "BULK SUPPLY CODE DRAFT - Jordan," [Online]. Available: https://www.emrc.gov.jo/echobusv3.0/systemassets/كود التزويد بالجملة.pdf.

[57] EMCR, "Periods of Peak Demand - 2021," [Online]. Available: https://www.emrc.gov.jo/echobusv3.0/systemassets/abb02815-d8a7-49ac-910f-a6ba3e7dcf60_فترة الذروة لاغراض الموقع 2021-1-1 من اعتباراً.pdf.

[58] D. S. Kirschen, G. Strbac, P. Cumperayot, and D. D. P. Mendes, "Factoring the Elasticity of Demand in Electricity Prices," vol. 15, no. 2, pp. 612–617, 2000.

[59] S. Ajlouni, "Price and Income Elasticities of Residential Demand for Electricity in Jordan : An ARDL Bounds Testing Approach to Cointegration," *Dirasat Adm. Sci.*, vol. 43, no. 1, pp. 335–349, 2016, doi: 10.12816/0028467.

[60] M. Leshno, V. Y. Lin, A. Pinkus, and S. Schocken, "Multilayer feedforward networks with a nonpolynomial activation function can approximate any function," *Neural Networks*, vol. 6, no. 6, pp. 861–867, 1993, doi: 10.1016/S0893-6080(05)80131-5.

[61] S. Ryu, J. Noh, and H. Kim, "Deep neural network based demand side short term load forecasting," *Energies*, vol. 10, no. 1, pp. 1–20, 2017, doi: 10.3390/en10010003.

[62] B. Karlik and A. Olgac, "Performance analysis of various activation functions in generalized MLP architectures of neural networks," *Int. J. Artif. Intell. Expert Syst.*, 2010.

[63] C. E. Nwankpa, W. Ijomah, A. Gachagan, and S. Marshall, "Activation functions: Comparison of trends in practice and research for deep learning," *arXiv*, pp. 1–20, 2018.

[64] R. M. Neal, "Connectionist learning of belief networks," *Artif. Intell.*, vol. 56, no. 1, pp. 71–113, 1992, doi: 10.1016/0004-3702(92)90065-6.

[65] J. Feng and S. Lu, "Performance Analysis of Various Activation Functions in Artificial Neural Networks," *J. Phys. Conf. Ser.*, vol. 1237, no. 2, pp. 111–122, 2019, doi: 10.1088/1742-6596/1237/2/022030.

[66] V. Nair and G. E. Hinton, "Rectified Linear Units Improve Restricted Boltzmann Machines. BT - Proceedings of the 27th International Conference on Machine Learning (ICML-10), June 21-24, 2010, Haifa, Israel." pp. 807–814, 2010, [Online]. Available: https://icml.cc/Conferences/2010/papers/432.pdf.

[67] M. D. Zeiler *et al.*, "On rectified linear units for speech processing," in *2013 IEEE International Conference on Acoustics, Speech and Signal Processing*, 2013, pp. 3517–3521, doi: 10.1109/ICASSP.2013.6638312.

[68] Ian Goodfellow and Yoshua Bengio and Aaron Courville, *Deep Learning*. MIT Press, 2016.

[69] X. Glorot, A. Bordes, and Y. B. B. T.-P. of the F. I. C. on A. I. and Statistics, "Deep Sparse Rectifier Neural Networks." PMLR , pp. 315–323, Jun. 14, 2011, [Online]. Available: http://proceedings.mlr.press/v15/glorot11a/glorot11a.pdf.

[70] A. L. Maas, A. Y. Hannun, and A. Y. Ng, "Rectifier nonlinearities improve neural network acoustic models," *ICML Work. Deep Learn. Audio, Speech Lang. Process.*, vol. 28, 2013.

[71] D. A. Clevert, T. Unterthiner, and S. Hochreiter, "Fast and accurate deep network learning by exponential linear units (ELUs)," *4th Int. Conf. Learn. Represent. ICLR 2016 - Conf. Track Proc.*, pp. 1–14, 2016.

[72] L. Trottier, P. Gigure, and B. Chaib-Draa, "Parametric exponential linear unit for deep convolutional neural networks," *Proc. - 16th IEEE Int. Conf. Mach. Learn. Appl. ICMLA 2017*, vol. 2017-Decem, pp. 207–214, 2017, doi: 10.1109/ICMLA.2017.00038.

[73] A. Krizhevsky, I. Sutskever, and G. E. Hinton, "ImageNet Classification with Deep Convolutional Neural Networks," pp. 1–1432, 2012, doi: 10.1201/9781420010749.

[74] S. Ruder, "An overview of gradient descent optimization algorithms," pp. 1–14, 2016, [Online]. Available: http://arxiv.org/abs/1609.04747.

[75] N. Qian, "On the momentum term in gradient descent learning algorithms," *Neural Networks*, vol. 12, no. 1, pp. 145–151, 1999, doi: 10.1016/S0893-6080(98)00116-6.

[76] G. Hinton, N. Srivastava, and K. Swersky, "Overview of mini-batch gradient descent." http://www.cs.toronto.edu/~tijmen/csc321/slides/lecture_slides_lec6.pdf.

[77]   D. P. Kingma and J. L. Ba, "Adam: A method for stochastic optimization," *3rd Int. Conf. Learn. Represent. ICLR 2015 - Conf. Track Proc.*, pp. 1–15, 2015.

[78]   A. Botchkarev, "A new typology design of performance metrics to measure errors in machine learning regression algorithms," *Interdiscip. J. Information, Knowledge, Manag.*, vol. 14, pp. 45–76, 2019, doi: 10.28945/4184.

[79]   D. L. J. Alexander, A. Tropsha, and D. A. Winkler, "Beware of R2: Simple, Unambiguous Assessment of the Prediction Accuracy of QSAR and QSPR Models," *J. Chem. Inf. Model.*, vol. 55, no. 7, pp. 1316–1322, 2015, doi: 10.1021/acs.jcim.5b00206.

[80]   W. Kong, Z. Y. Dong, Y. Jia, D. J. Hill, Y. Xu, and Y. Zhang, "Short-Term Residential Load Forecasting Based on LSTM Recurrent Neural Network," *IEEE Trans. Smart Grid*, vol. 10, no. 1, pp. 841–851, 2019, doi: 10.1109/TSG.2017.2753802.

[81]   J. F. Hastie, Trevor, Robert Tibshirani, *The Elements of Statistical Learning*. 2009.

[82]   N. Srivastava, G. Hinton, A. Krizhevsky, I. Sutskever, and R. Salakhutdinov, "Dropout: A simple way to prevent neural networks from overfitting," *J. Mach. Learn. Res.*, 2014.

[83]   L. Prechelt, "Automatic early stopping using cross validation: Quantifying the criteria," *Neural Networks*, vol. 11, no. 4, pp. 761–767, 1998, doi: 10.1016/S0893-6080(98)00010-0.

[84]   I. Guyon and A. Elisseeff, "An Introduction to Variable and Feature Selection," *J. Mach. Learn. Res.*, vol. 3, no. null, pp. 1157–1182, Mar. 2003.

[85]   A. J. Del Real, F. Dorado, and J. Durán, "Energy demand forecasting using deep learning: Applications for the French grid," *Energies*, vol. 13, no. 9, 2020, doi: 10.3390/en13092242.

[86]   P. Schober and L. A. Schwarte, "Correlation coefficients: Appropriate use and interpretation," *Anesth. Analg.*, vol. 126, no. 5, pp. 1763–1768, 2018, doi: 10.1213/ANE.0000000000002864.

[87]   A. Lahouar and J. Ben Hadj Slama, "Day-ahead load forecast using random forest and expert input selection," *Energy Convers. Manag.*, vol. 103, pp. 1040–1051, 2015, doi: 10.1016/j.enconman.2015.07.041.

[88]   The Department of Statistics (DoS) - Jordan, "Distribution of Housing Units by Household Appliances and Private Car and Governorate and Urban-Rural (%)," 2017.

[89]   Energyusecalculator, "Electricity usage of a Water Heater." https://energyusecalculator.com/electricity_waterheater.htm.

[90]   B. J. Johnson, M. R. Starke, O. A. Abdelaziz, R. K. Jackson, and L. M. Tolbert, "A dynamic simulation tool for estimating demand response potential from residential loads," *2015 IEEE Power Energy Soc. Innov. Smart Grid Technol. Conf. ISGT 2015*, no. Dlc, pp. 1–5, 2015, doi: 10.1109/ISGT.2015.7131867.

[91]   Z. Wang and R. Paranjape, "Optimal Residential Demand Response for Multiple Heterogeneous Homes with Real-Time Price Prediction in a Multiagent Framework," *IEEE Trans. Smart Grid*, vol. 8, no. 3, pp. 1173–1184, 2017, doi: 10.1109/TSG.2015.2479557.